Chapter 17
Surface and Interface Physics

Reference Textbook:

- Solid State Physics, Gerald Burns
- Solid State Physics, Ashcroft and Mermin
- Physics at Surfaces, Andrew Zangwill
- Modern techniques of surface science, D. P. Woodruff and T. A. Delchar
- Introduction to Synchrotron Radiation, G. Margaritondo

What makes surface different?

- 3D vs 2D
- Surface is what we usually “see”.
- Technology:
  - Semiconductors
  - Catalysis

Surface Structures

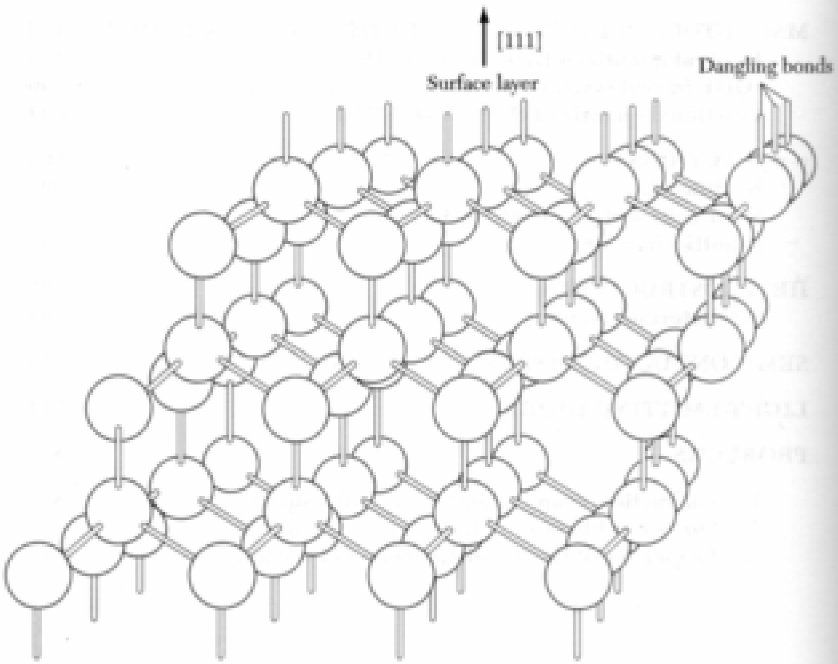

Figure 1 Dangling bonds from the (111) surface of a covalently bonded diamond cubic structure. (After M. Prutton, *Surface physics*, Clarendon, 1975.)

Surface Reconstruction and Relaxation

- 2D crystalline structure
- Atoms on surface
- truncation

Surface Crystalography

- Notations
- LEED
- RHEED

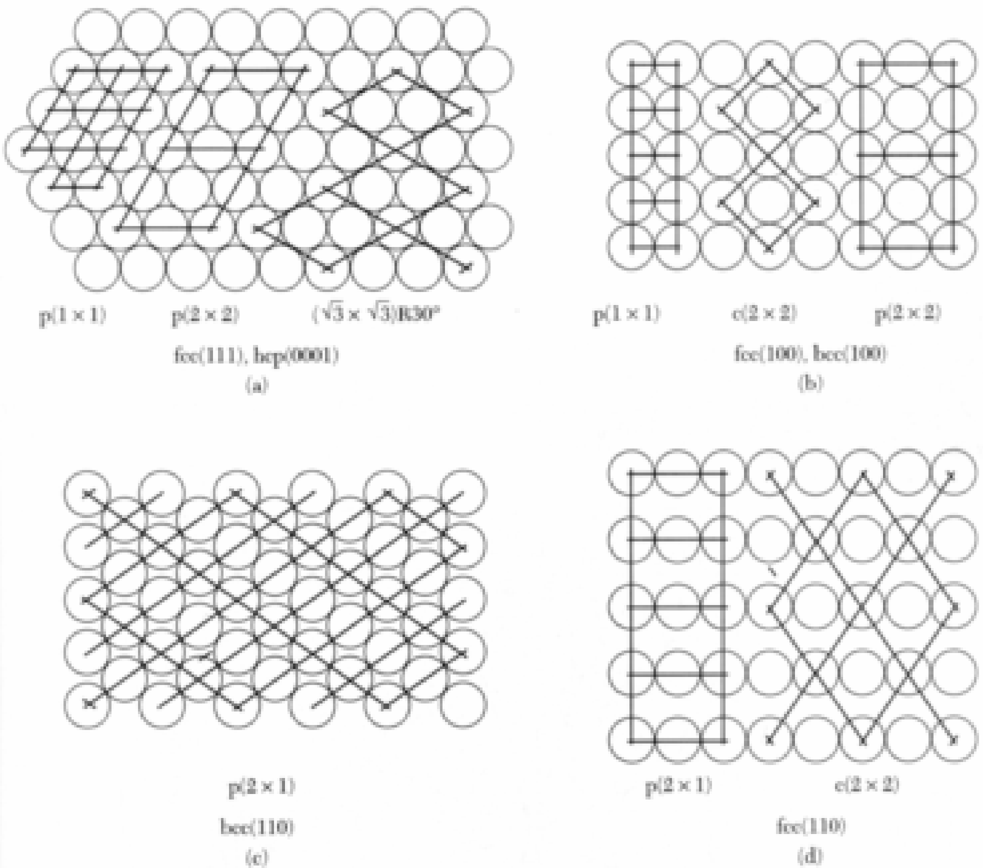

Figure 2 Surface nets of adsorbed atoms. The circles represent atoms in the top layer of the substrate. In (a) the designation fcc(111) means the (111) face of an fcc structure. This face determines a reference net. The lines represent ordered overlayers, with adatoms at the intersections of two lines. The intersection points represent diperiodic nets (lattices in two dimensions). The designation p(1 × 1) in (a) is a primitive mesh unit for which the basis is identical with the basis of the reference net. In (b) the c(2 × 2) mesh unit is a centered mesh with basis vectors twice as long as those of the reference net. Atomic adsorption on metals takes place most often into those surface sites (hollow sites) that maximize the number of nearest-neighbor atoms on the substrate. (After Van Hove.)

LEED

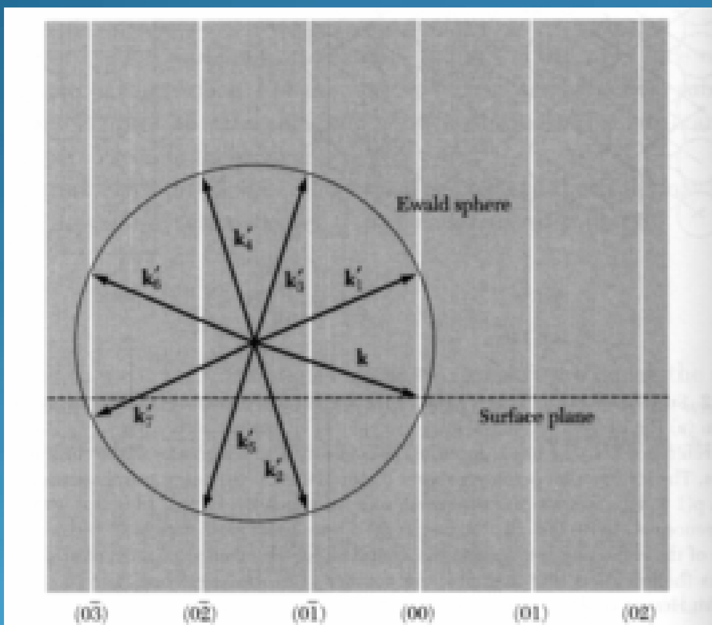

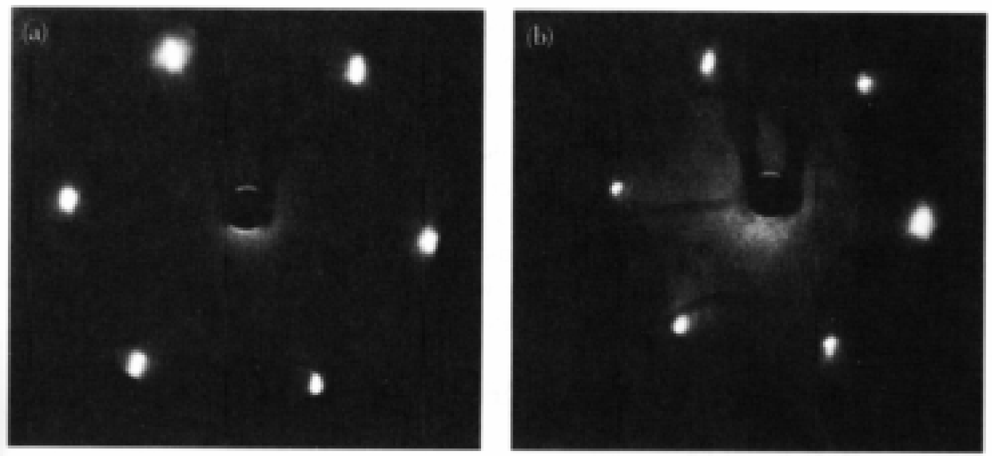

Figure 5 LEED patterns from a Pt(111) crystal surface for incident electron energies of 51 and 63.5 *eV*. The diffraction angle is greater at the lower energy. (After G. A. Somorjai, *Chemistry in two dimensions: surfaces*, Cornell, 1981.)

RHEED

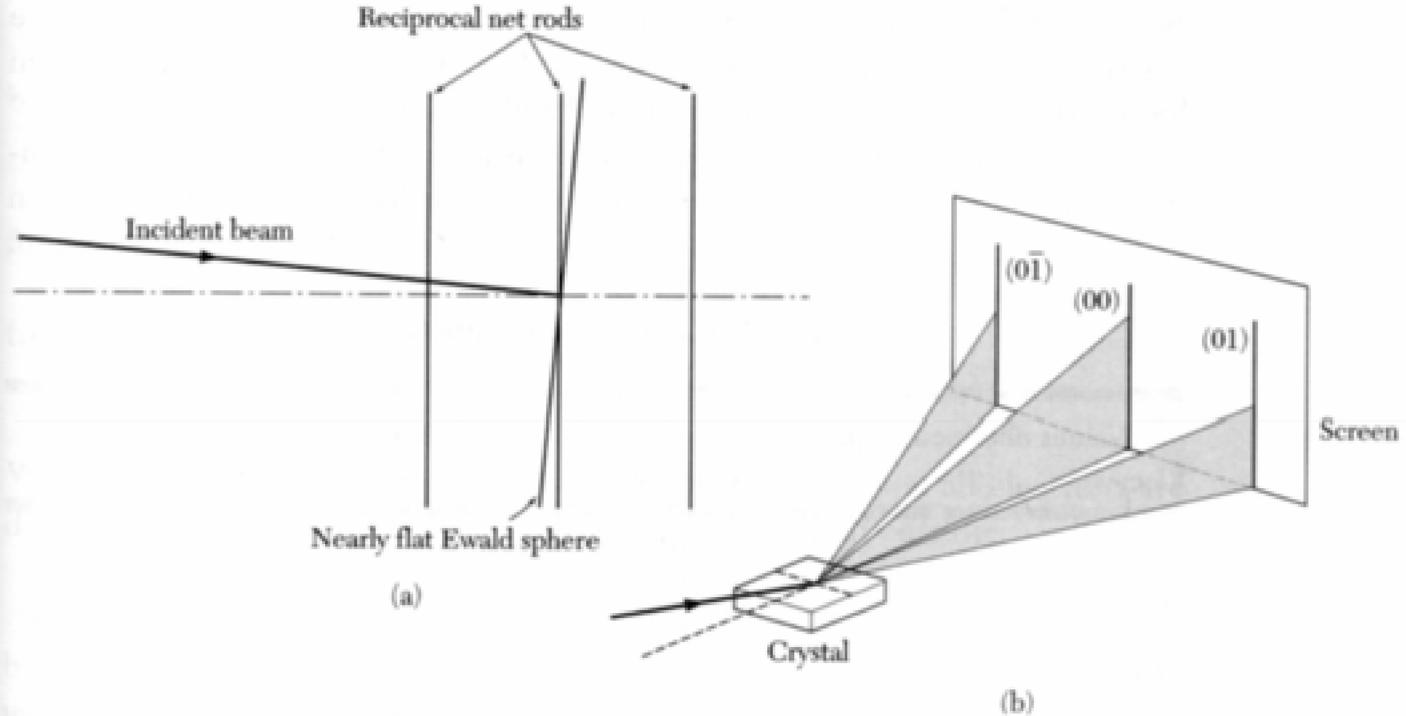

Figure 6 The RHEED method. In (a) the high-energy incident electron beam at a glancing angle to the crystal surface is associated with an Ewald sphere of large radius, so large that the surface is nearly flat in relation to the separation between adjacent rods of the reciprocal net. The formation of diffraction lines on a plane screen is shown in (b). (After Prutton.)

Surface electronic structures

- Work function
- Thermionic Emission
- Surface State
- Tangential Surface Transport

Work Function

- Difference in potential energy of an electron between the vacuum level and the Fermi level.
- Work functions depends on the orientation of the exposed crystal face.
- Photoemission

Table 1 Electron work functions[a]

(Values obtained by photoemission, except tungsten obtained by field emission.)

Element	Surface plane	Work function, in eV
Ag	(100)	4.64
	(110)	4.52
	(111)	4.74
Cs	polycrystal	2.14
Cu	(100)	4.59
	(110)	4.48
	(111)	4.98
Ge	(111)	4.80
Ni	(100)	5.22
	(110)	5.04
	(111)	5.35
W	(100)	4.63
	(110)	5.25
	(111)	4.47

[a]After H. D. Hagstrum.

Thermionic Emission

- Rate of thermionic emission depends exponentially on the work function
- Rchardson-Dushman Equation

Surface States

Surface States

Fig. 4.20. Photoemission energy distribution curves from Cu(111) at different collection angles. Equation (4.32) has been used to express the electron kinetic energy in terms of the binding energy of the electron state (Kevan, 1983).

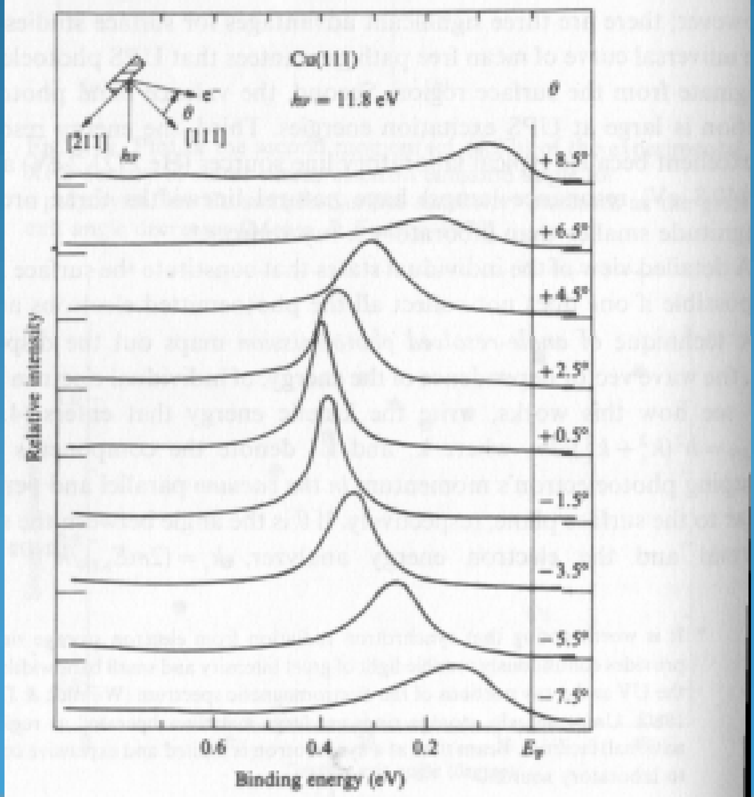

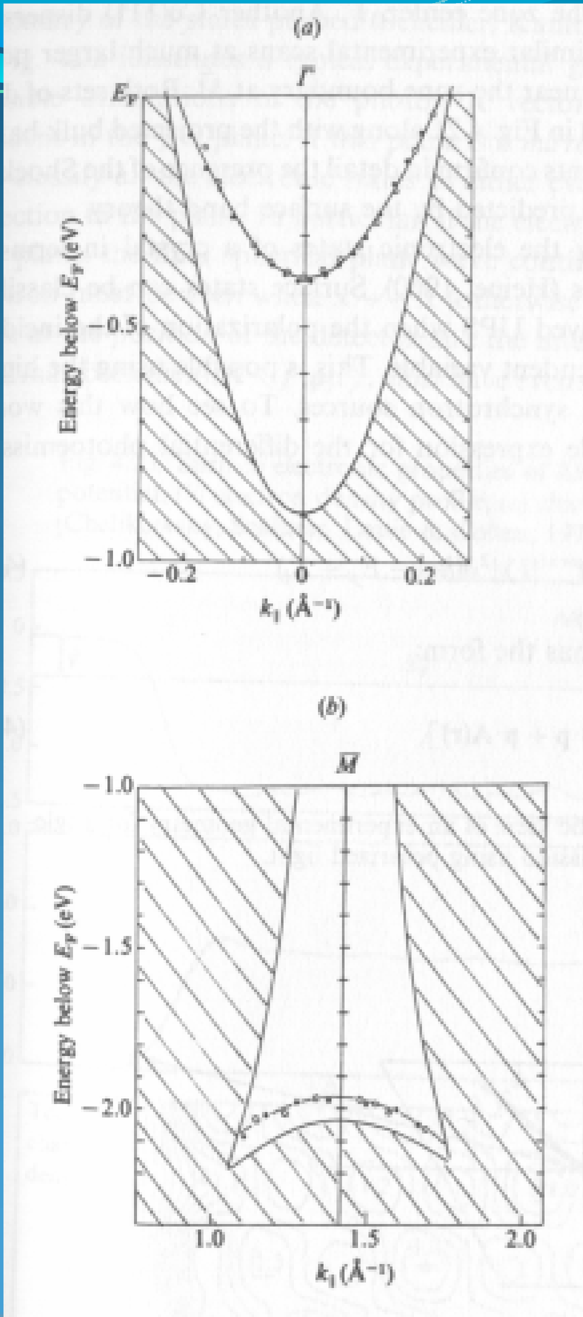

Tangential Surface Transport

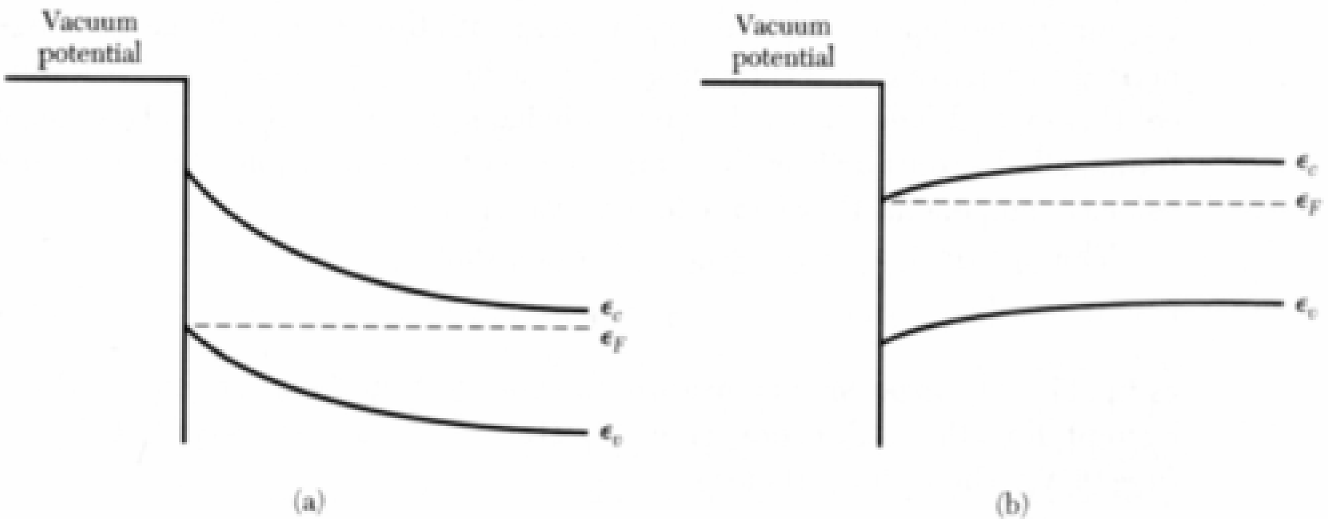

Figure 7 Band bending near a semiconductor surface that can give a highly conducting surface region. (a) Inversion layer on an *n*-type semiconductor. For the bending as shown, the hole concentration at the surface is far larger than the electron concentration in the interior. (b) Accumulation layer on an *n*-type semiconductor, with an electron concentration at the surface that is far higher than in the interior.

Fig. 3.18. The field ion microscope: (*a*) schematic view of image formation (Muller, 1977); (*b*) image of a tungsten tip of radius ~ 120 Å. [100] and [111] planes are well resolved (Tsong & Sweeney, 1979).

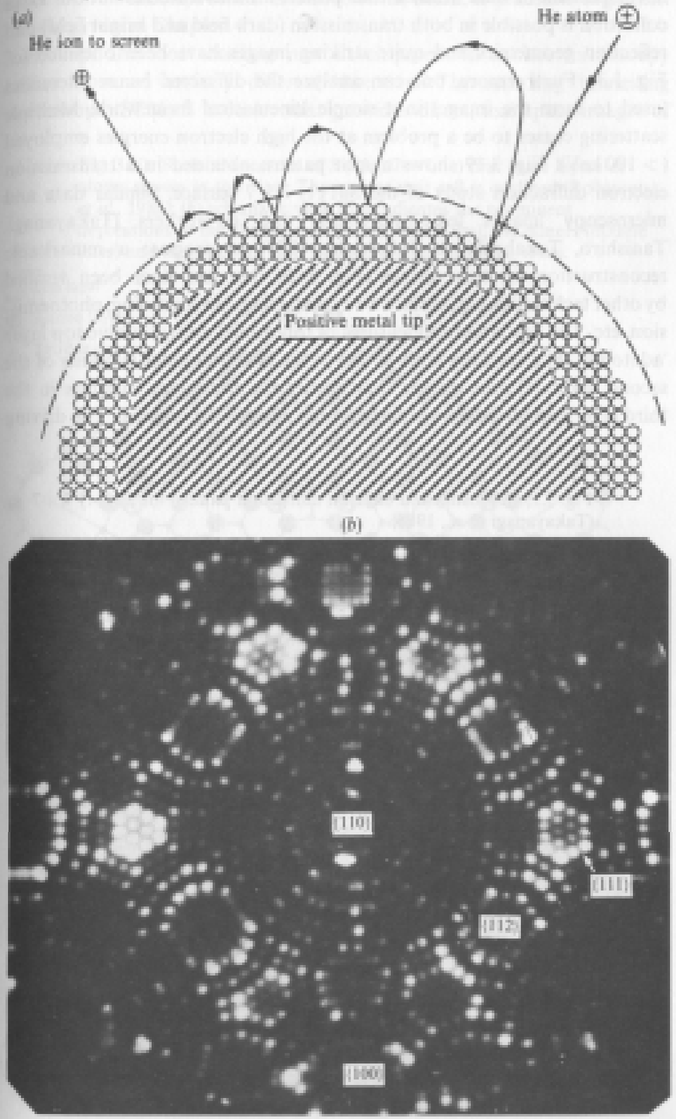

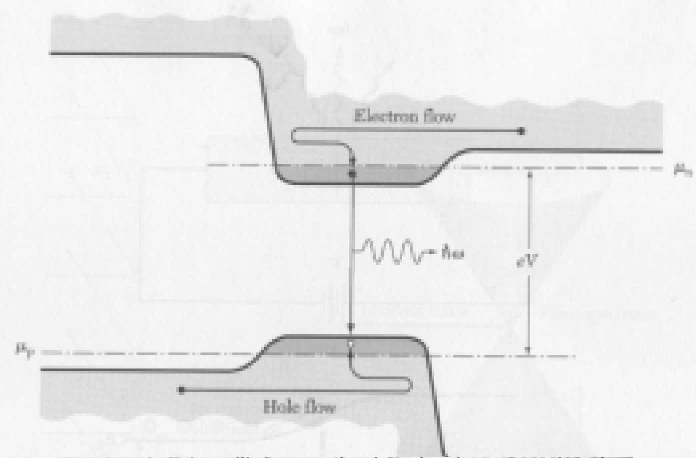

the optically-
vided by the
es flow from

two-dimensional periodicity will destroy the delta function character of the reciprocal lattice rods. Broadening and splittings will appear as one

Fig. 3.8. Possible surface defect structures, the corresponding modification of the reciprocal lattice rods and the resultant LEED spot profile (Henzler, 1982).

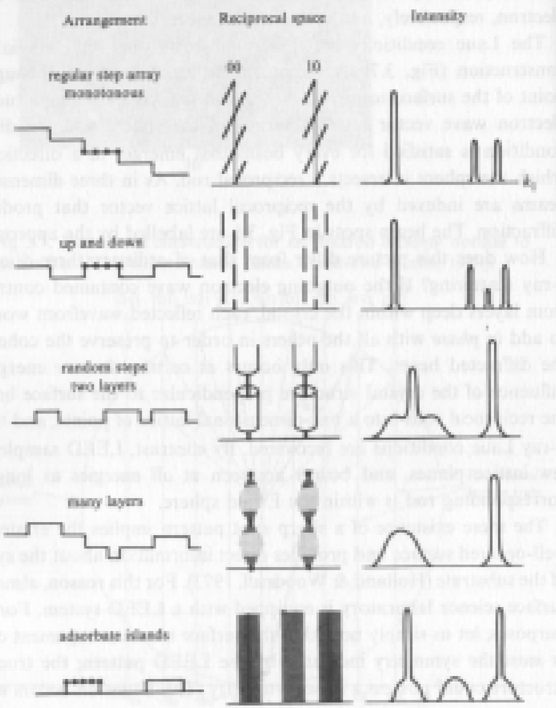

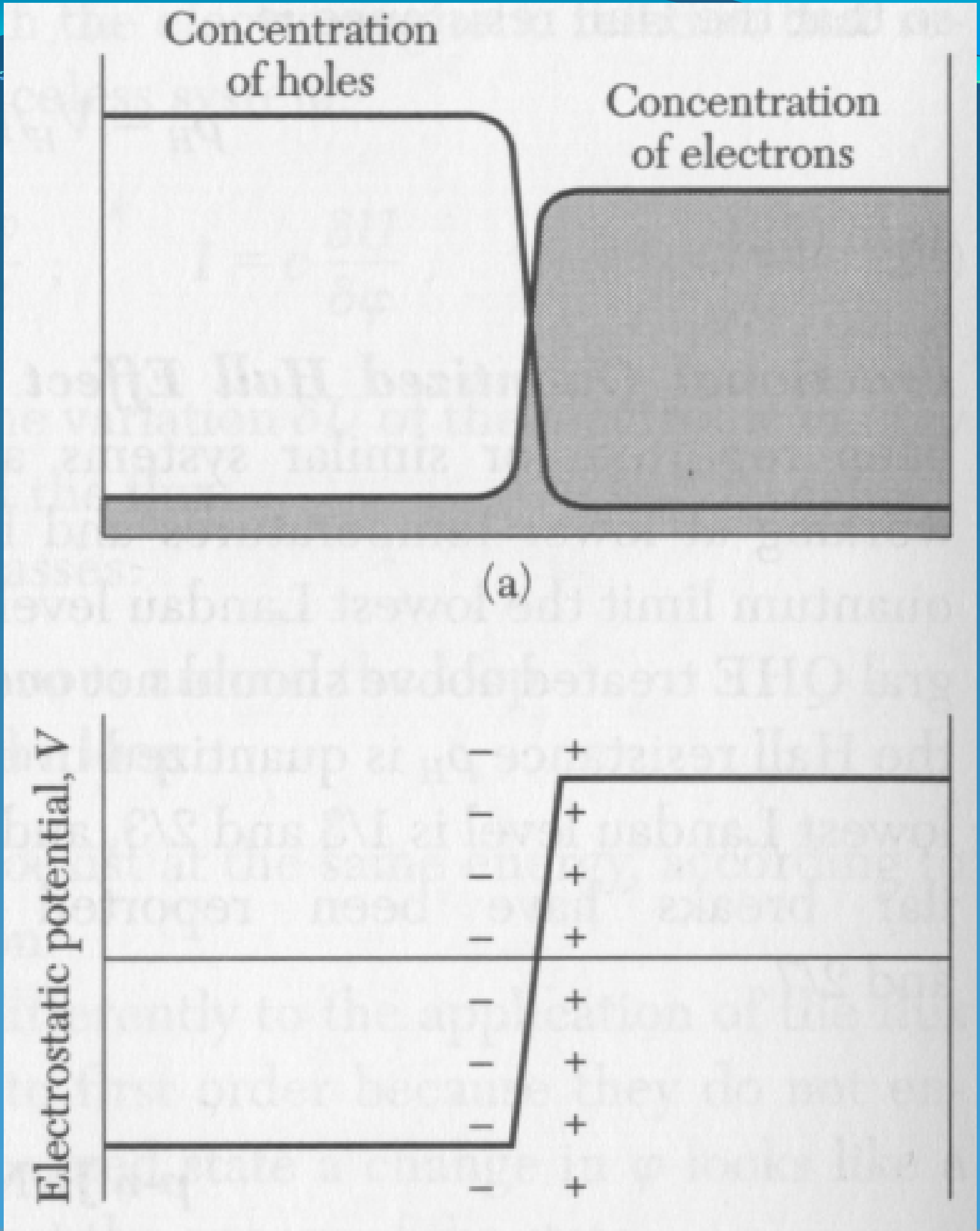
Concentration of holes
Concentration of electrons
(a)
Electrostatic potential, V
− +
− +
− +
− +
− +
− +
− +
− +

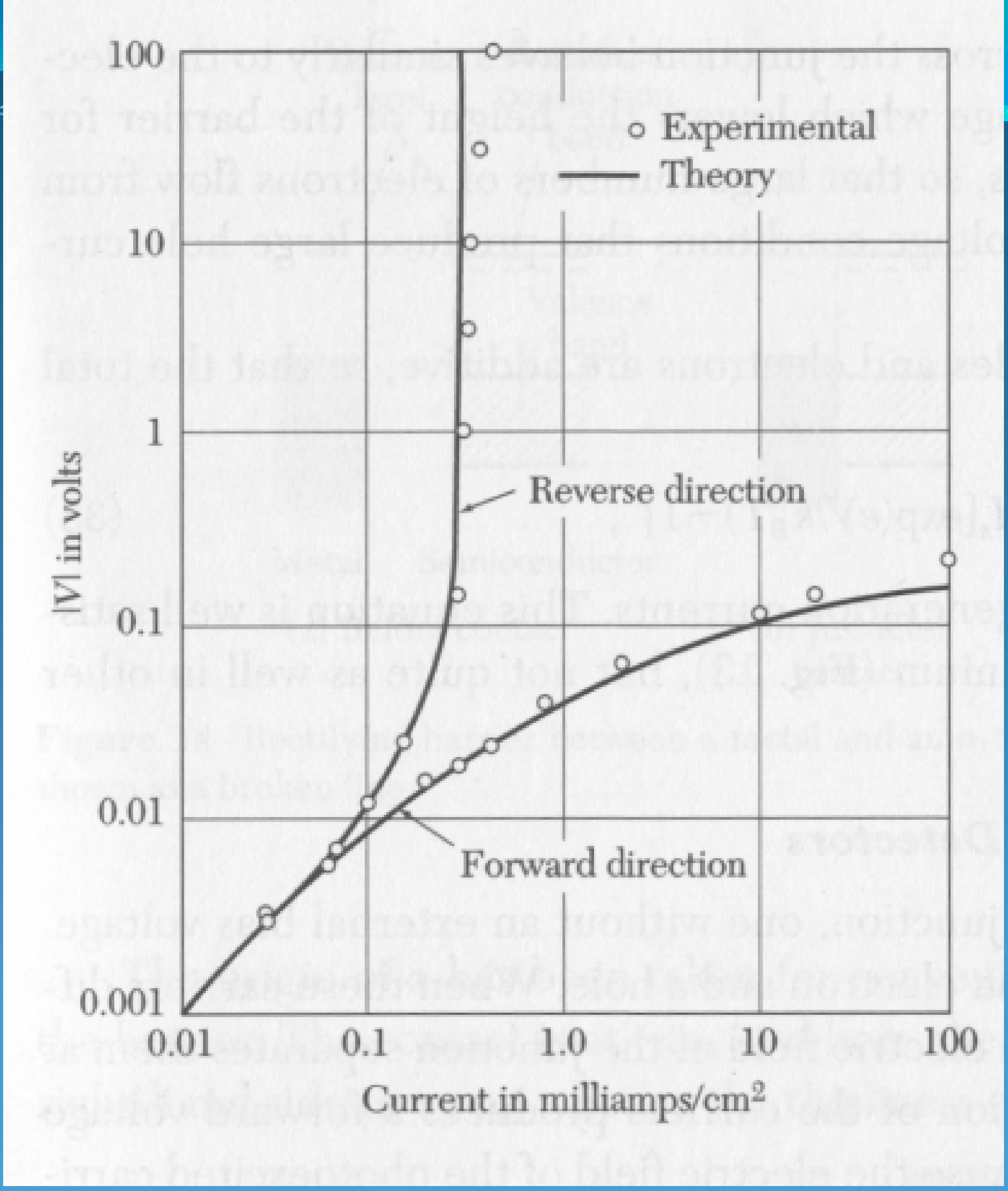

Experimental
Theory
Reverse direction
Forward direction
|V| in volts
Current in milliamps/cm²
100
10
1
0.1
0.01
0.001
0.01
0.1
1.0
10
100

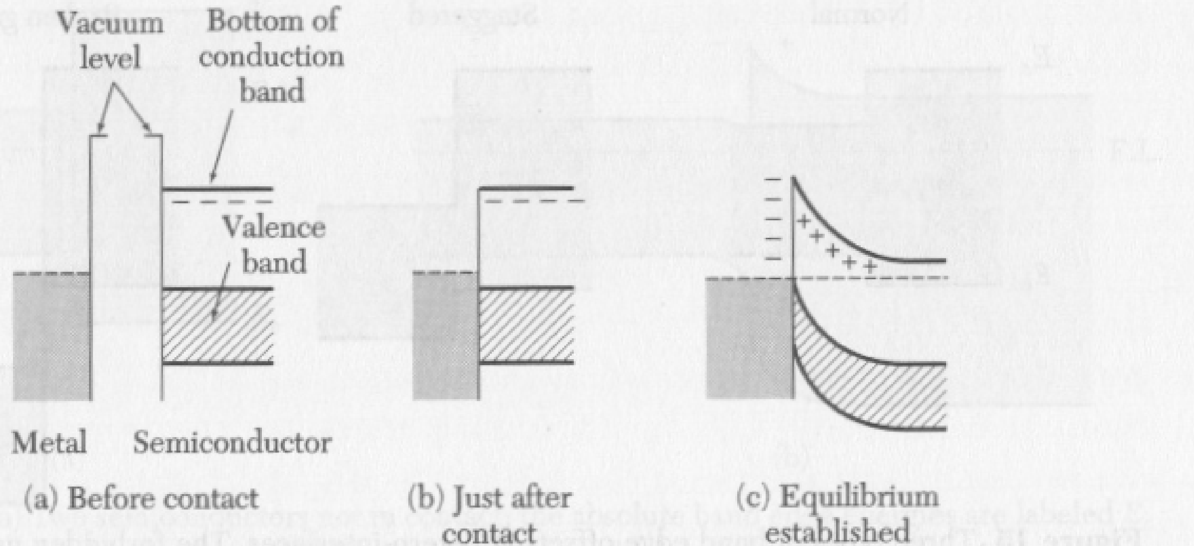

Figure 14 Rectifying barrier between a metal and an *n*-type semiconductor. The Fermi level is shown as a broken line.

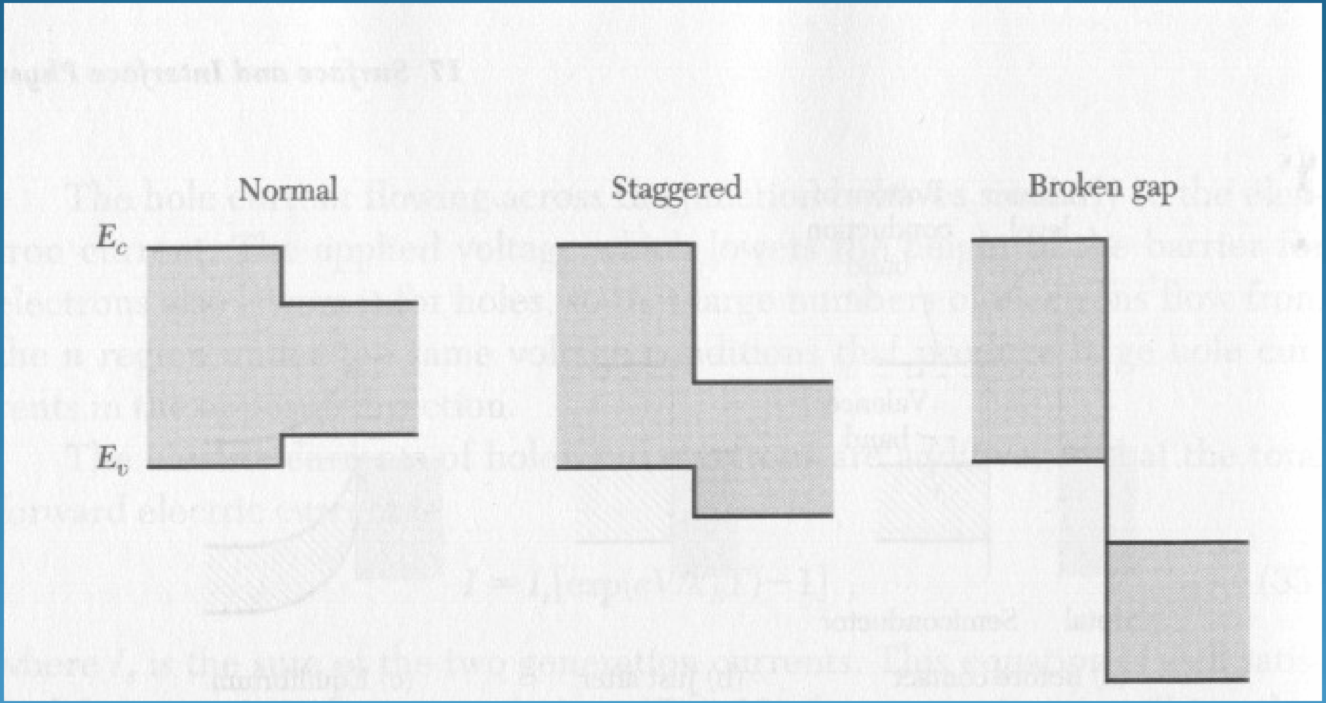

Normal
Staggered
Broken gap
E_c
E_v

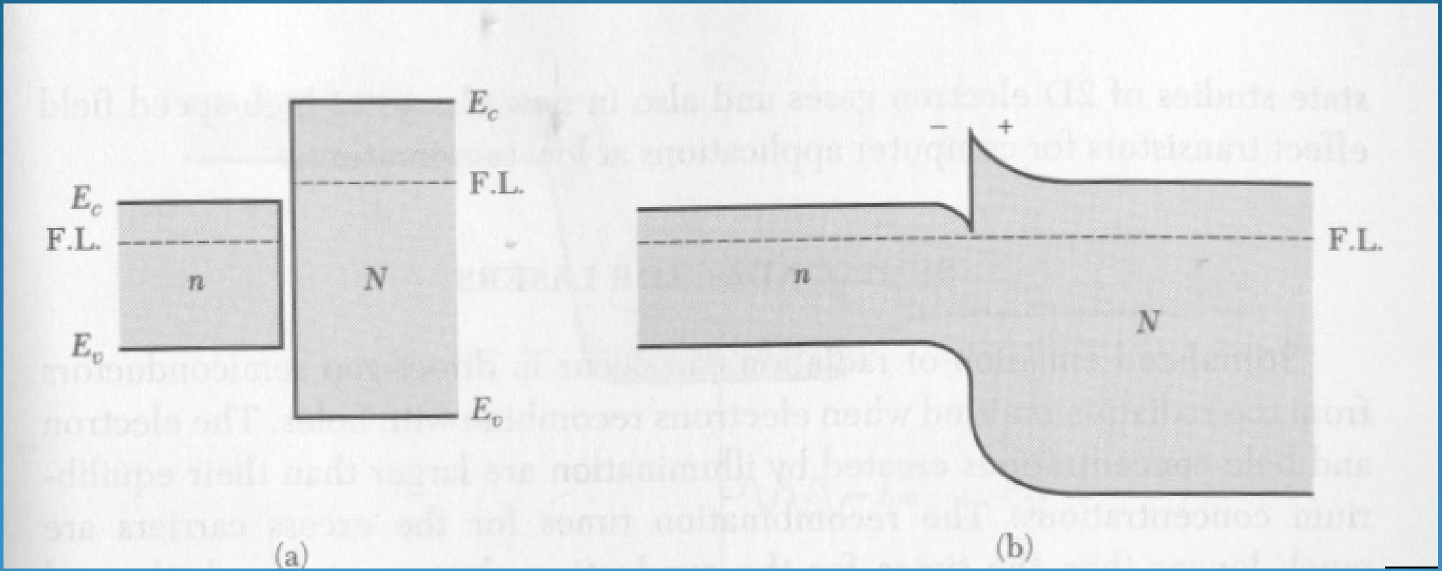
E_c
F.L.
n
E_v
N
E_c
F.L.
E_v
(a)
−
+
F.L.
n
N
(b)

Fig. 3.9. Comparison of LEED theory and experiment for Cu(100) (Davis & Noonan, 1982).

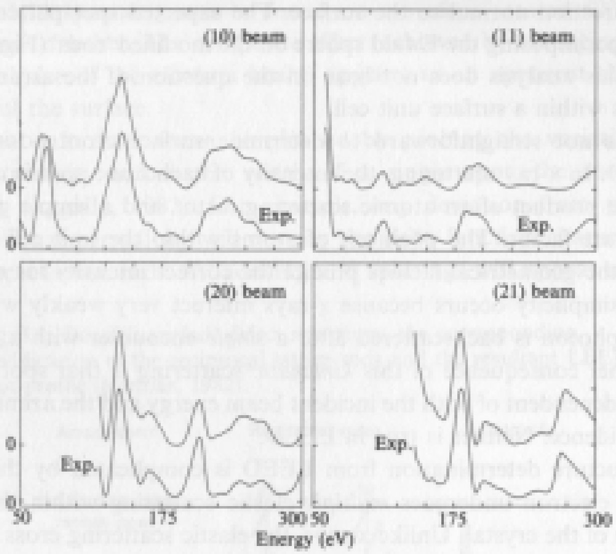

Fig. 3.10. Top layer relaxation for iron versus surface roughness (inverse surface ion density) (Sokolov, Jona & Marcus, 1984).

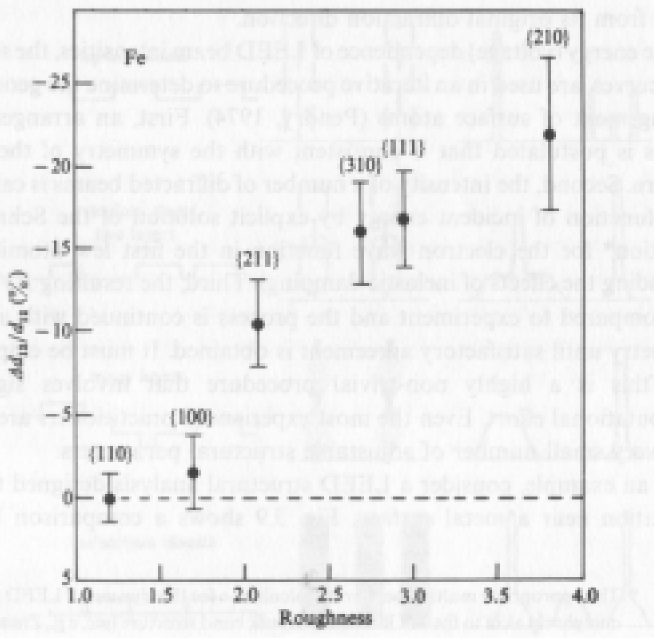

Fig. 3.11. Comparison of LEED theory and experiment for Si(111) 1 × 1 (Zehner, Noonan, Davis & White, 1981; Jones & Holland, 1985).

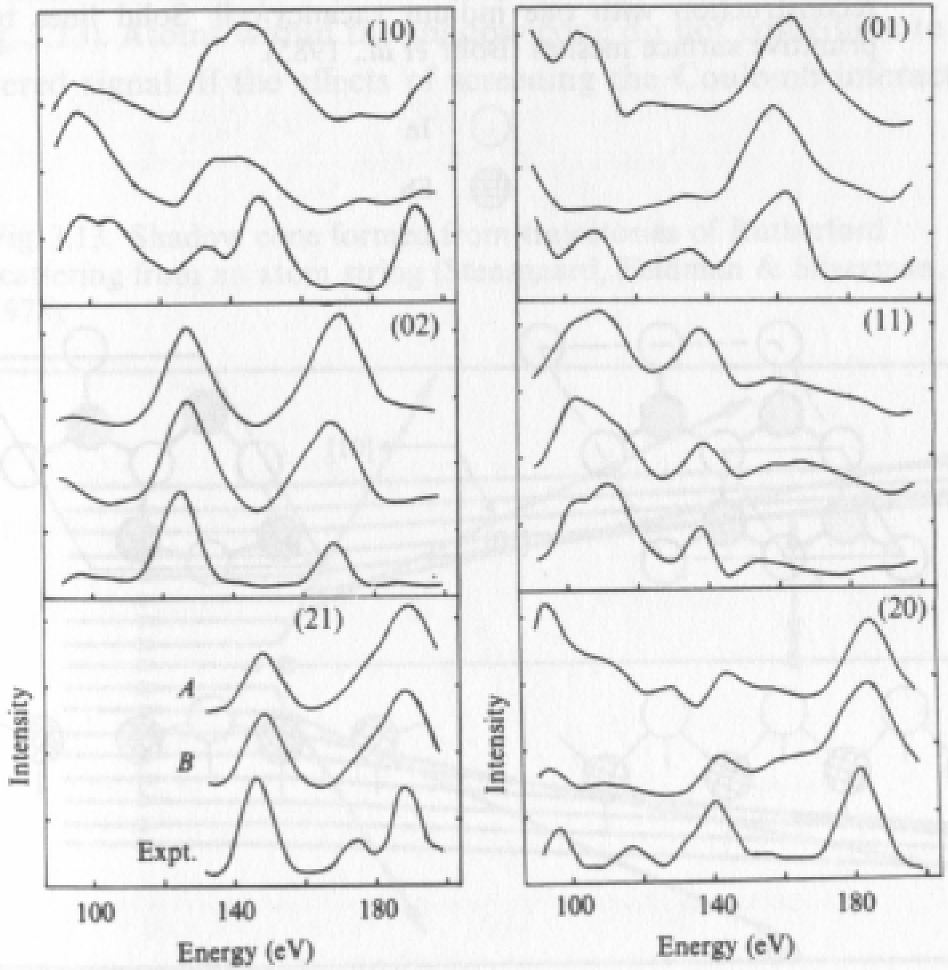

Surface preparation

- Ultrahigh Vacuum
- Surface cleaning
- Cleaving crystals to expose fresh surface
- In vacuum deposition

Surface Characterization

- Photon
- Electron
- SPM
- Ion

p-n JUNCTIONS

- Rectification
- Solar Cells and Photovoltaic Detector
- Schottky Barrier

p-n Junctions

- Donor and acceptor

Rectification

Schottky Barrier

- Fermi Level alignment
- Band Bending

Solar Cells and Photovoltaic Detectors

- Photovoltaic effect
- The basic requirements
  - the absorption of photons through the creation of electron-hole pairs;
  - the separation of the electron and hole so that their recombination is inhibited and the electric field within the semiconductor is altered
  - the collection of the electrons and holes, separately, by each of two current-collecting electrodes so that current can be induced to flow in a circuit external to the semiconductor itself.

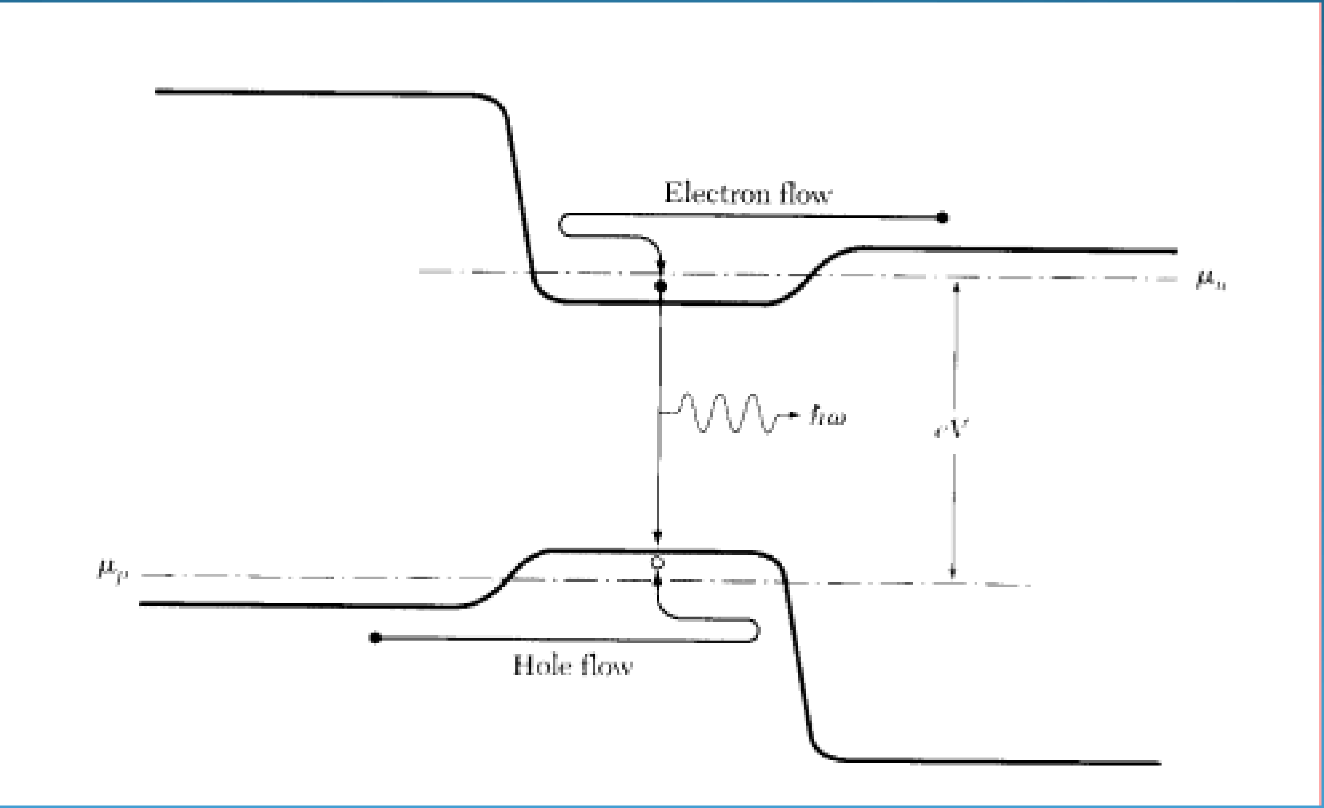

Electron flow
μ_n
$\hbar\omega$
eV
μ_p
Hole flow

HETEROSTRUCTURES

- n-N Heterojunction

SEMICONDUCTOR LASERS

LIGHT-EMITTING DIODES

Optical Absorption Process

- UV, Soft-x-ray
- X-ray

Fermi's Golden Rule

$$H_I = -\sum_i [\frac{e_i}{m_i c} \mathbf{A_R}(\mathbf{r_i}) \bullet \mathbf{p_i} + A_R^2(\mathbf{r_i})]$$

$$\Gamma_{i,f} = \frac{2\pi}{\hbar^2} \left| \langle f | H_{\text{int}} | i \rangle \right|^2 \delta\left(\omega - \boldsymbol{E}_f + \boldsymbol{E}_i\right)$$

Optical Absorption Process in Atoms --Transitions for the H atom

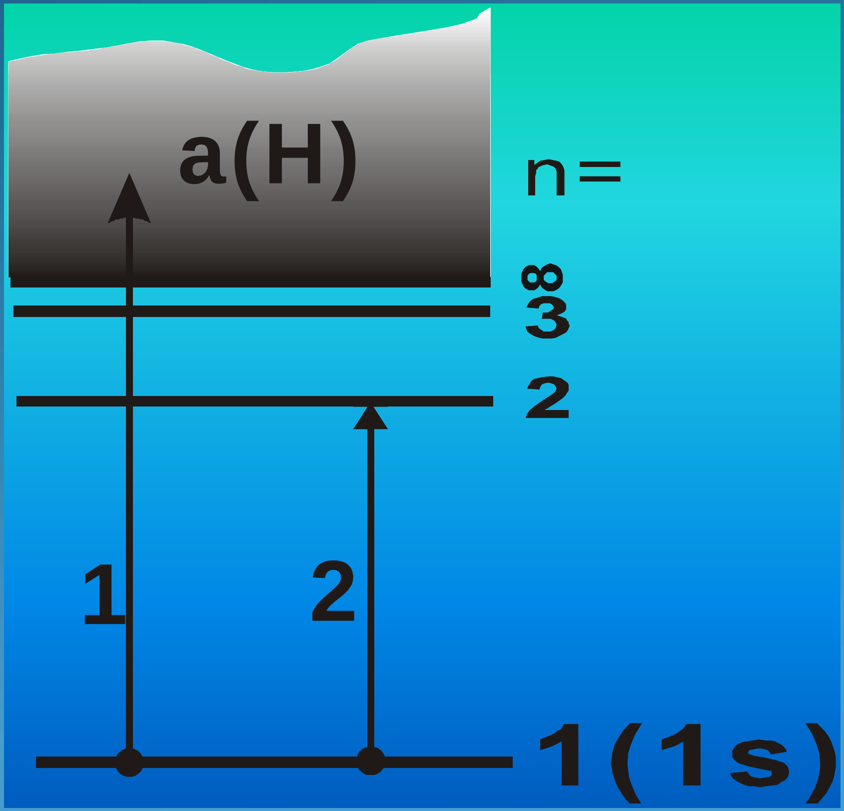

1. to an unbound state in the continuum above the ionization edge. Creates H^+ produces photon absorption in a spectral continuum, at photon energies above the threshold.
2. brings the electron to a bound excited state. produces a discrete line in the Rydberg series.

Other Atomic processes

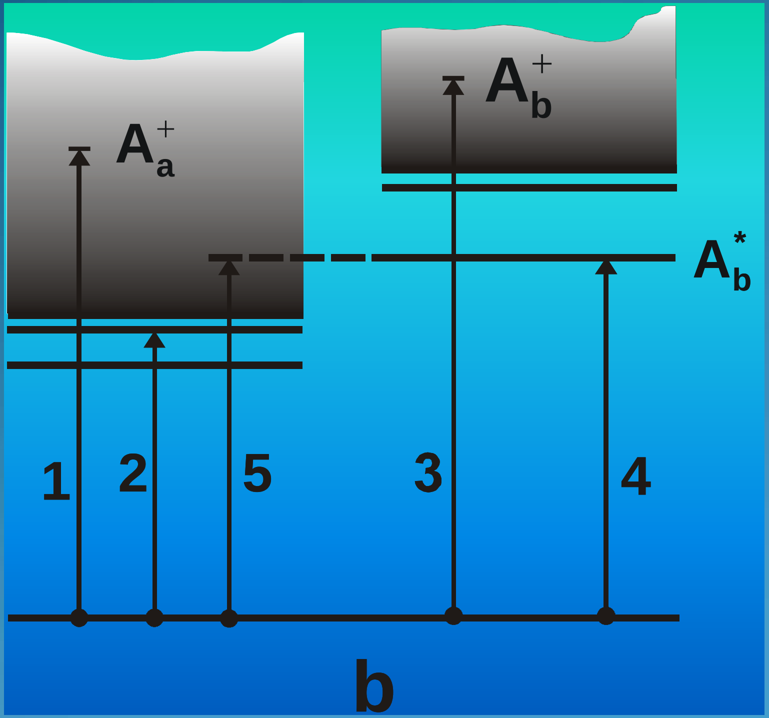

- The bound states of the Rydberg series which accompanies a given continuum can overlap the unbound states of another continuum. This is the case of the final state of process 4.
- 1, 5 and 3 are ionization processes, which produce two different kinds of ion states. 3 produce a different continuum than 1 and 5.
- 2 and 4 are excitations to two of the discrete bound states corresponding to these continua. They produce lines in the Rydberg series.
- Note that, after process 4 has taken place, the system can further evolve from the bound excited state to an ionization state without changing its energy. The combination of process and the transition to the ionized state is an example of an autoionization process.

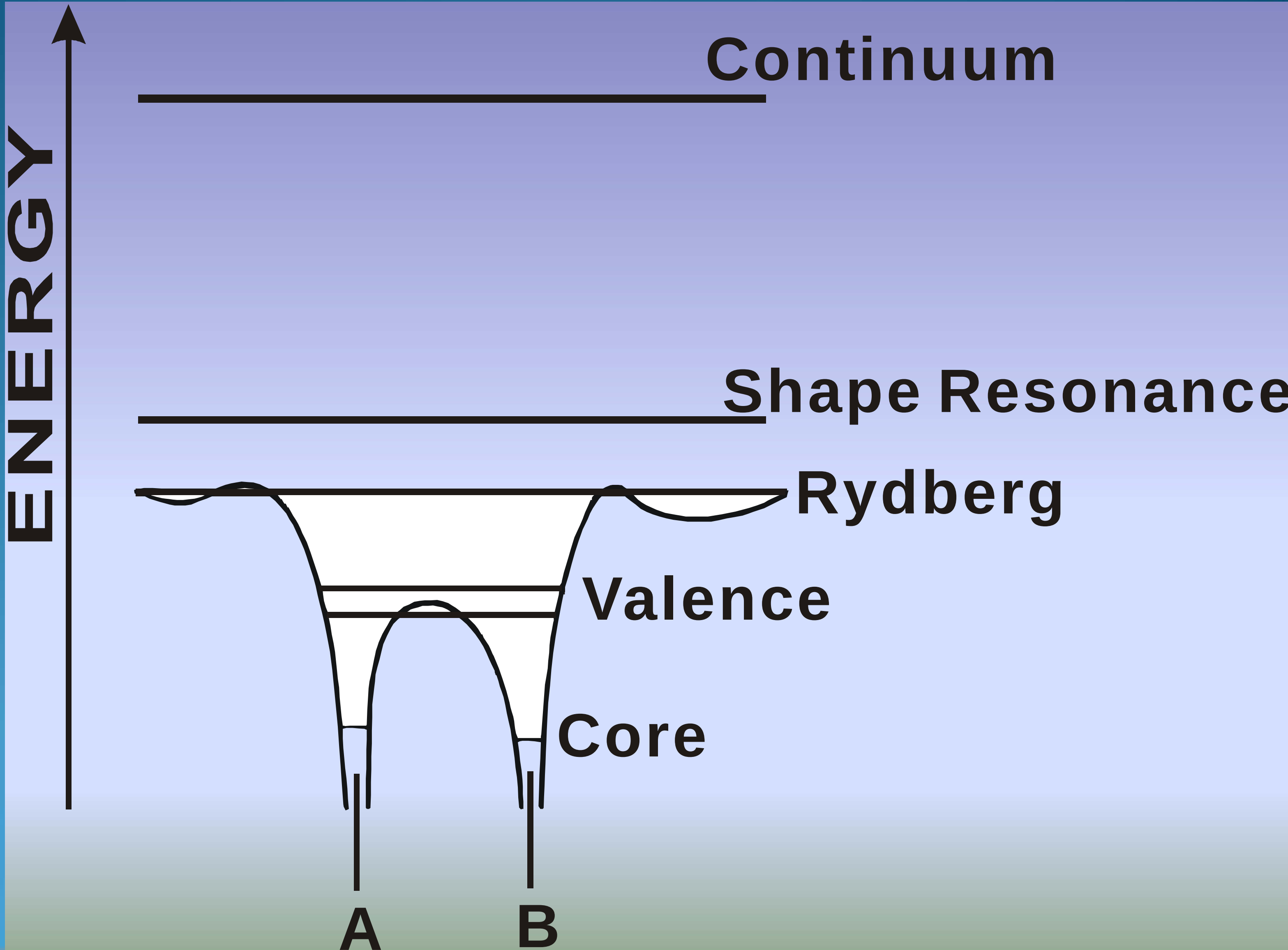

ENERGY
Continuum
Shape Resonance
Rydberg
Valence
Core
A
B

Electronic States of Molecules

- Bound Molecular Orbitals
  - Core
  - Valence
  - Rydberg
- Unbound Molecular Orbitals
  - Shape resonance
  - Continuum orbitals

Optical transition in Metal and Insulator

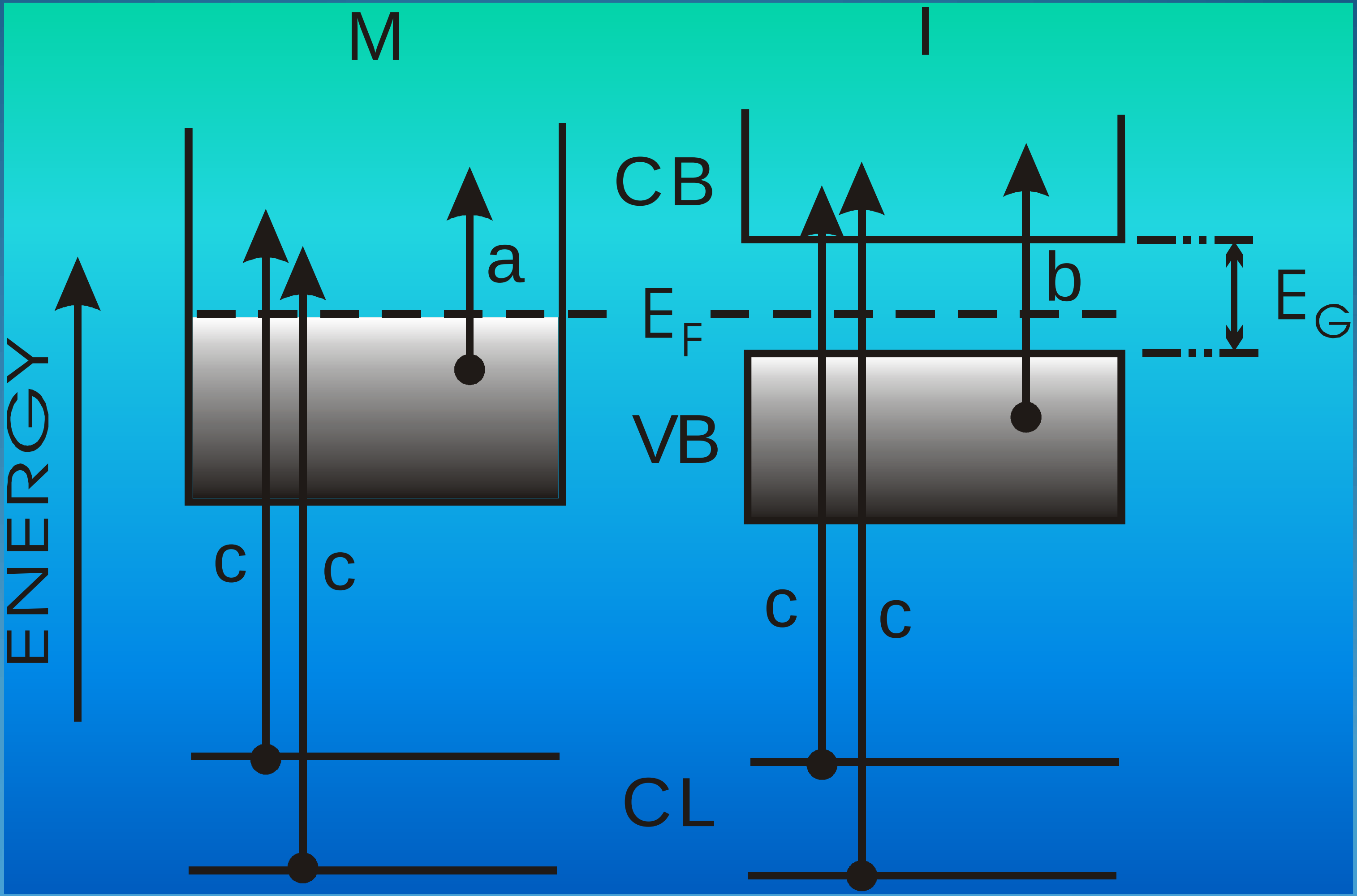

Optical Absorption Spectra

- Atoms and Molecules
  - Discrete states: Rydberg States
  - No EXAFS oscillation in XAS
- Solids
  - Band Structure
  - EXAFS oscillation

Core-Leve Absorption from Atom

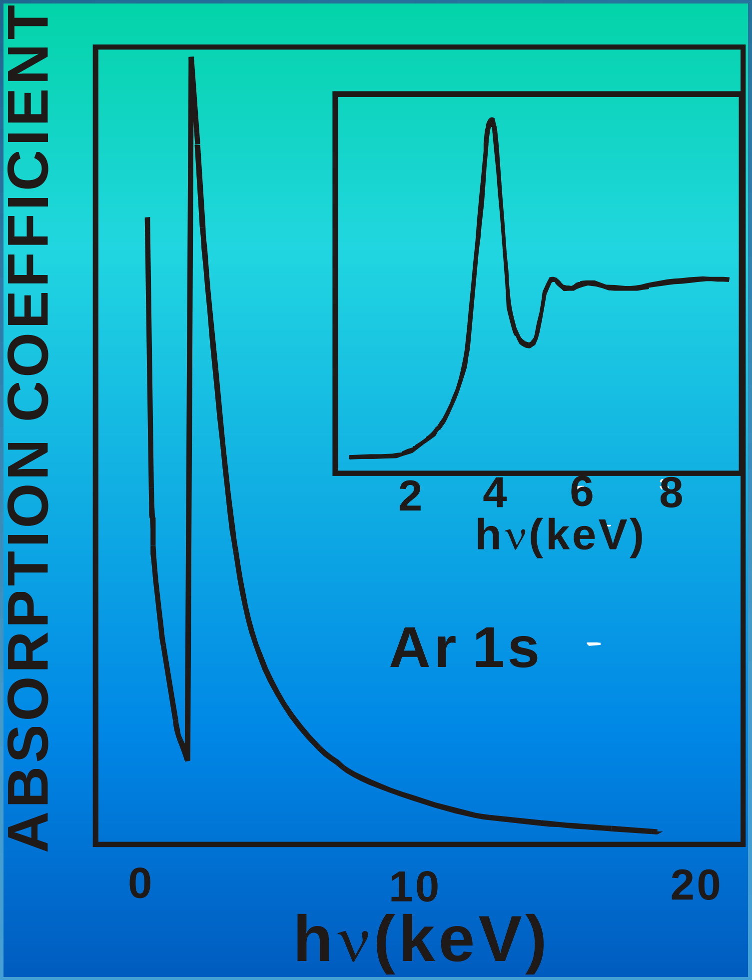

Example of a core-level optical absorption threshold, corresponding to the excitation of the is level in Ar. The inset shows the fine structure near this threshold due to its Rydberg series.

The Delay Onset

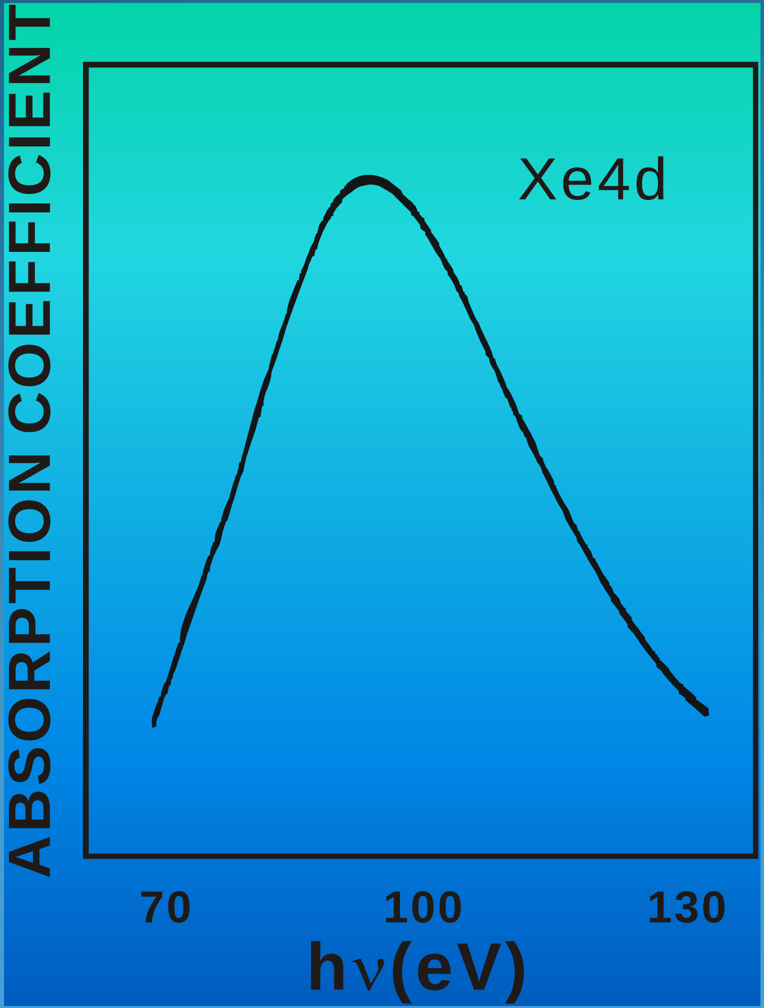

The delayed onset for the excitation of Xe electrons, due to the “centrifugal barrier” which tends to exclude the electrons from the core region.

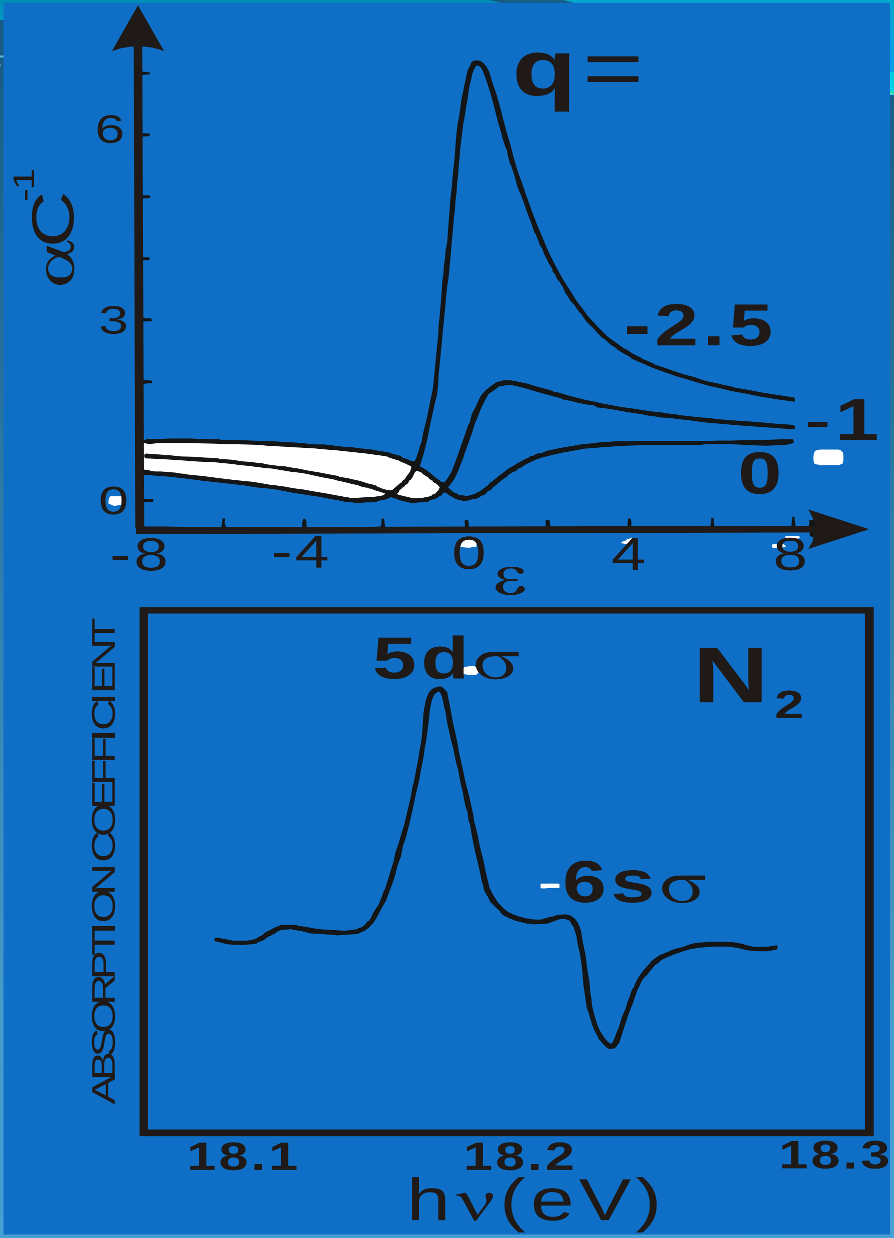

q=
αC^{-1}
6
3
0
-2.5
-1
0
-8
-4
0
4
8
ε
ABSORPTION COEFFICIENT
5dσ
N_2
6sσ
18.1
18.2
18.3
hν(eV)

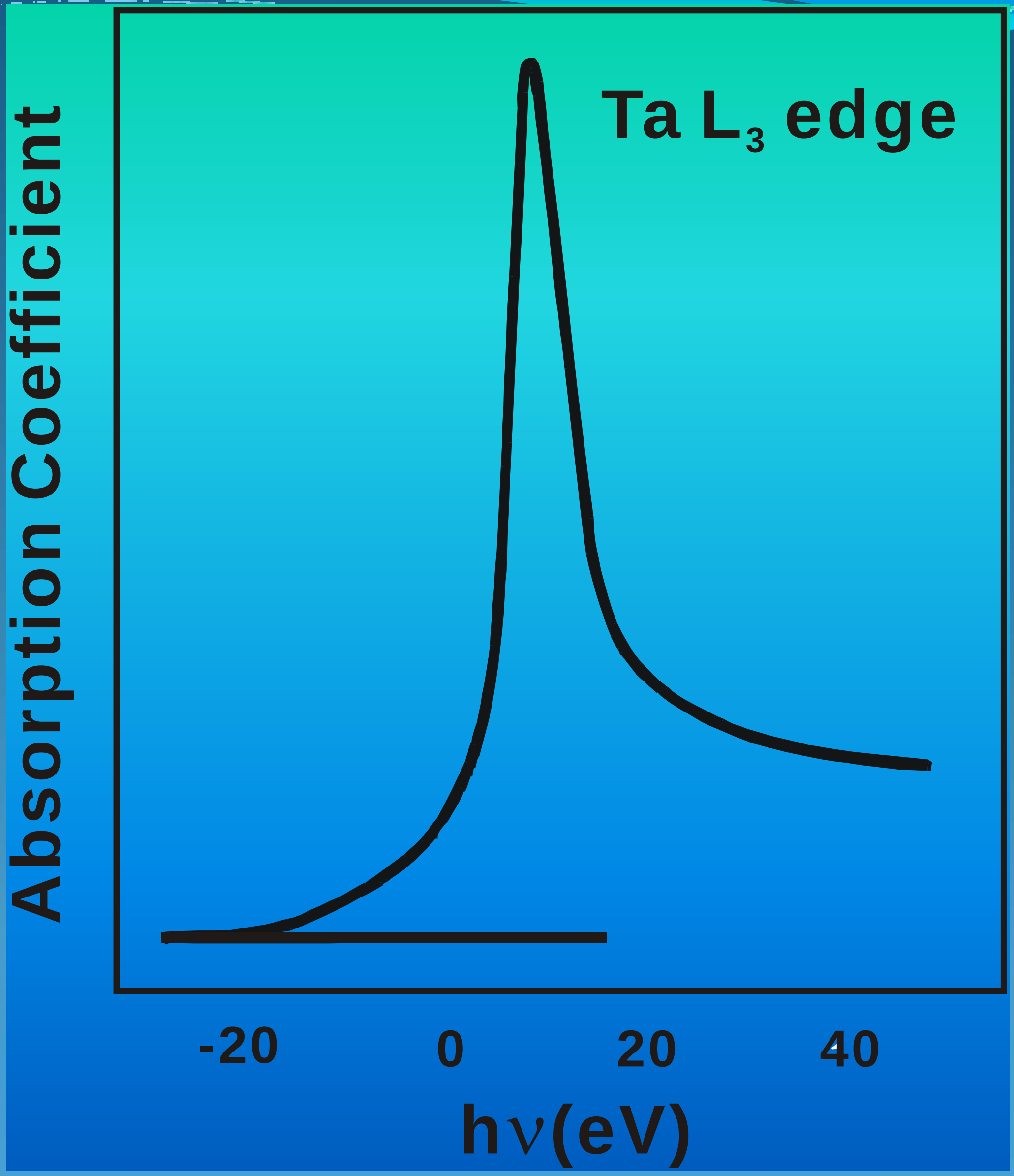
Ta L3 edge
Absorption Coefficient
-20
0
20
40
hν(eV)

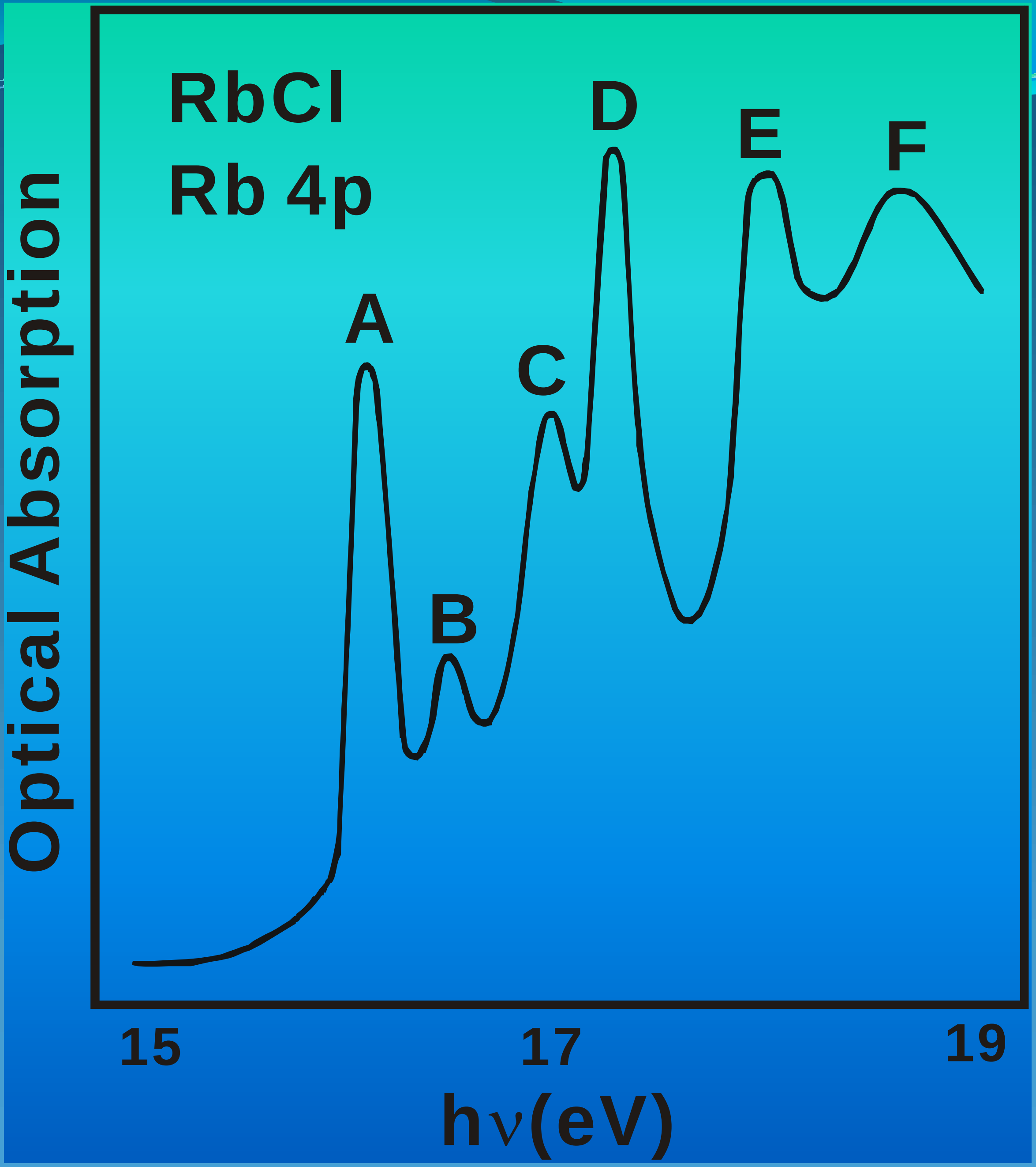

RbCl
Rb 4p
A
B
C
D
E
F
Optical Absorption
15
17
19
hν(eV)

Photoemission Spectroscopy

- General description
- “Electronic” Structure and Properties
- Gas phase—Atomic and Molecular process
- Solid state
  - 3 step description
  - Retrieving “initial” state information from final “free” electron state

Available information in the final free electron state

- Plan wave final state: $$\left|\psi_f^V\right\rangle = A_0 e^{i\boldsymbol{k_0}\cdot r}$$
- Kinetic Energy, E_k ($E_k = p^2/2m$)
- Momentum, $\boldsymbol{p} = \hbar \boldsymbol{k_0}$
- Spin

Electron Energy Analyzer

Cylindrical Mirror Analyzer

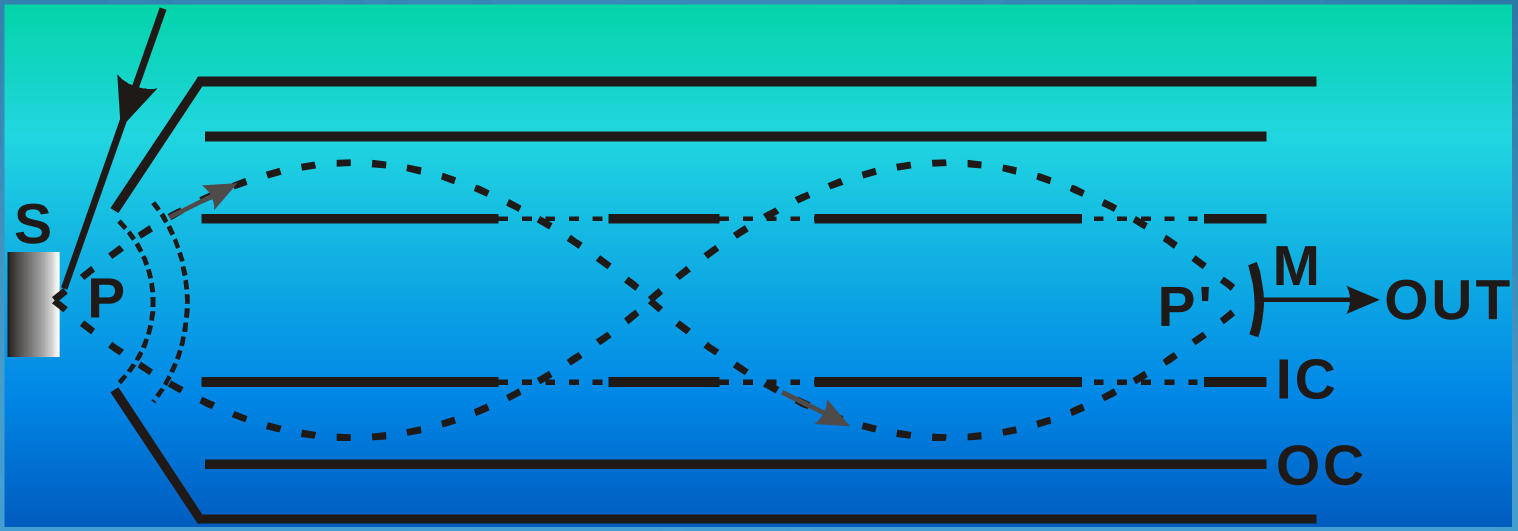

Hemispherical Analyzer

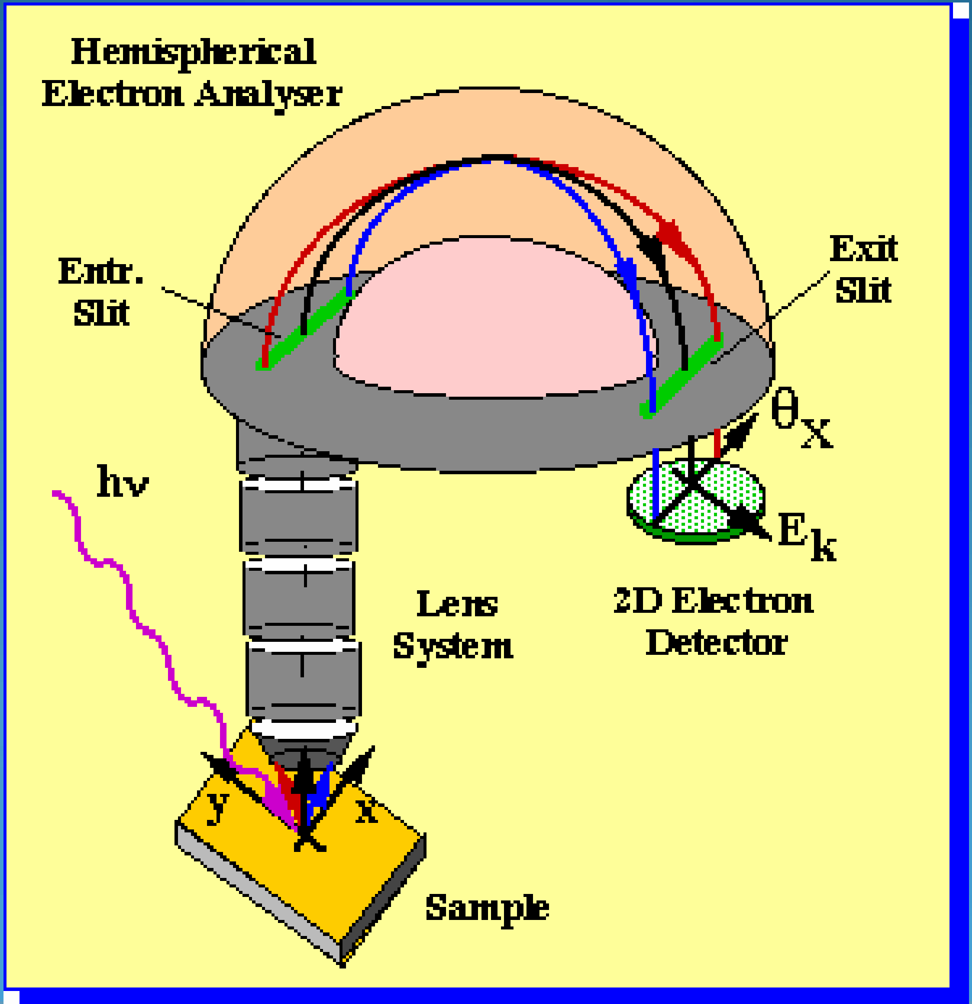

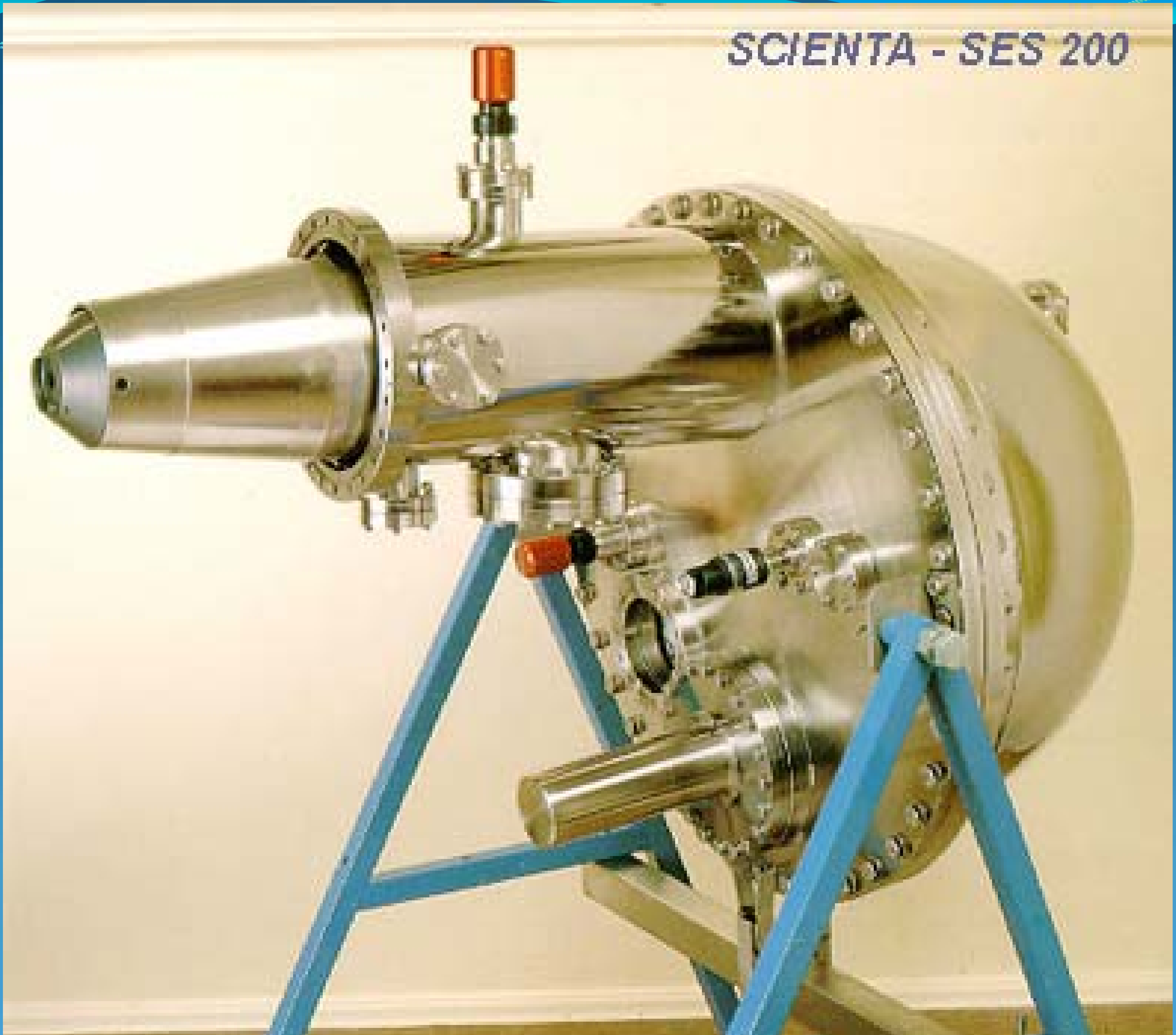
SCIENTA - SES 200

Photoelectro Energy Spectrum

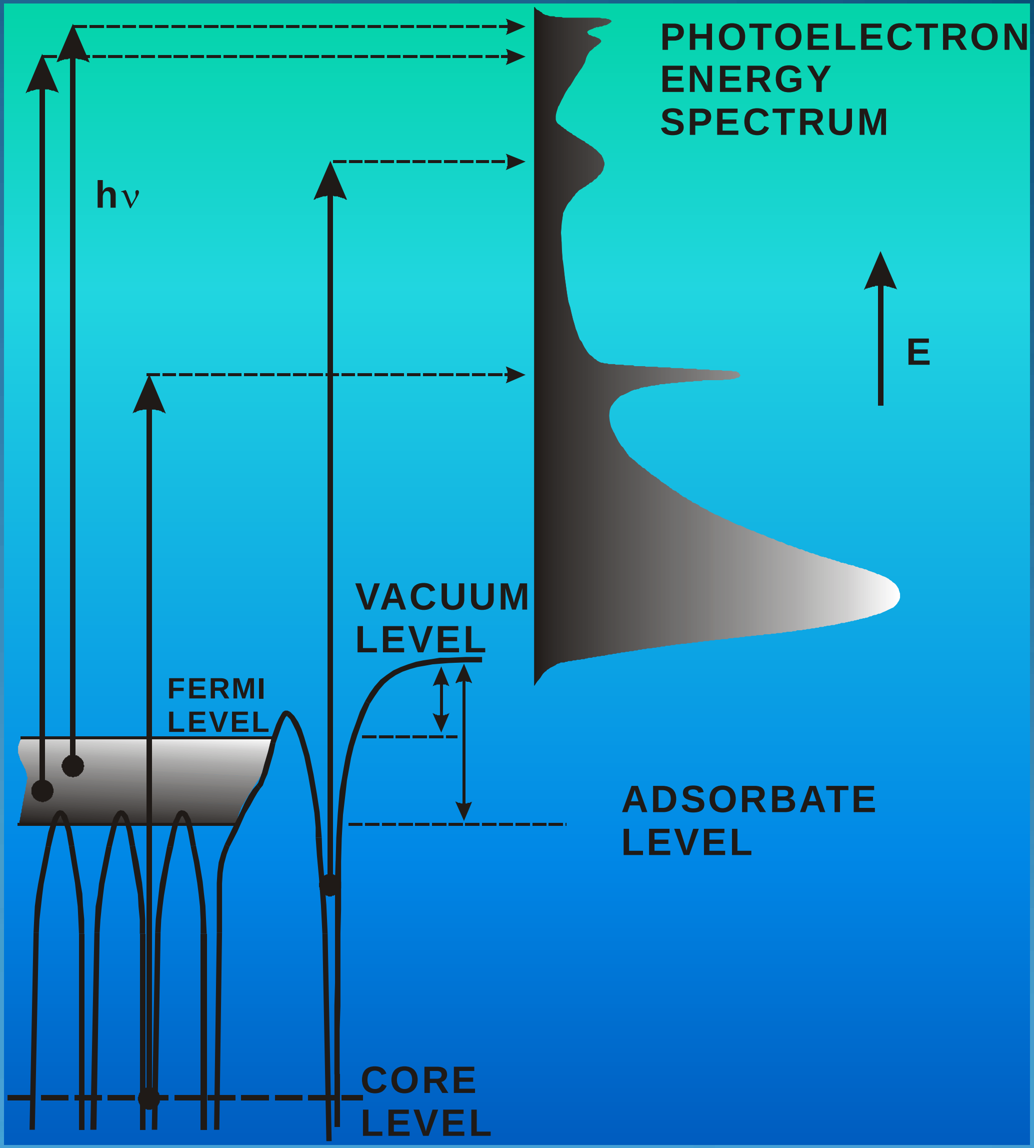

Photoemission Process

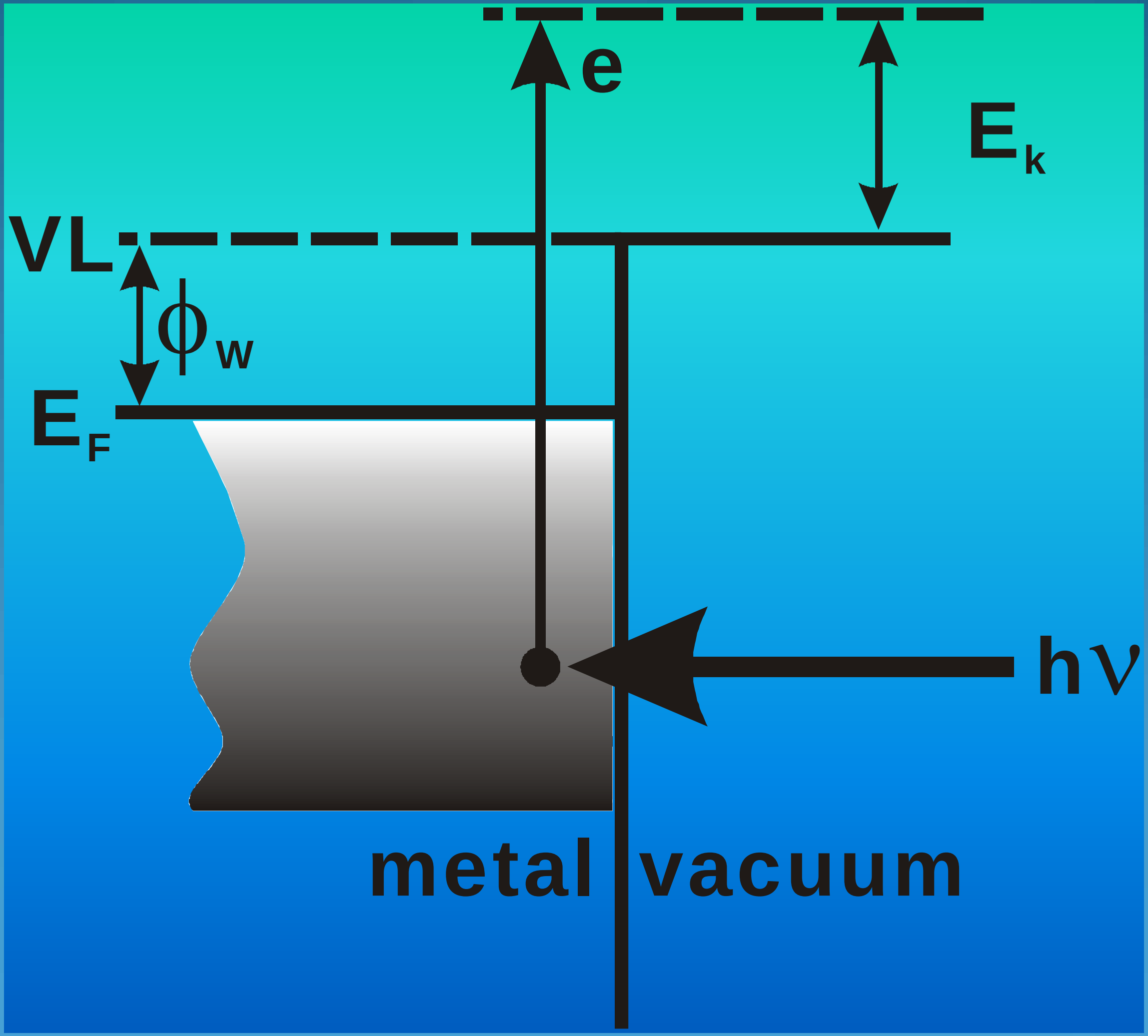

Angular dependence in PES

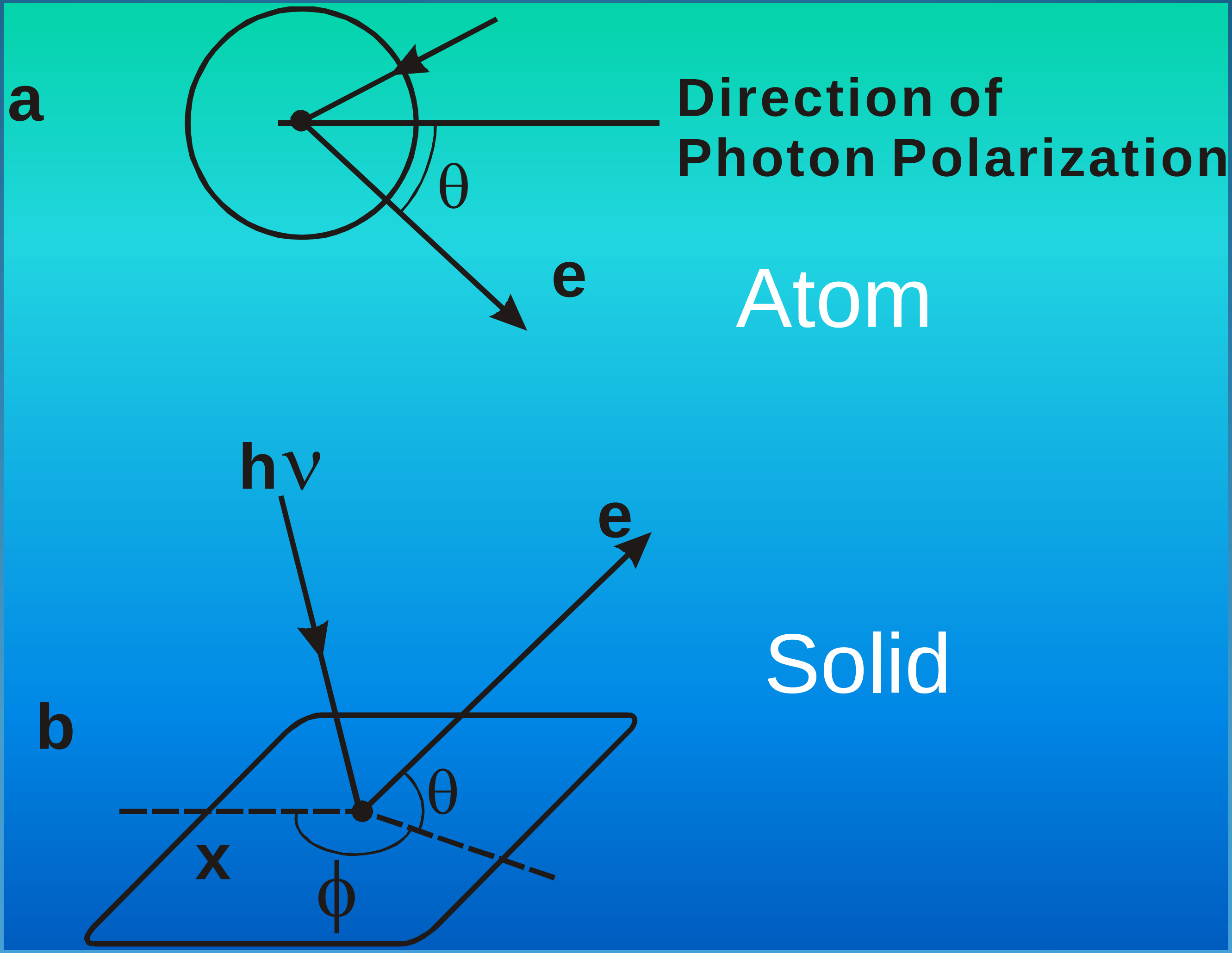

Total Photoionization Cross Section

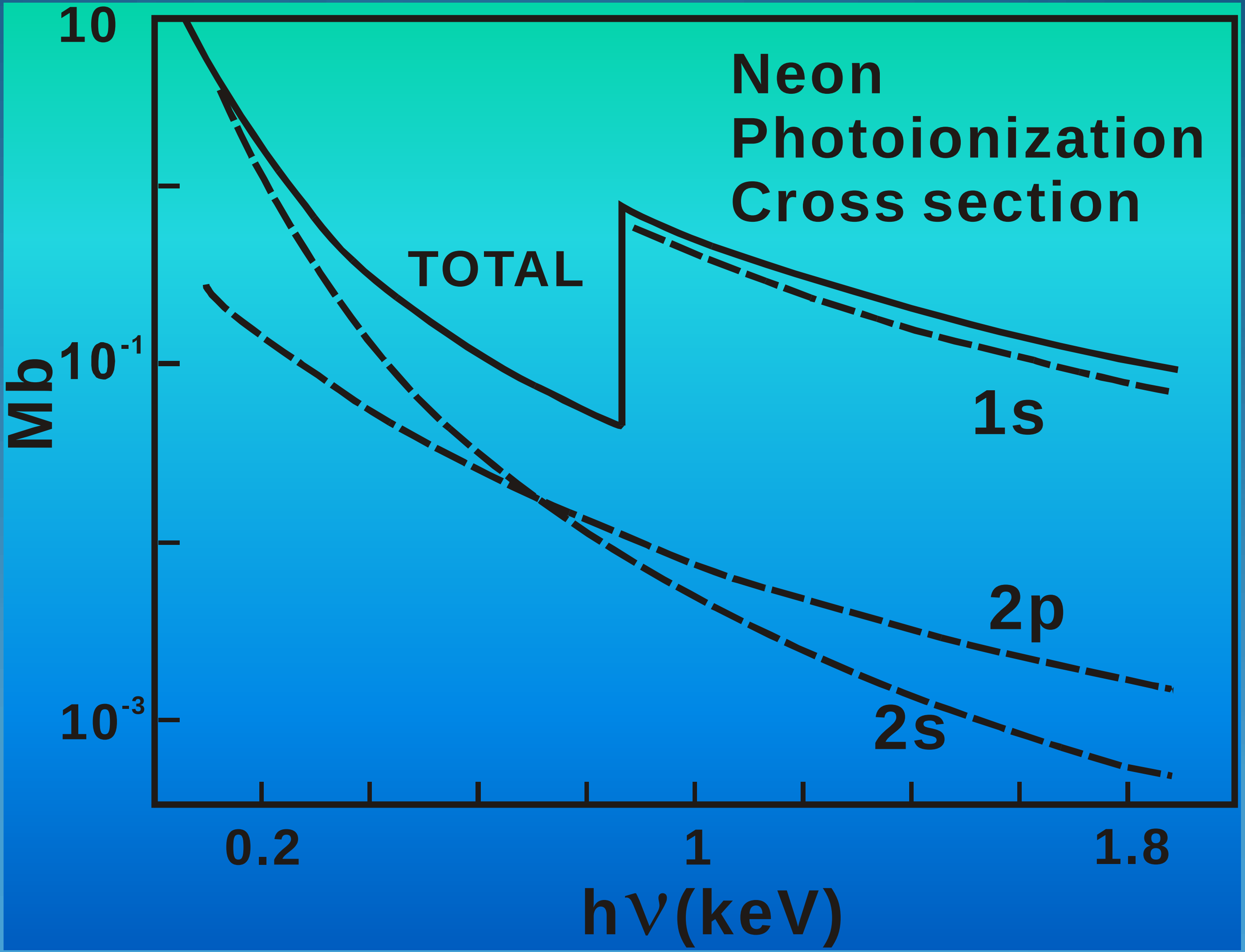

Cooper Minimum

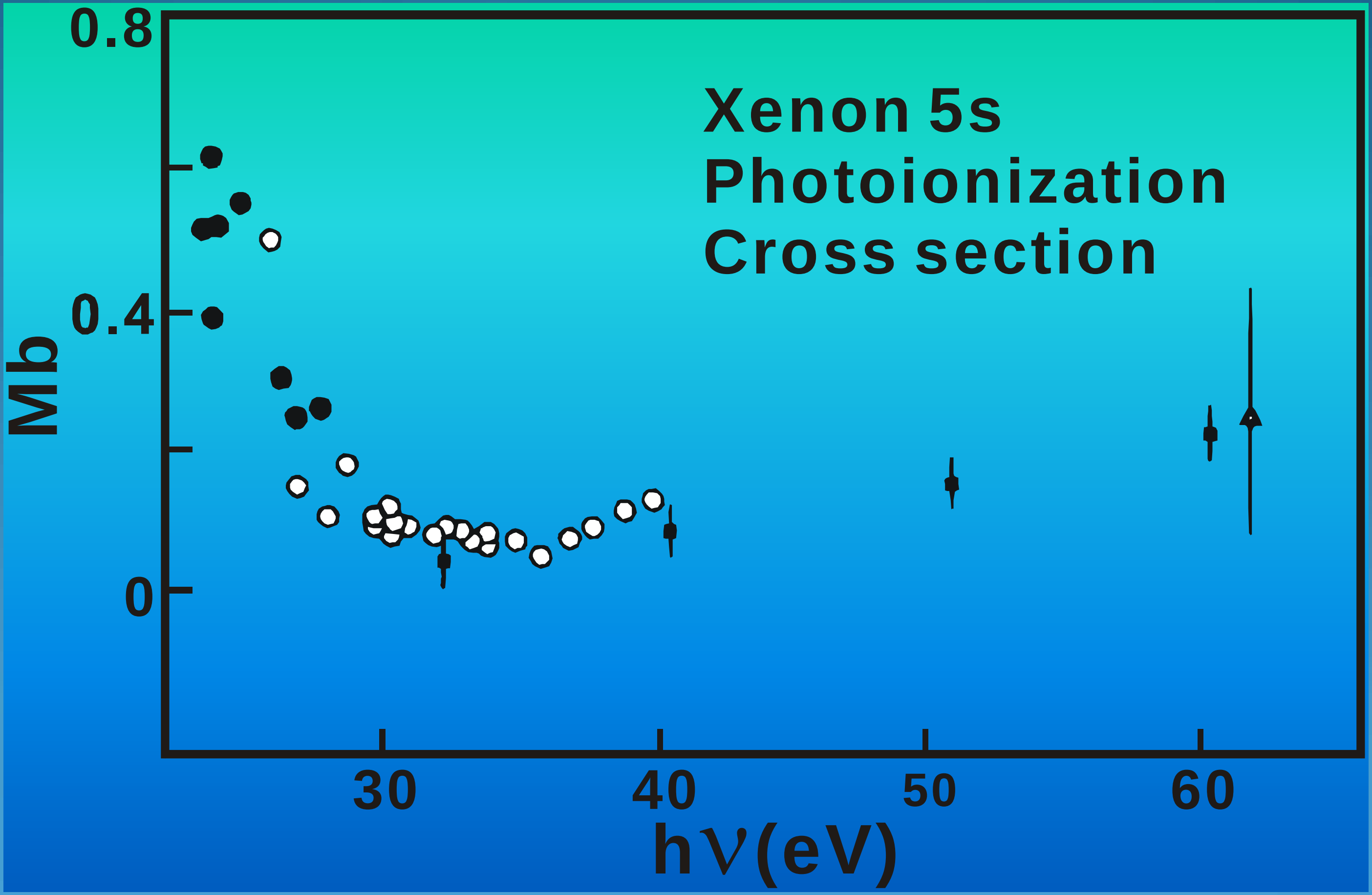

Photoemission Resonance

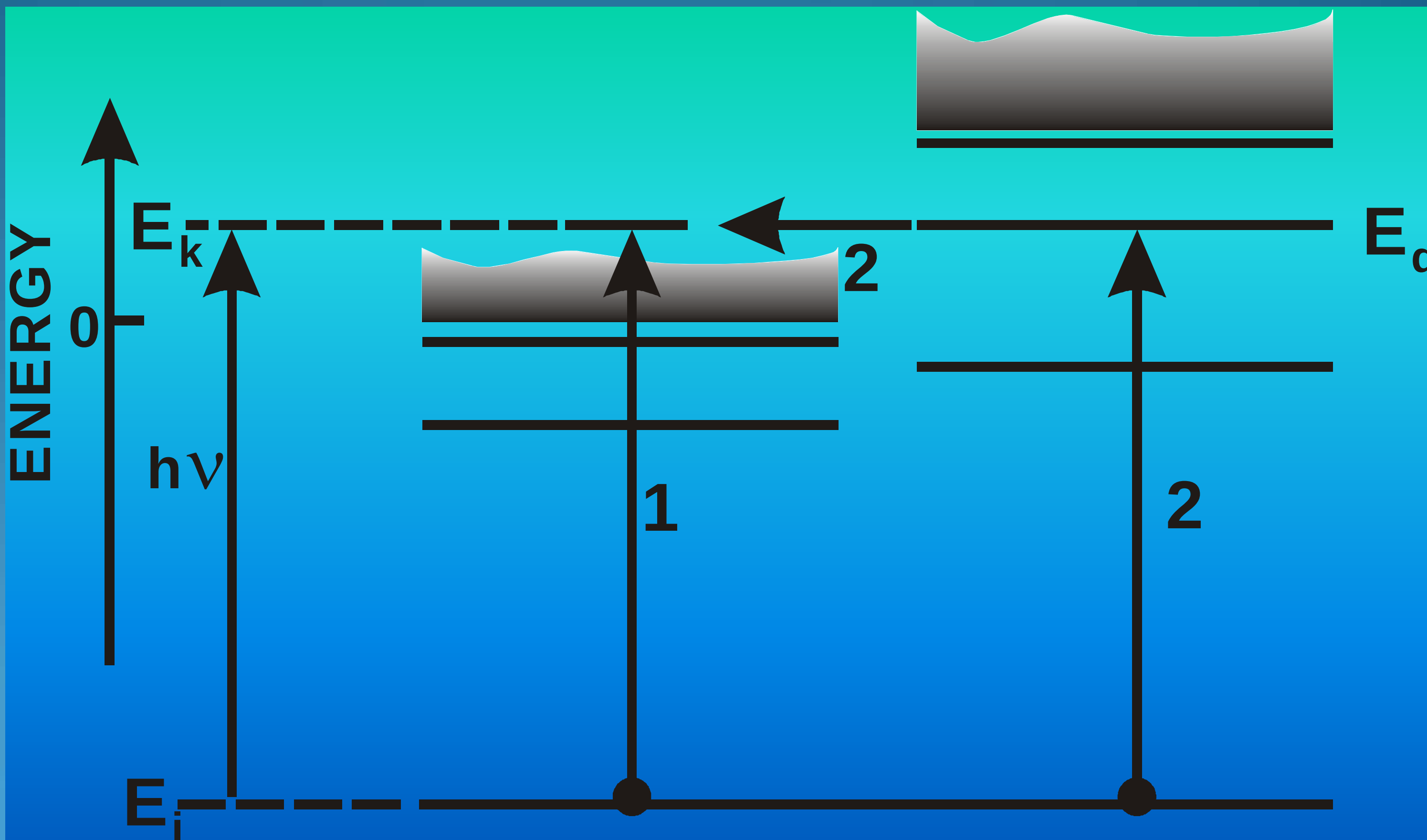

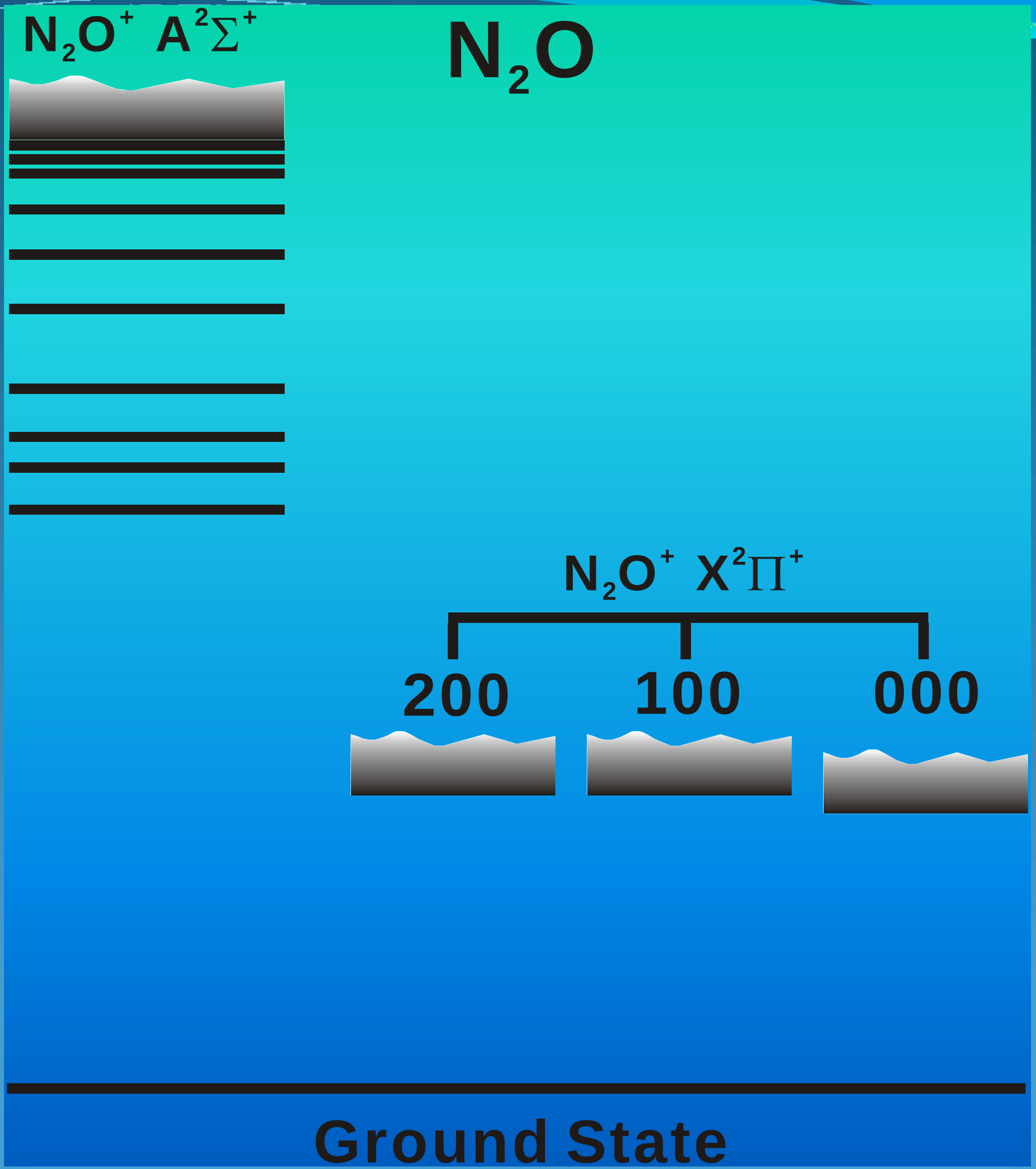
N2O+ A2Σ+
N2O
N2O+ X2Π+
200
100
000
Ground State

N_2O^+ $X^2\Pi^+(100)$ Resonance

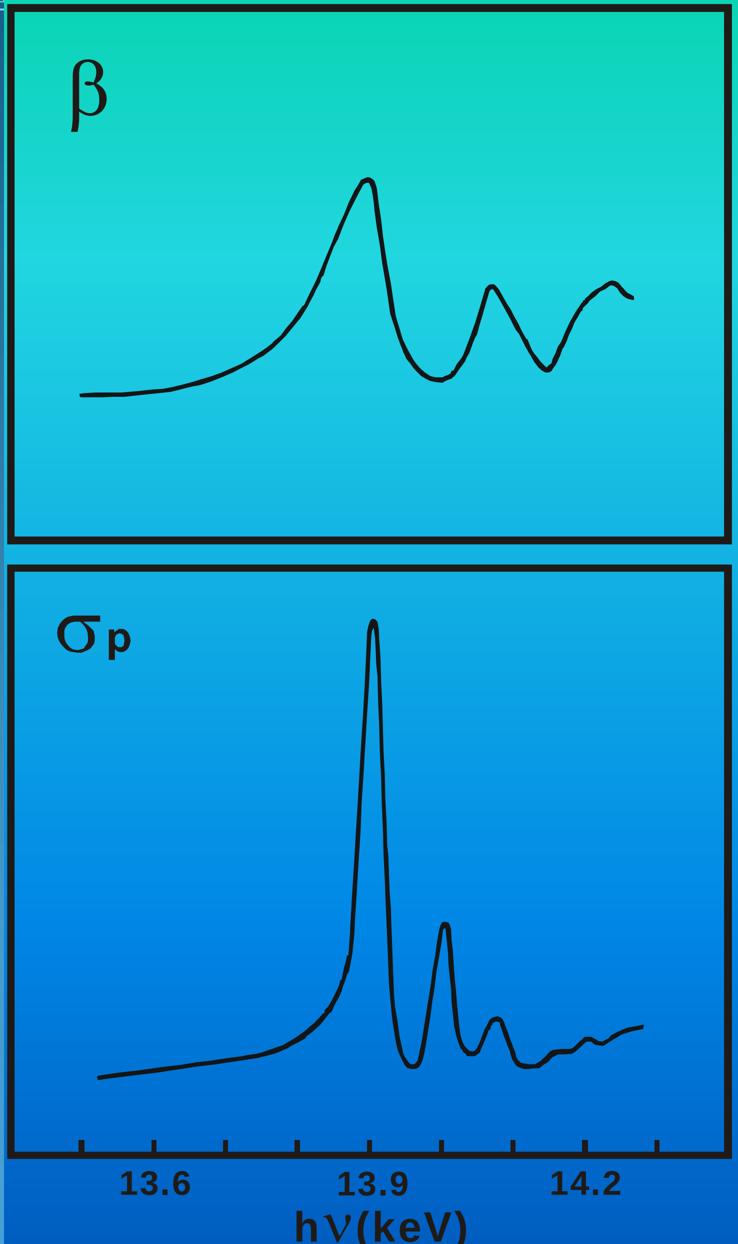

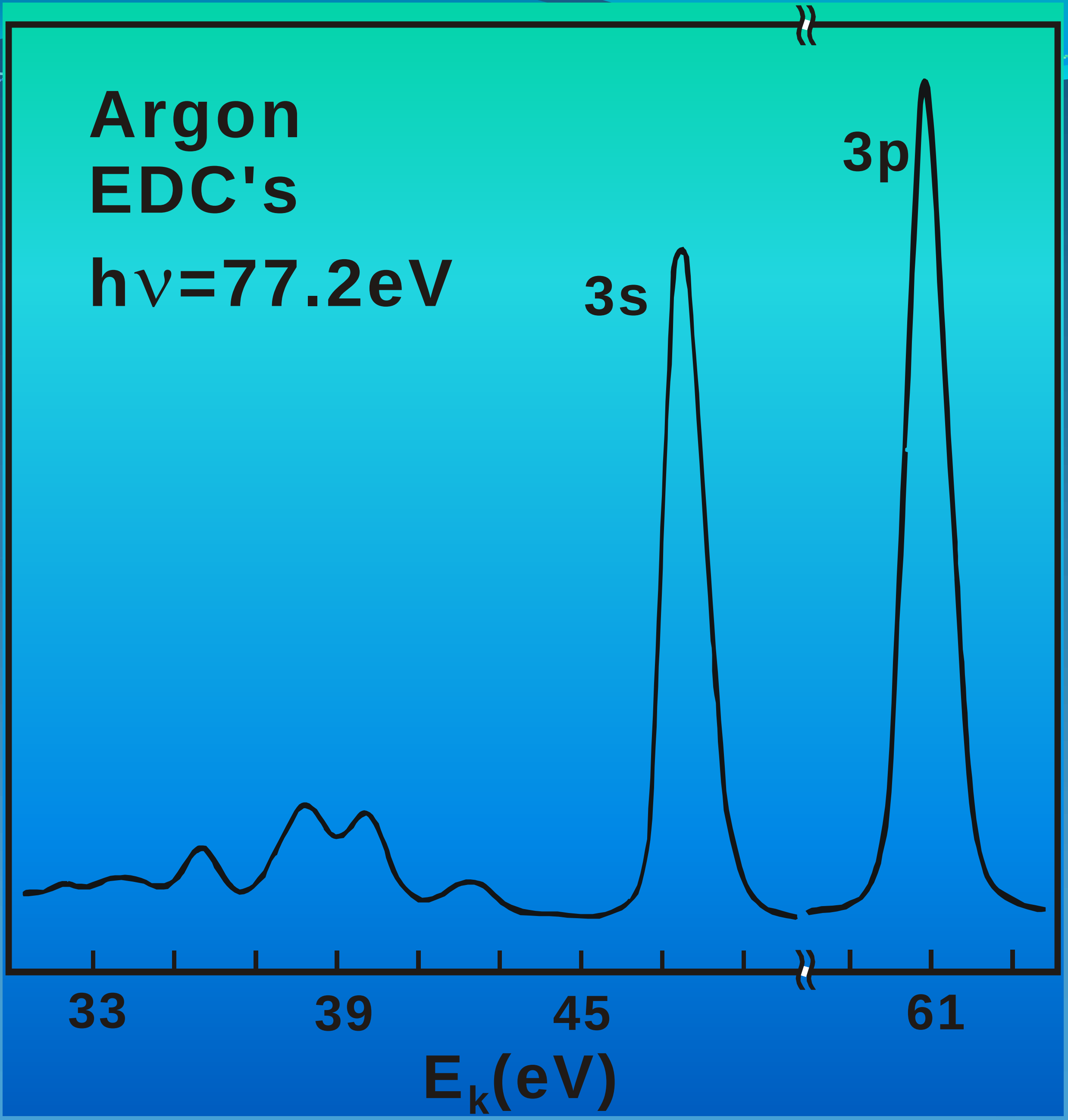
Argon
EDC's
hν=77.2eV
3s
3p
33
39
45
61
E_k(eV)

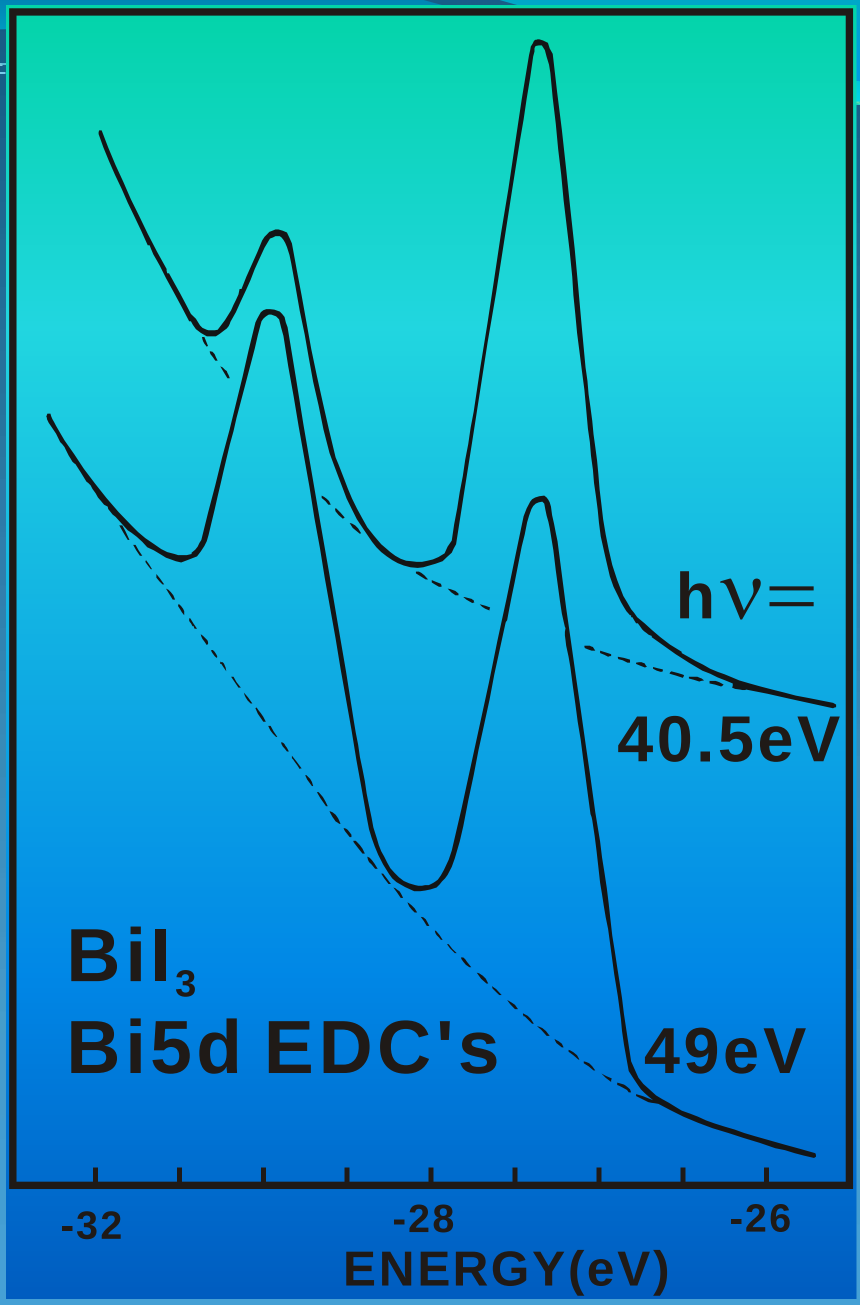

hν=
40.5eV
BiI3
Bi5d EDC's
49eV
-32
-28
-26
ENERGY(eV)

PES in Solid

- Extreme Surface Sensitivity
- EDC (Energy Distribution Curve) vs. DOS (Density of States)
- Bulk Solids
- Surface & Interfaces
- Photoelectron diffraction (PhD) and photoelectron holography

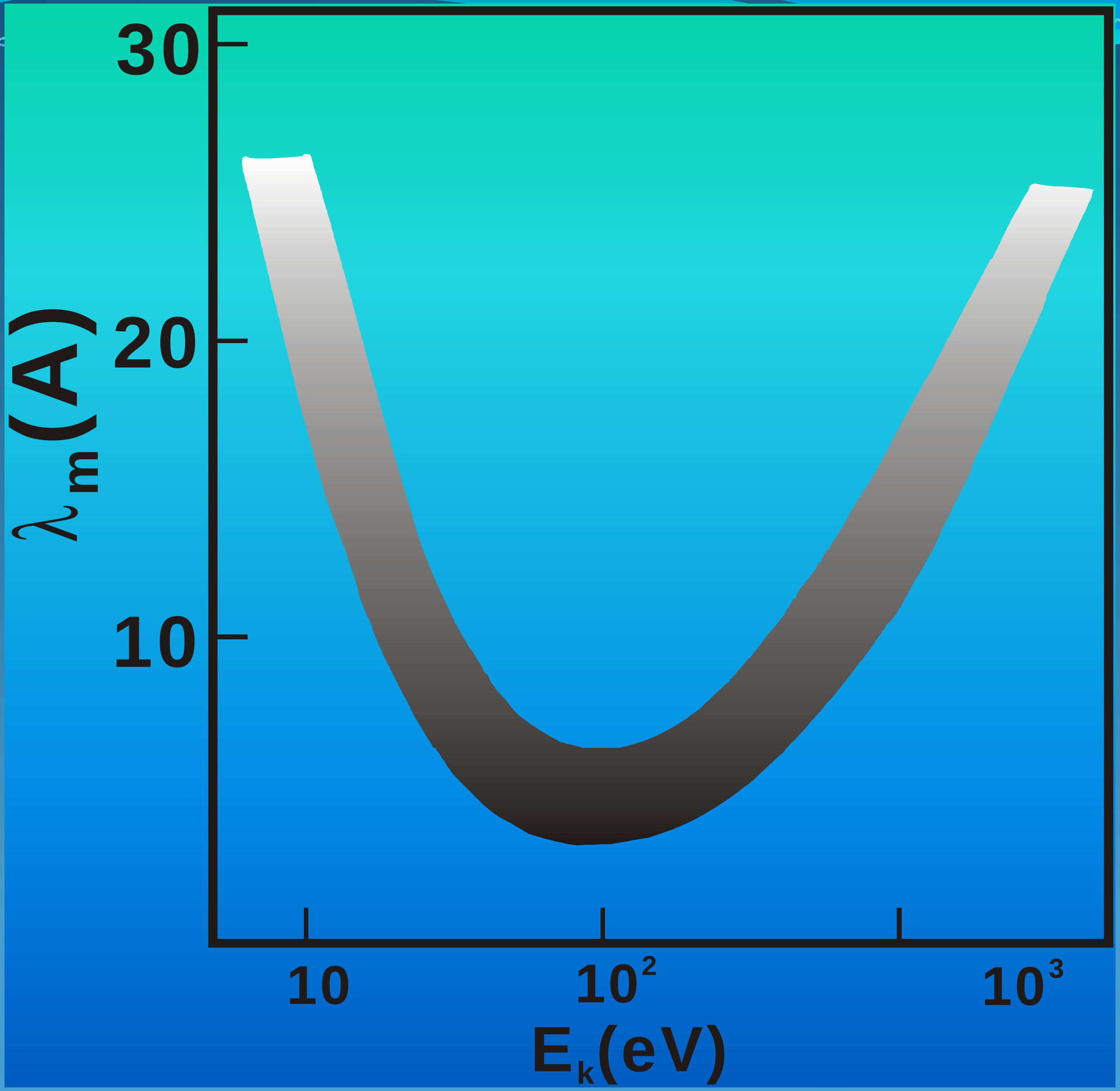

30
20
10
λm(A)
10
10²
10³
Ek(eV)

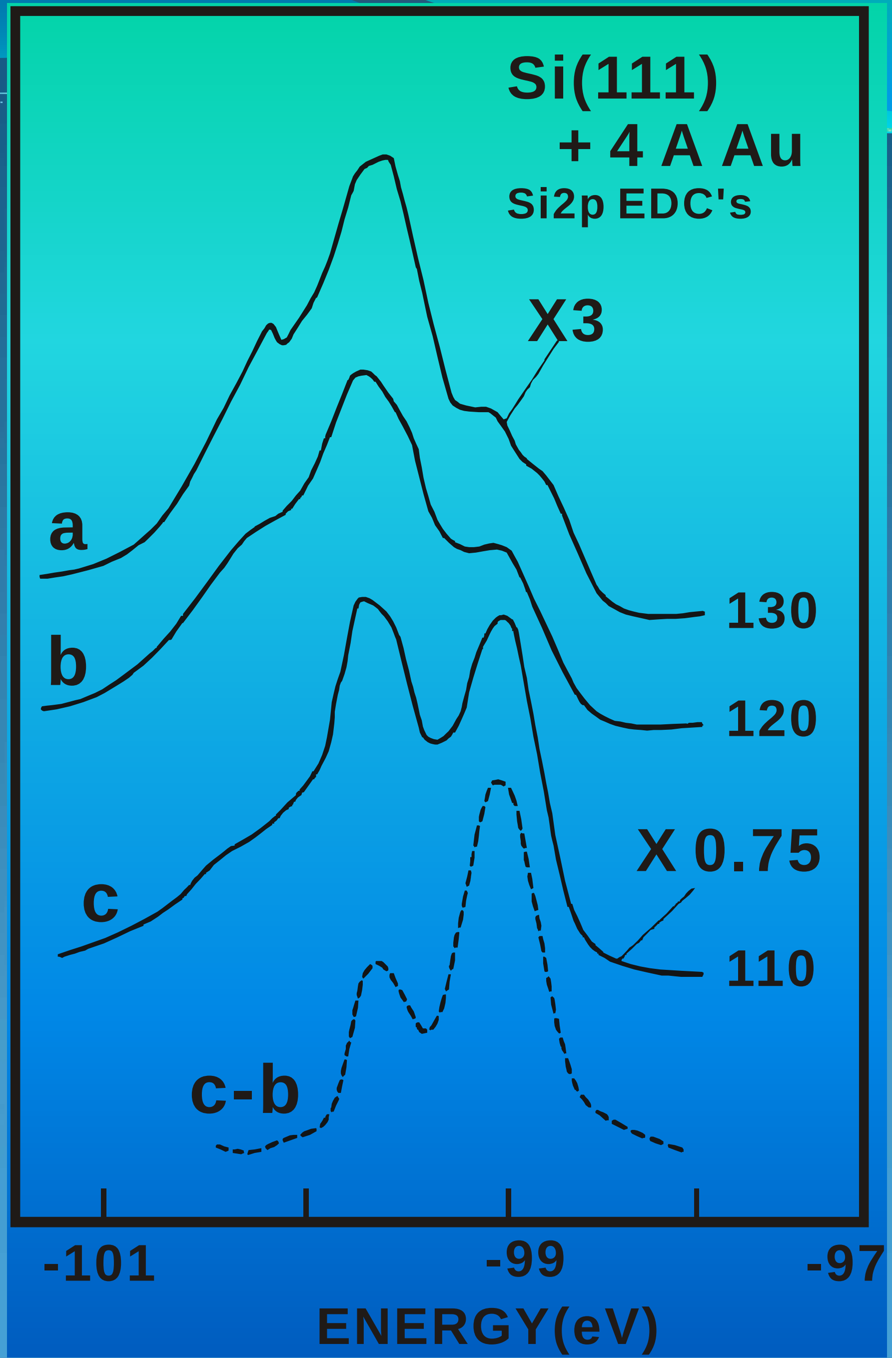
Si(111)
+ 4 A Au
Si2p EDC's
X3
a
b
c
c-b
130
120
X 0.75
110
-101
-99
-97
ENERGY(eV)

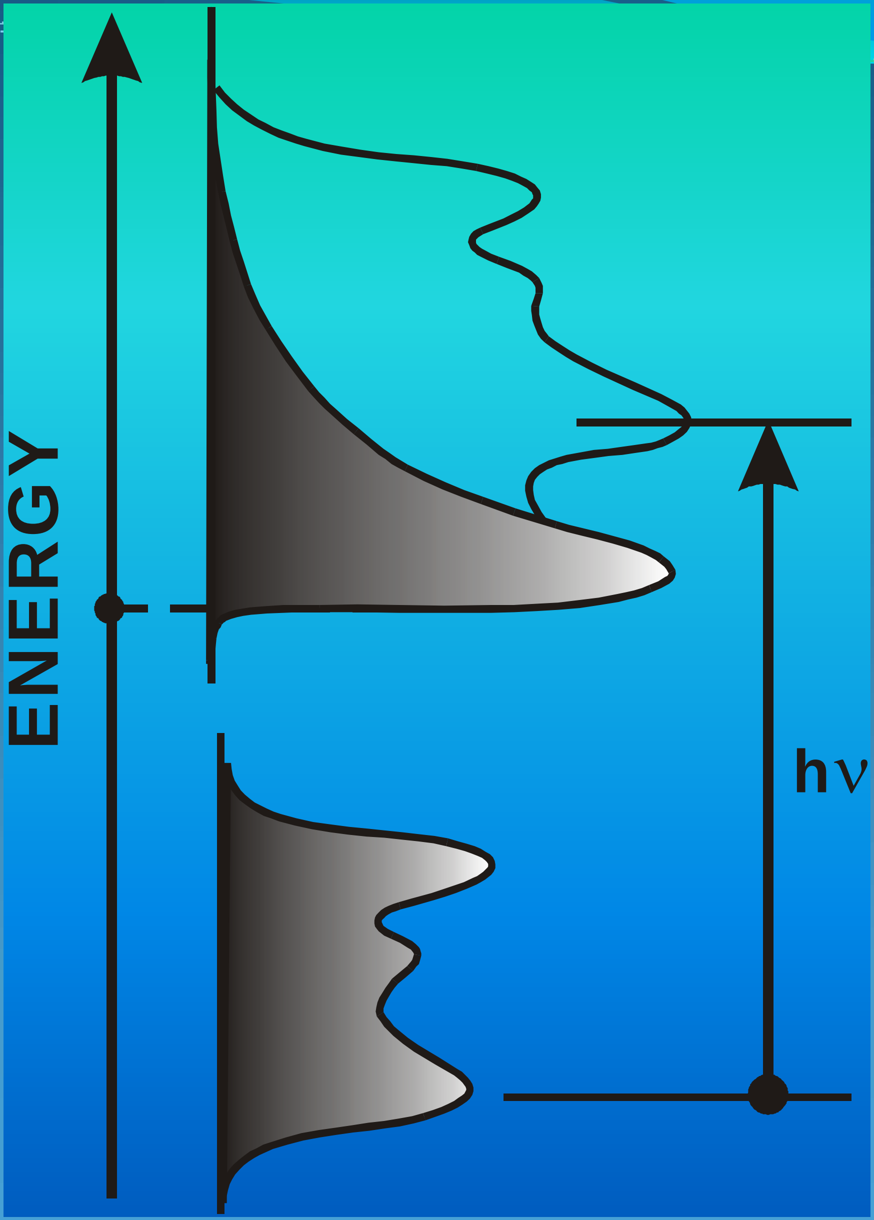
ENERGY
hν

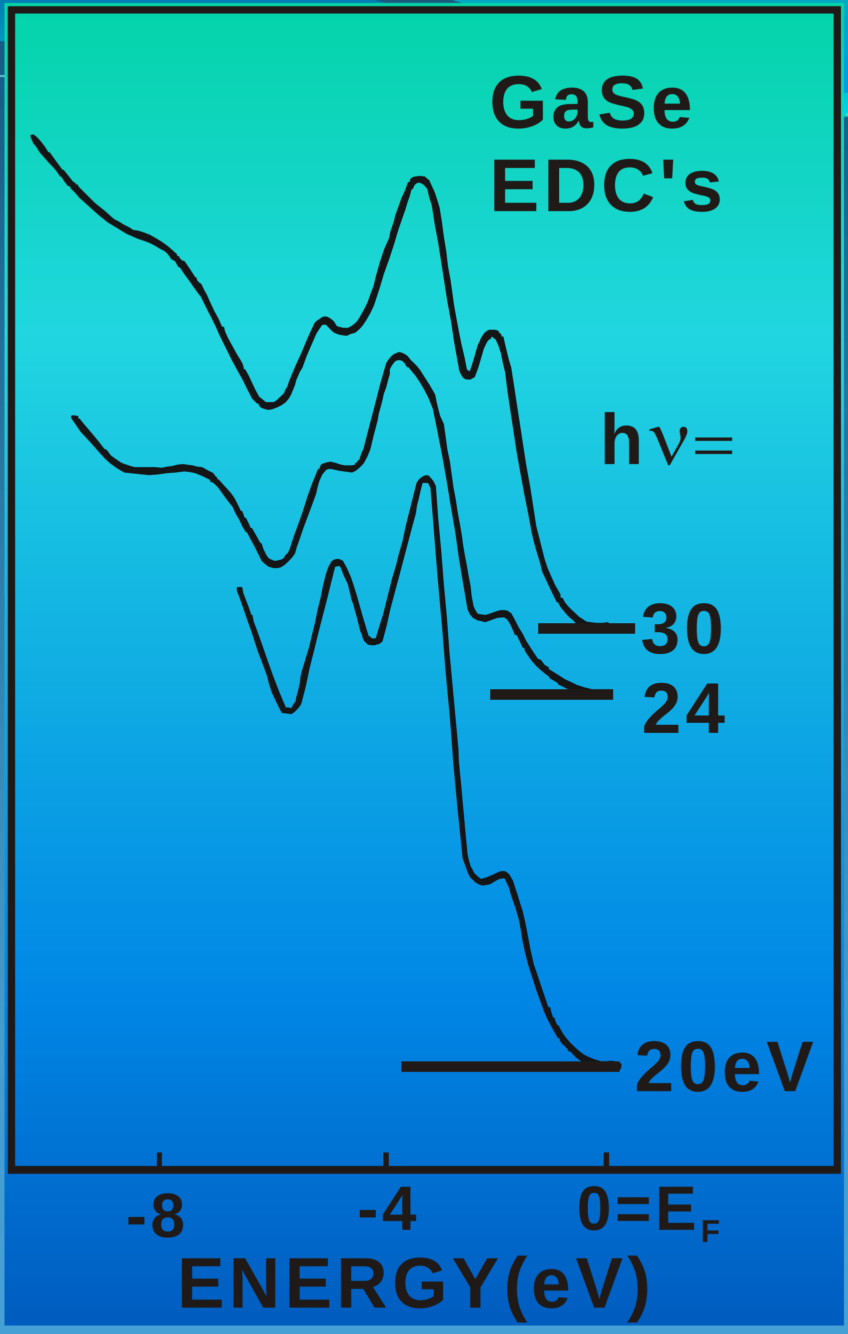

GaSe
EDC's
hν=
30
24
20eV
-8
-4
0=E_F
ENERGY(eV)

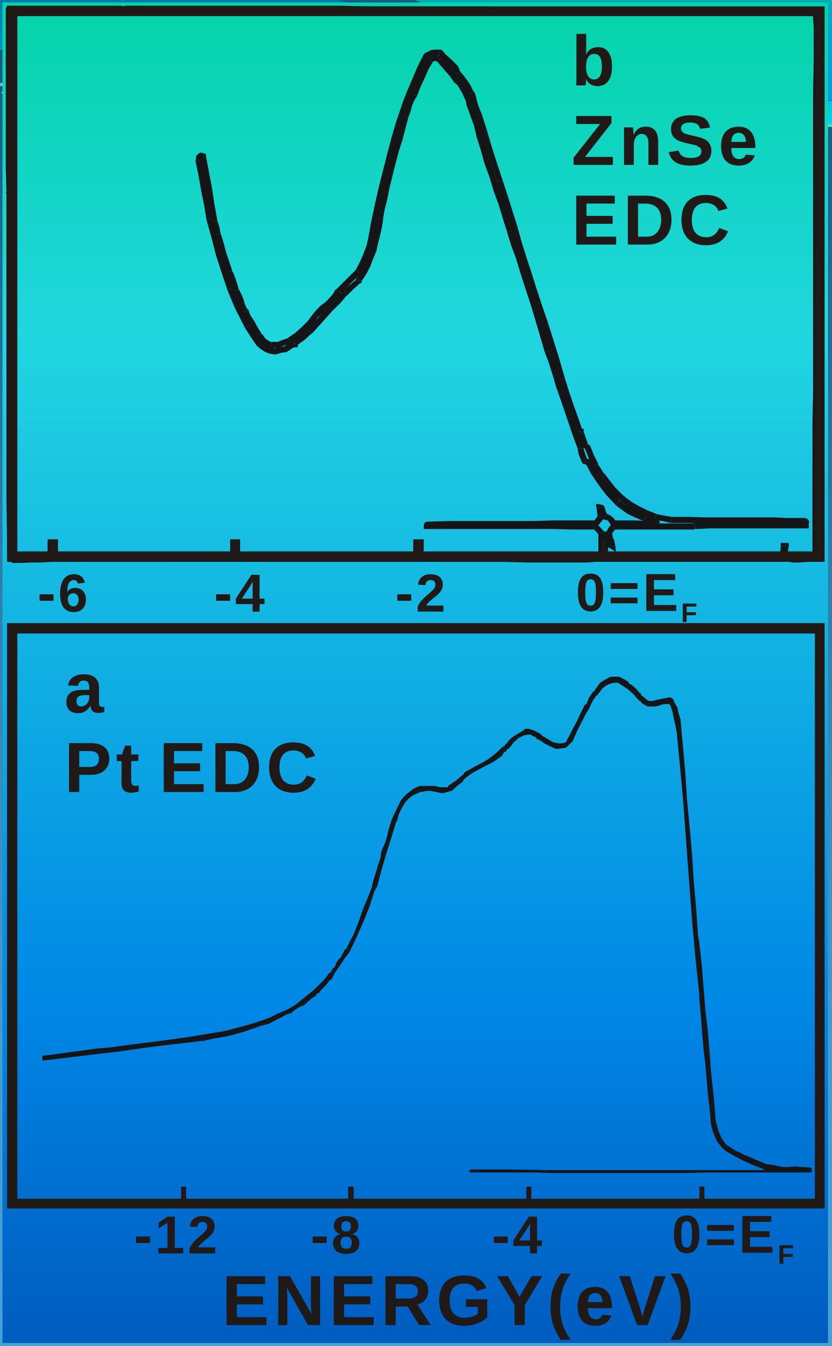

b
ZnSe
EDC
-6
-4
-2
0=E_F
a
Pt EDC
-12
-8
-4
0=E_F
ENERGY(eV)

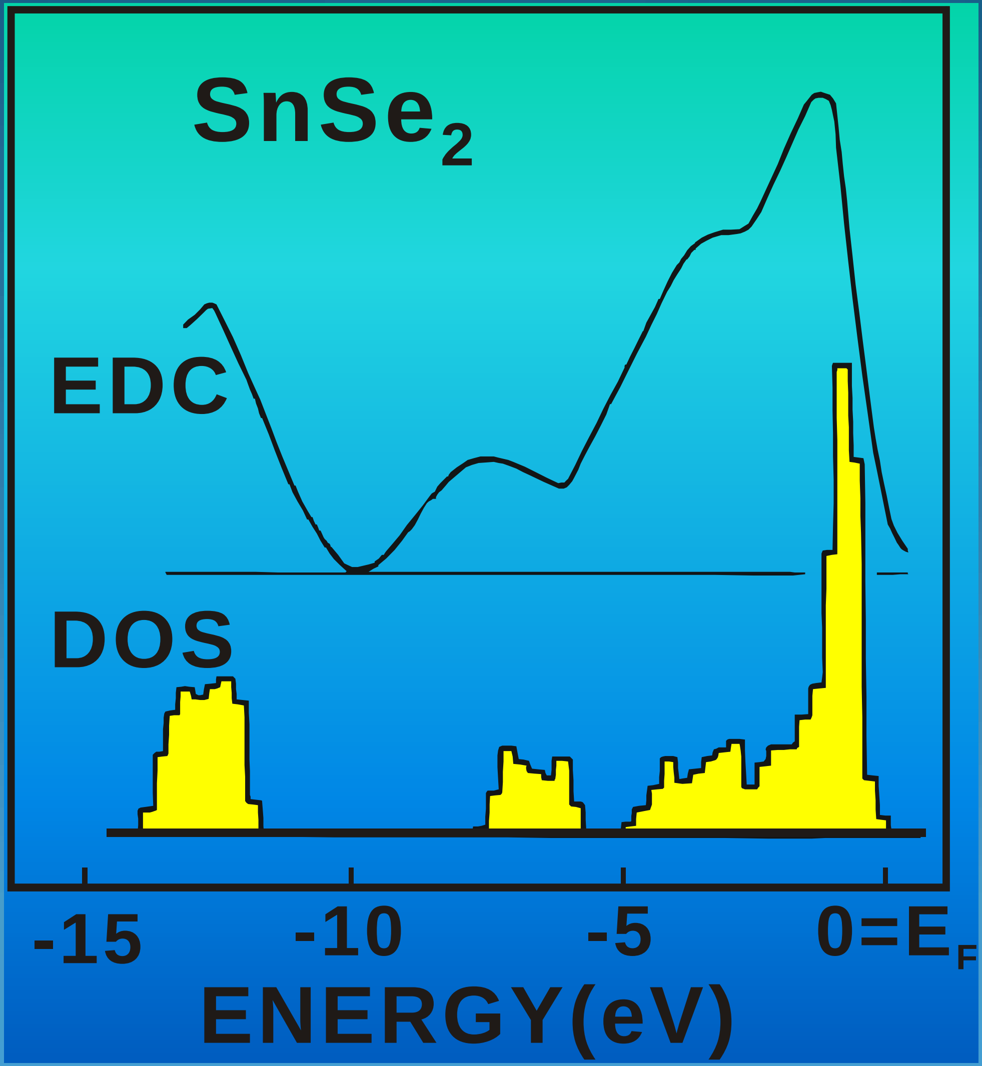

SnSe2
EDC
DOS
-15
-10
-5
0=EF
ENERGY(eV)

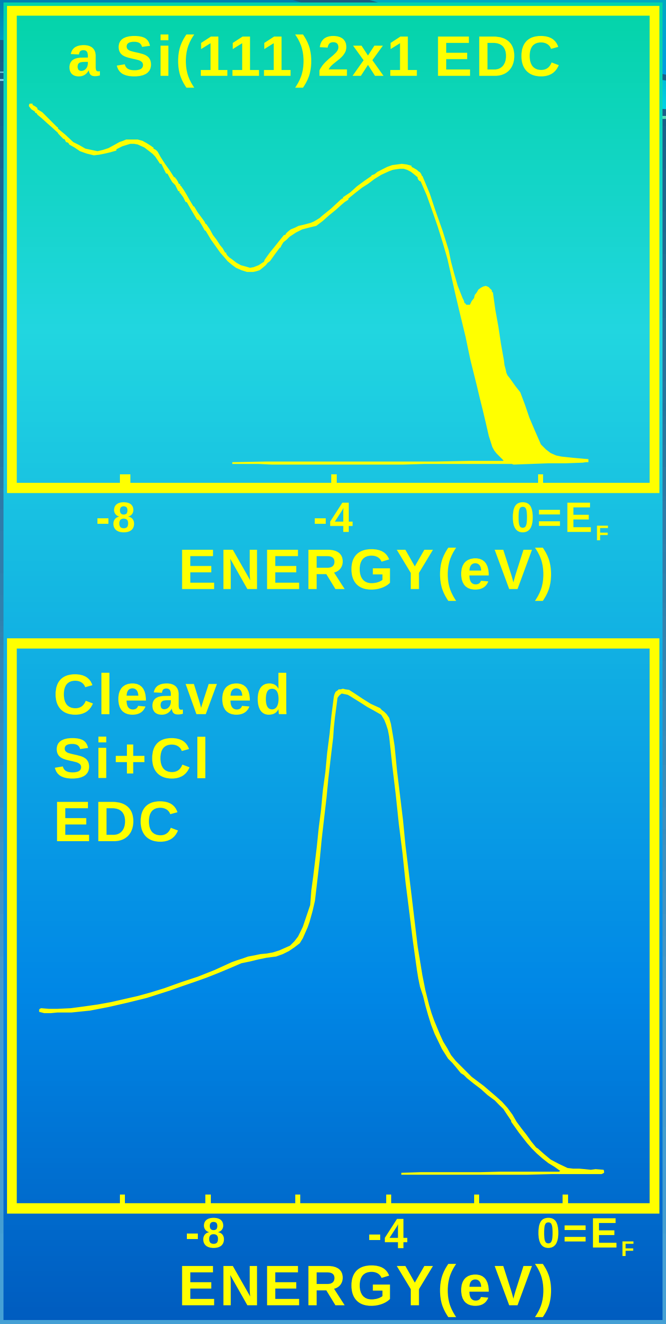

a Si(111)2x1 EDC
-8
-4
0=E_F
ENERGY(eV)
Cleaved
Si+Cl
EDC
-8
-4
0=E_F
ENERGY(eV)

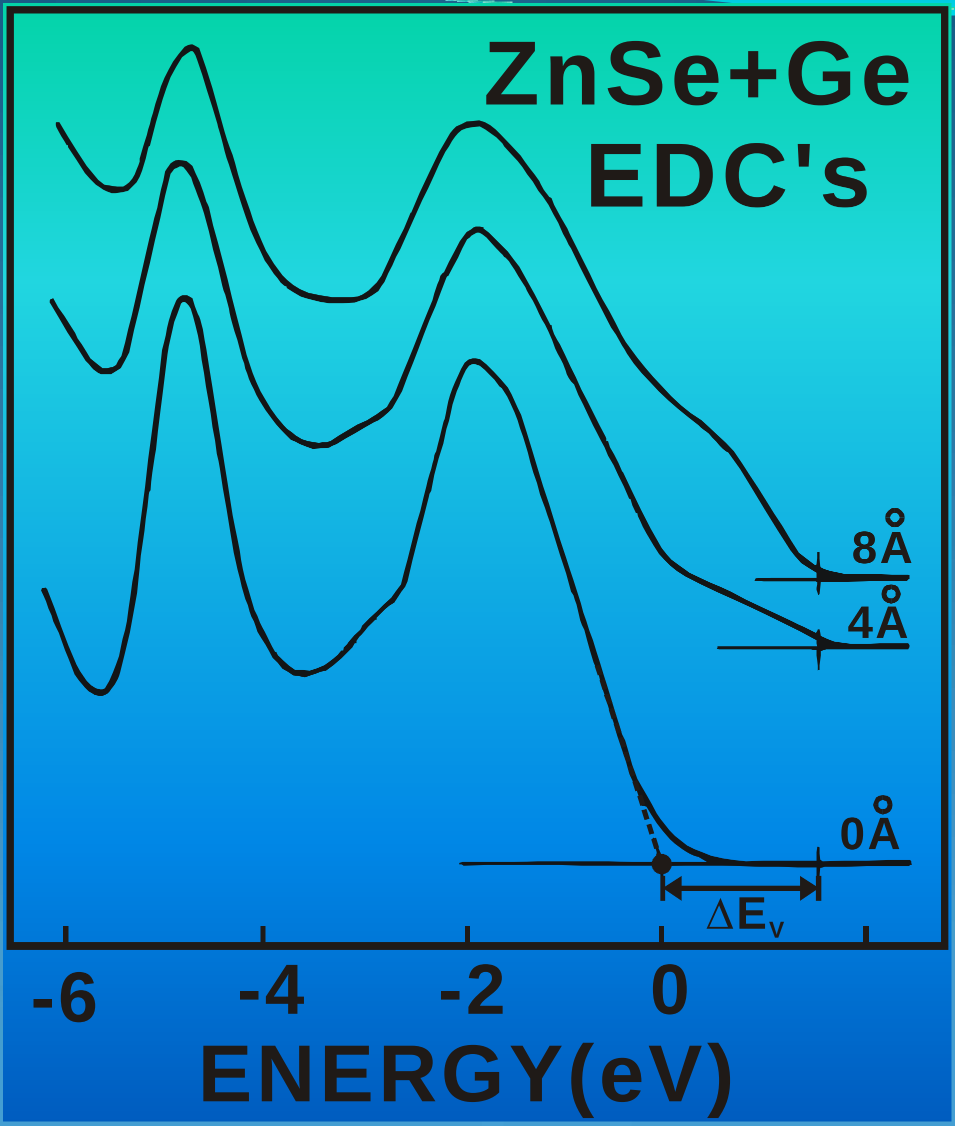
ZnSe+Ge
EDC's
8Å
4Å
0Å
ΔEv
-6
-4
-2
0
ENERGY(eV)

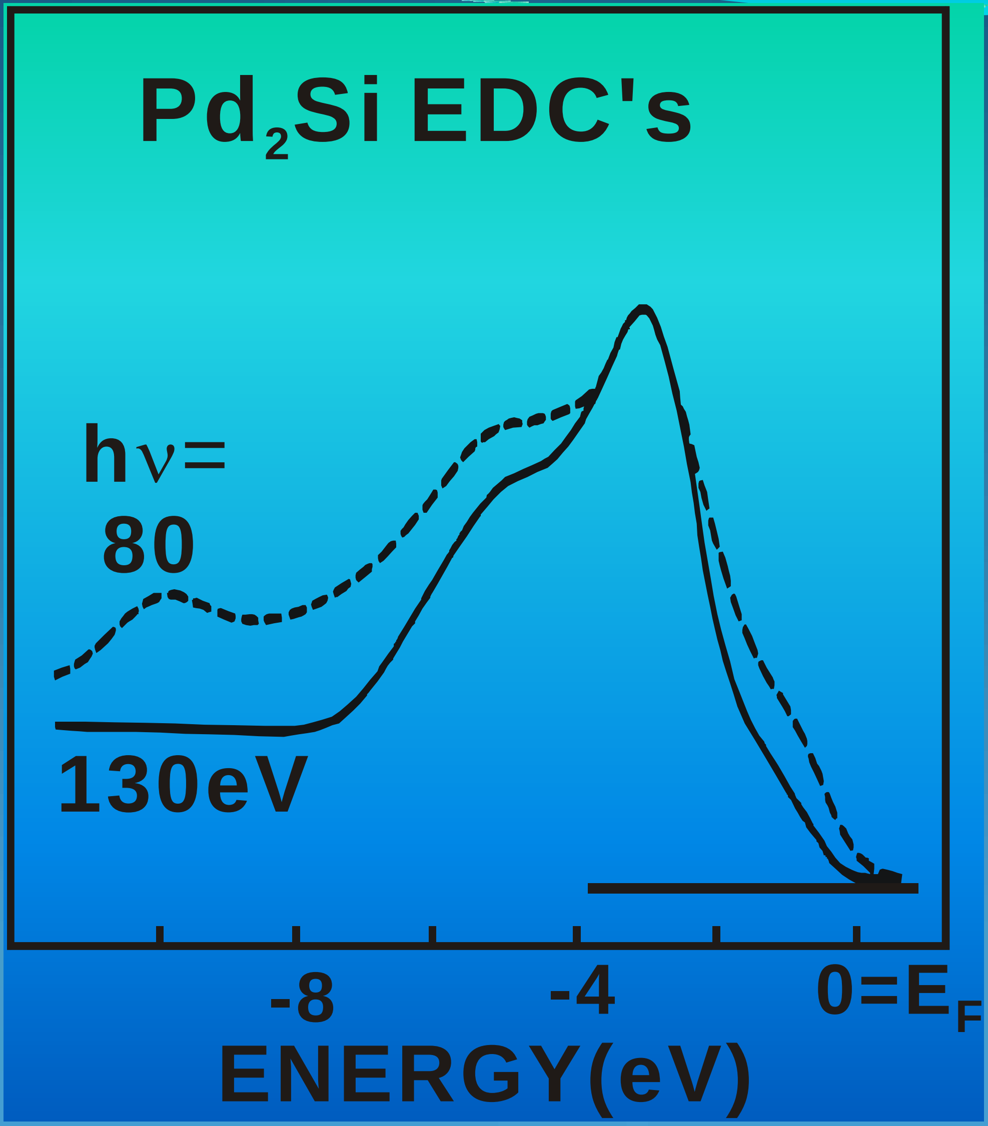

Pd2Si EDC's
hν=
80
130eV
-8
-4
0=EF
ENERGY(eV)

Band Structure Mapping

- ARPES (ARUPS) is the ONLY method to map the band structure in Solid
- The tunability of SR UV reduced the ambiguity of ARUPS in determining the band structure
- High energy and angular (momentum space) resolution has enabled the determination of quasi-particle electronic structure of highly correlated electronic system

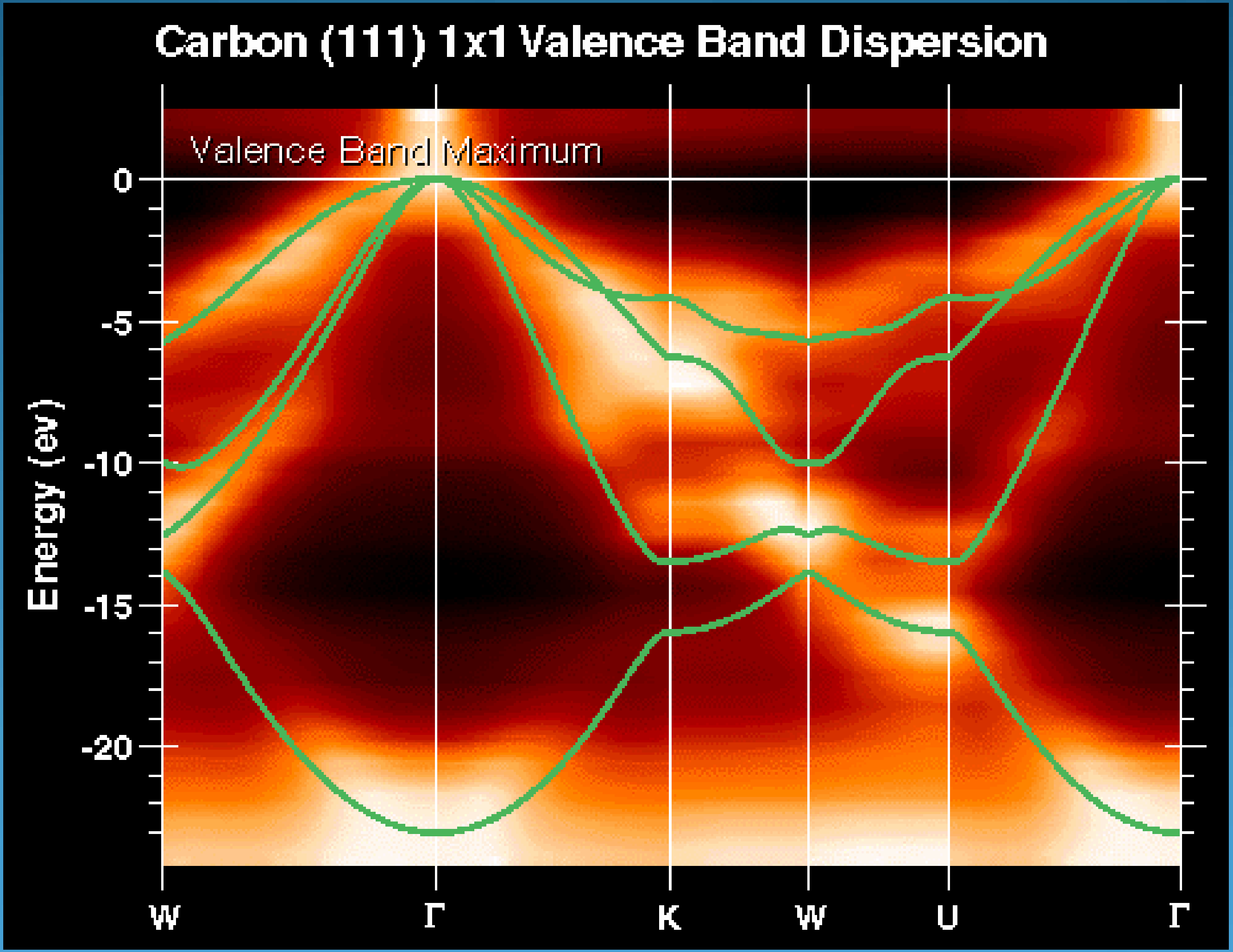

Carbon (111) 1x1 Valence Band Dispersion
Valence Band Maximum
Energy (ev)
0
-5
-10
-15
-20
W
Γ
K
W
U
Γ

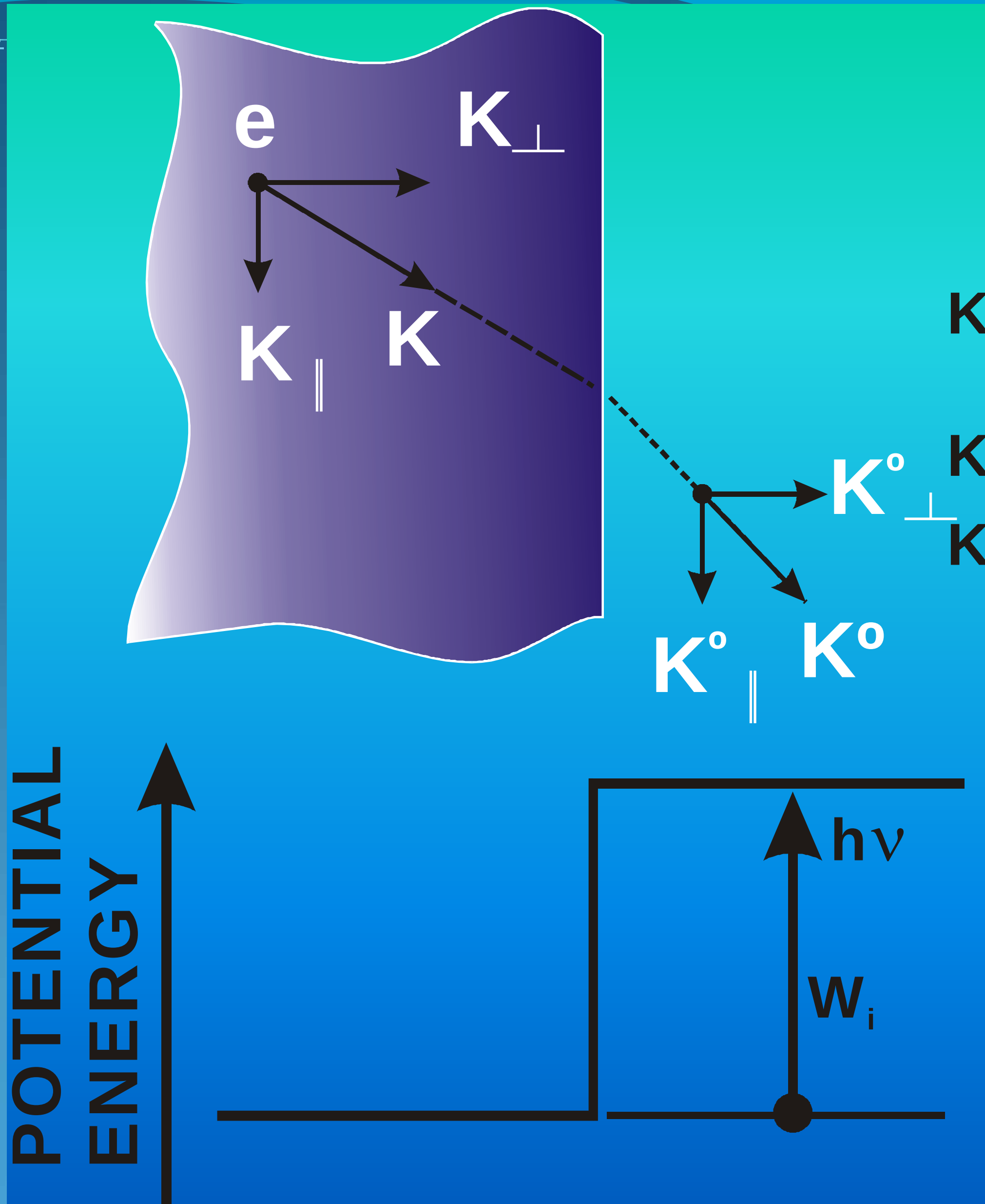

e
K⊥
K∥
K
K
K
K
K°⊥
K°∥
K°
hν
Wi
POTENTIAL
ENERGY

Direct Interband Transition

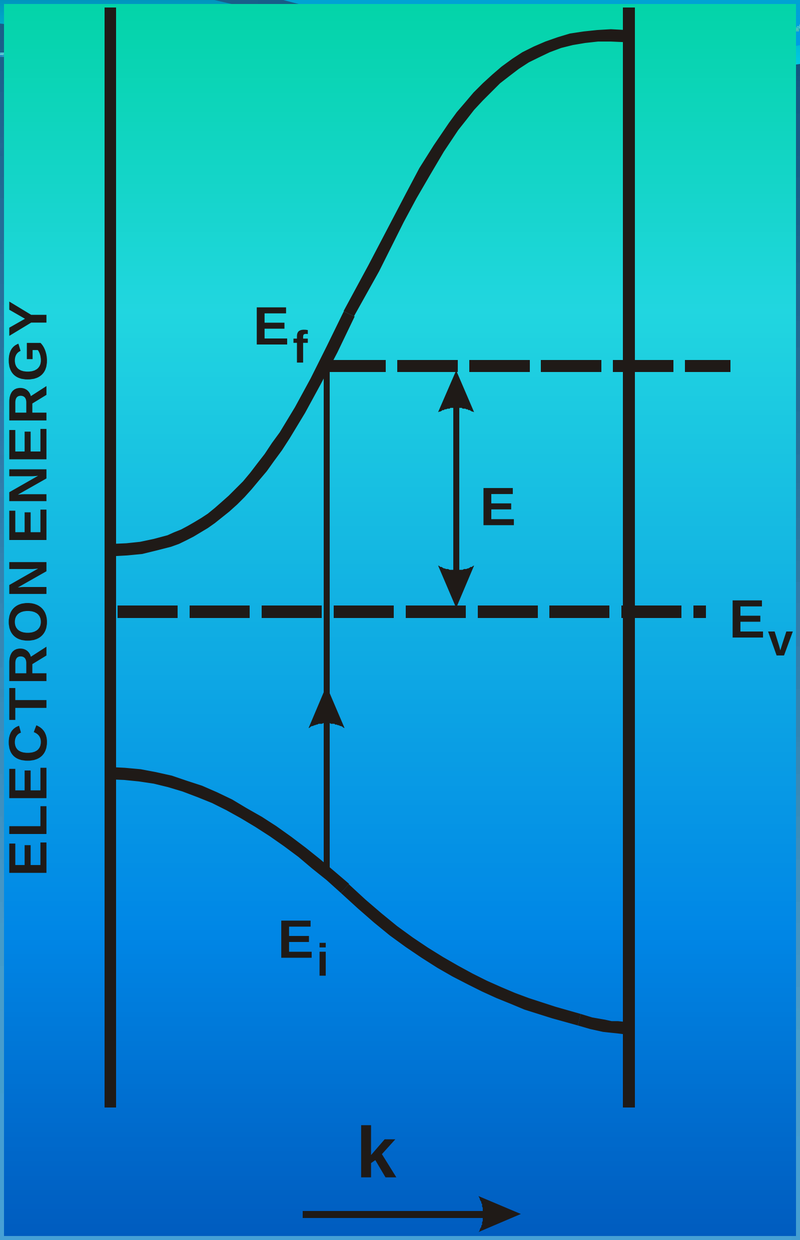

Band dispersion GaAs(110) Normal emission

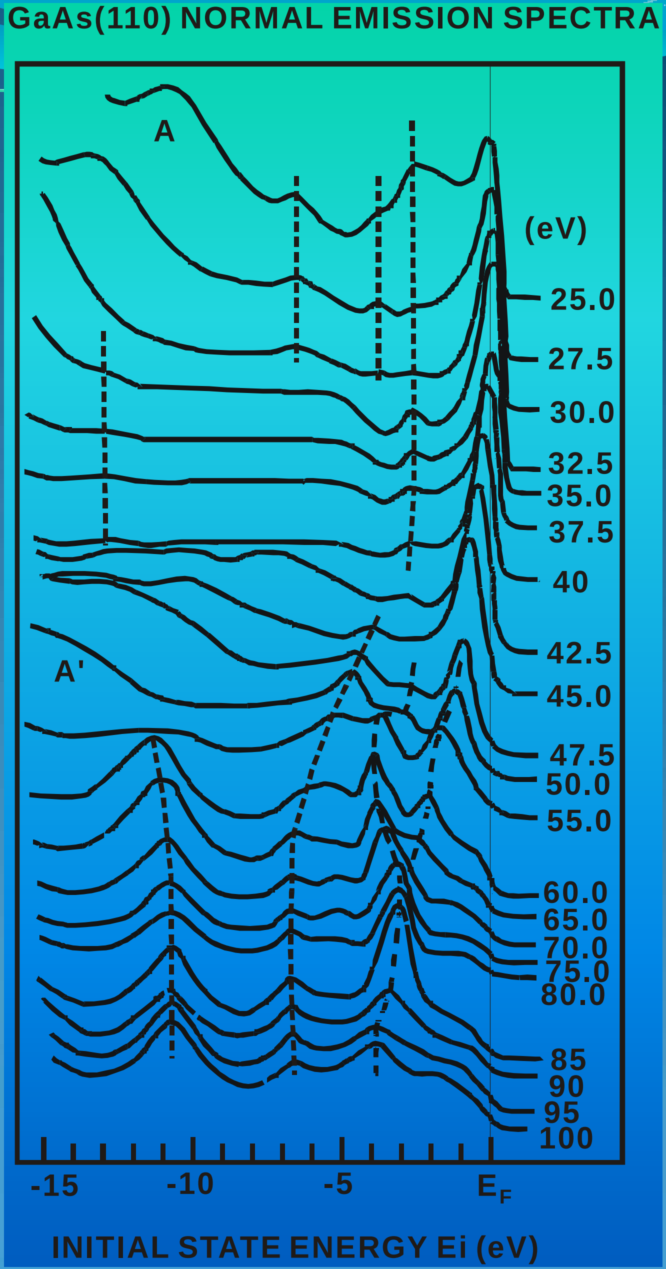

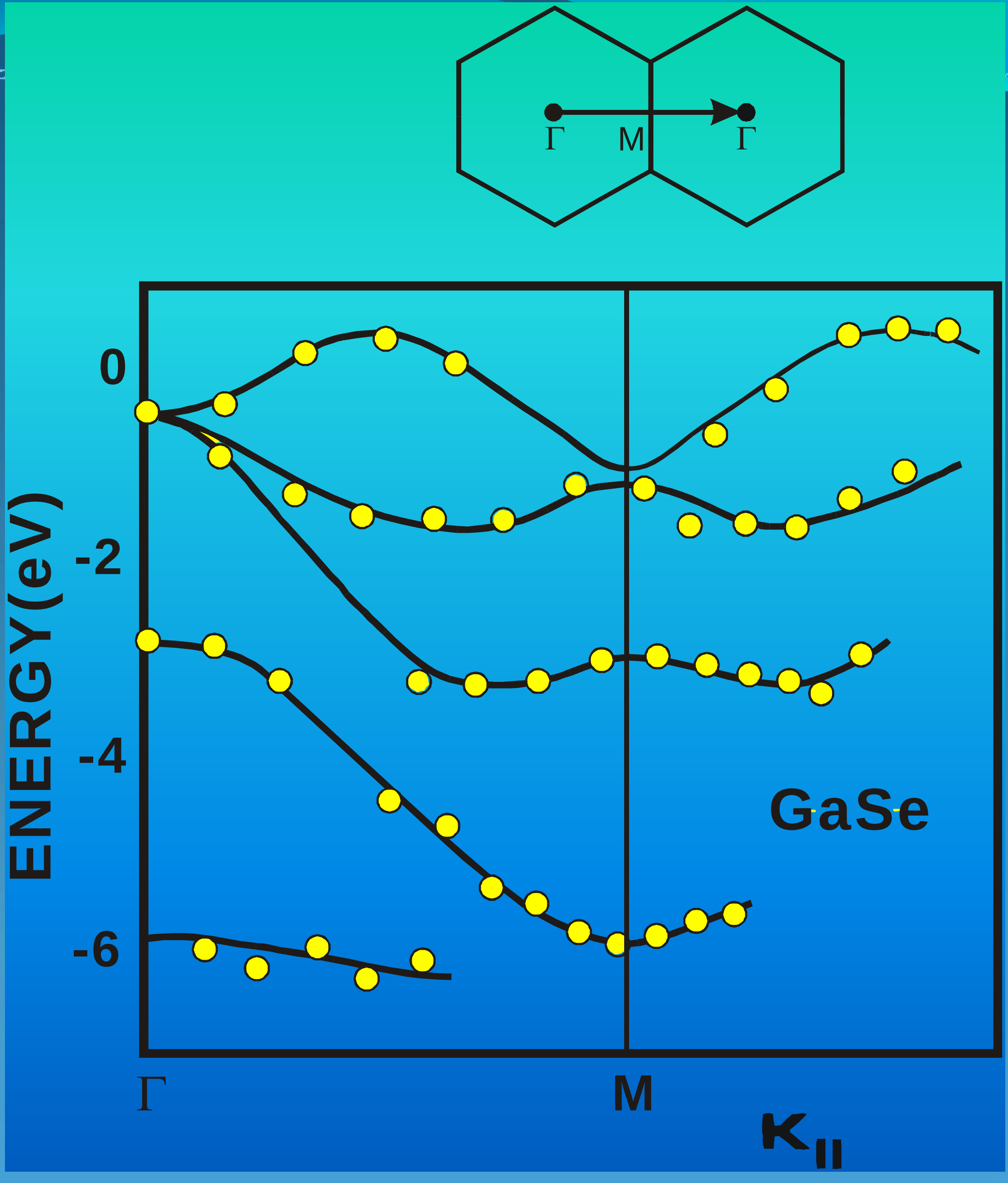

Γ
M
Γ
0
-2
-4
-6
ENERGY(eV)
GaSe
Γ
M
K||

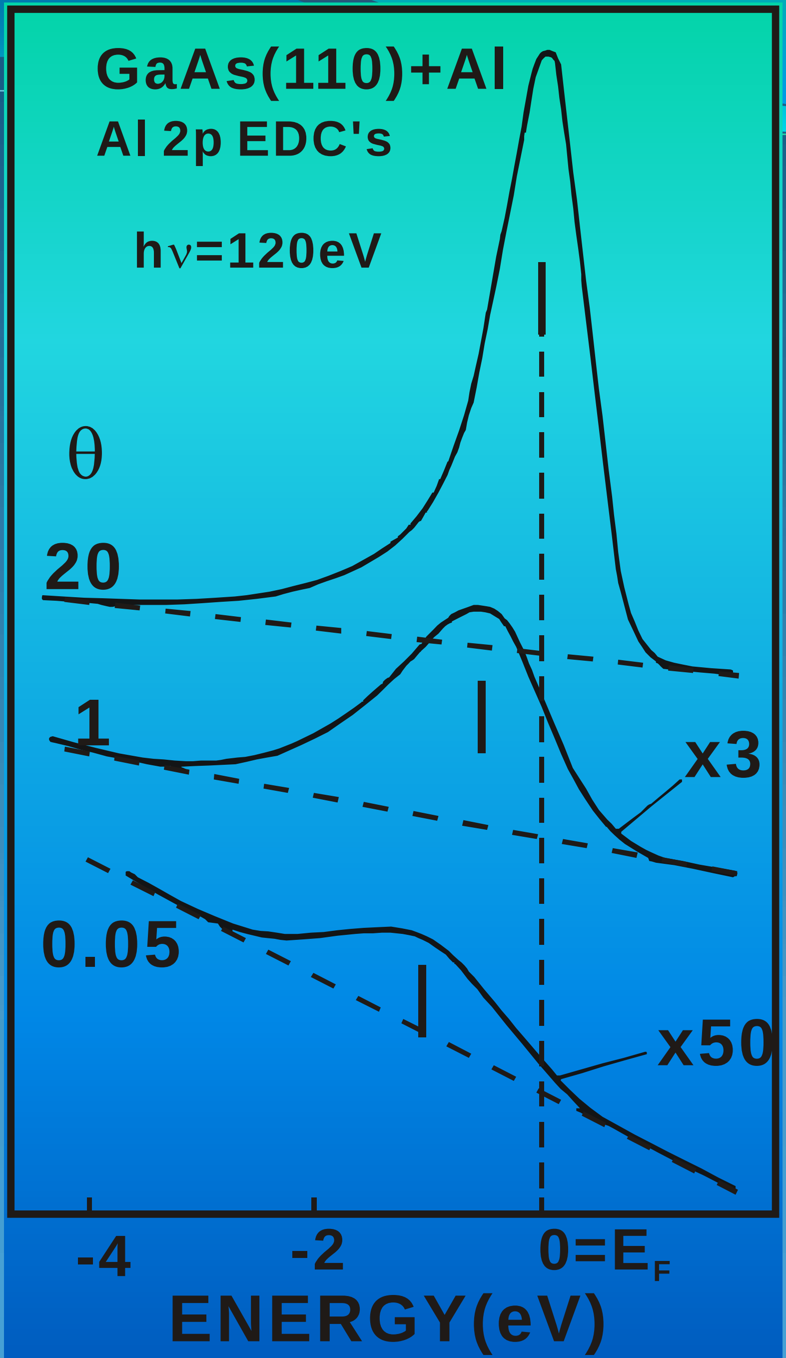

GaAs(110)+Al
Al 2p EDC's
hν=120eV
θ
20
1
0.05
x3
x50
-4
-2
0=E_F
ENERGY(eV)

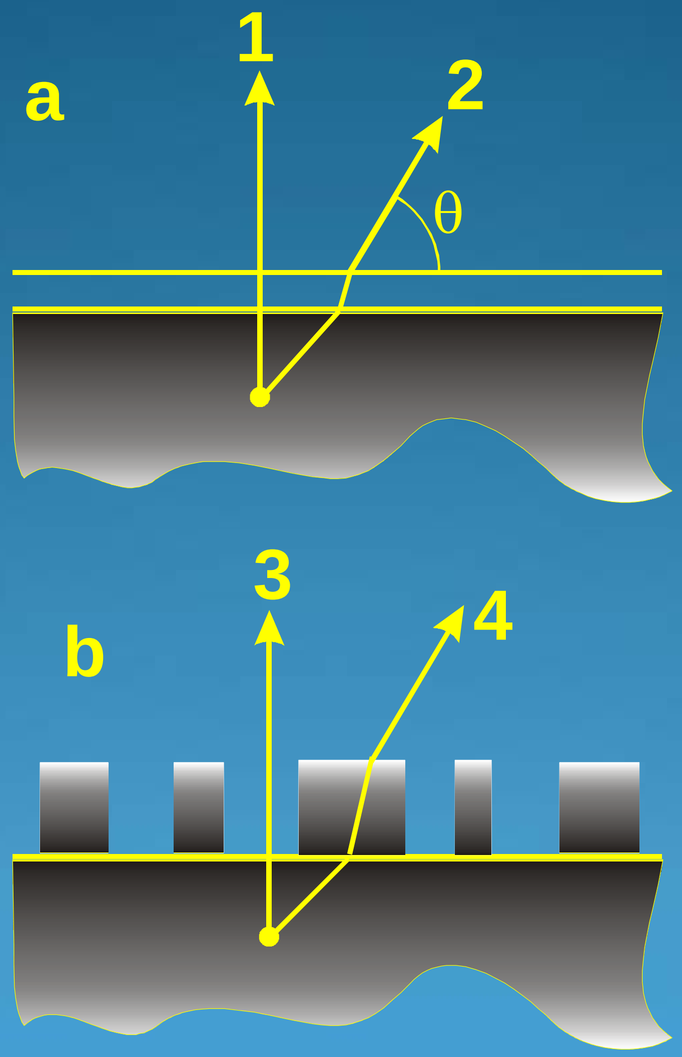

a
1
2
θ
b
3
4

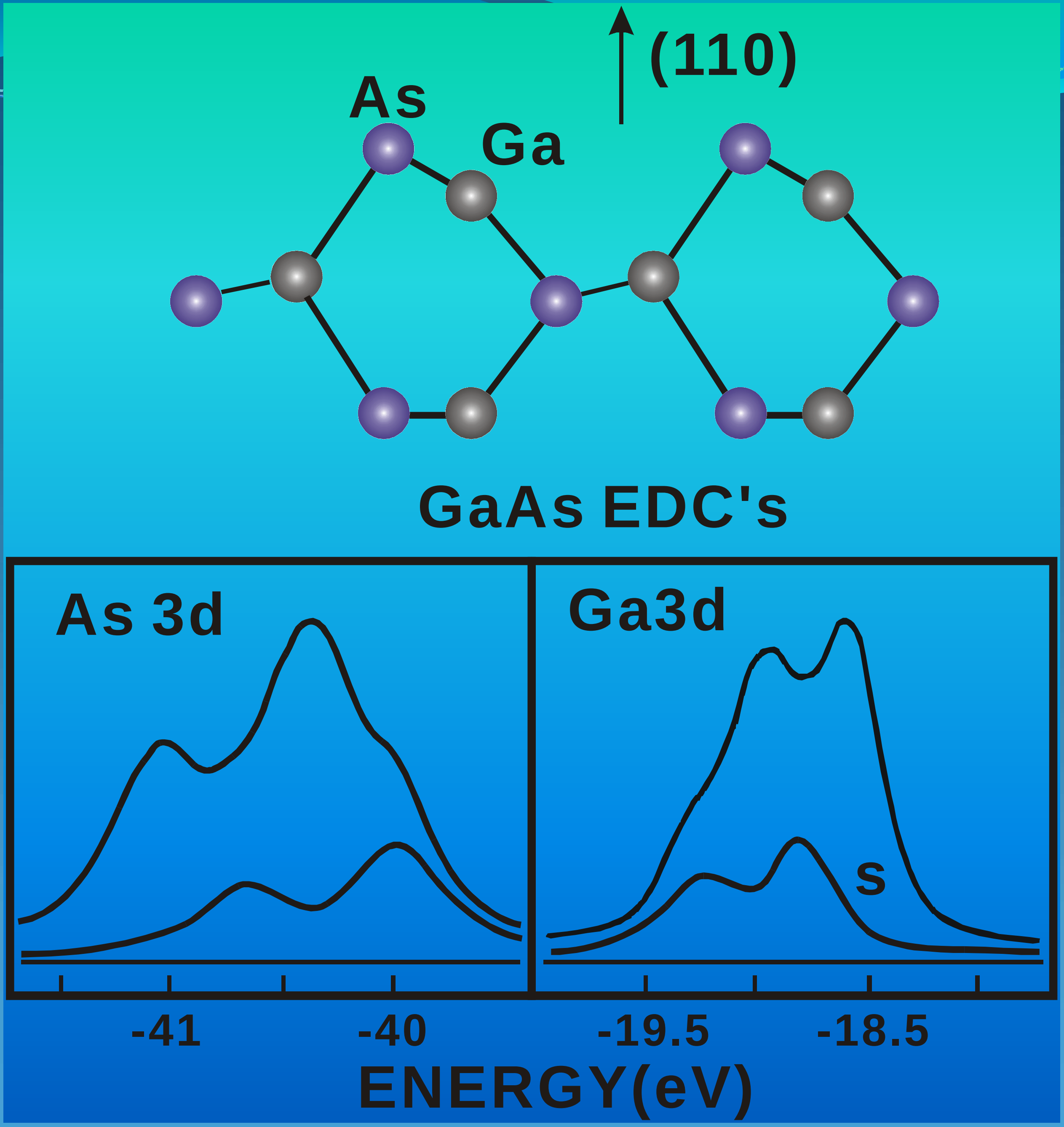

(110)
As
Ga
GaAs EDC's
As 3d
Ga3d
S
-41
-40
-19.5
-18.5
ENERGY(eV)

Taking Advantage of The Tunability

- Constant Initial State PES
- Constant Final State PES
- Resonance PES

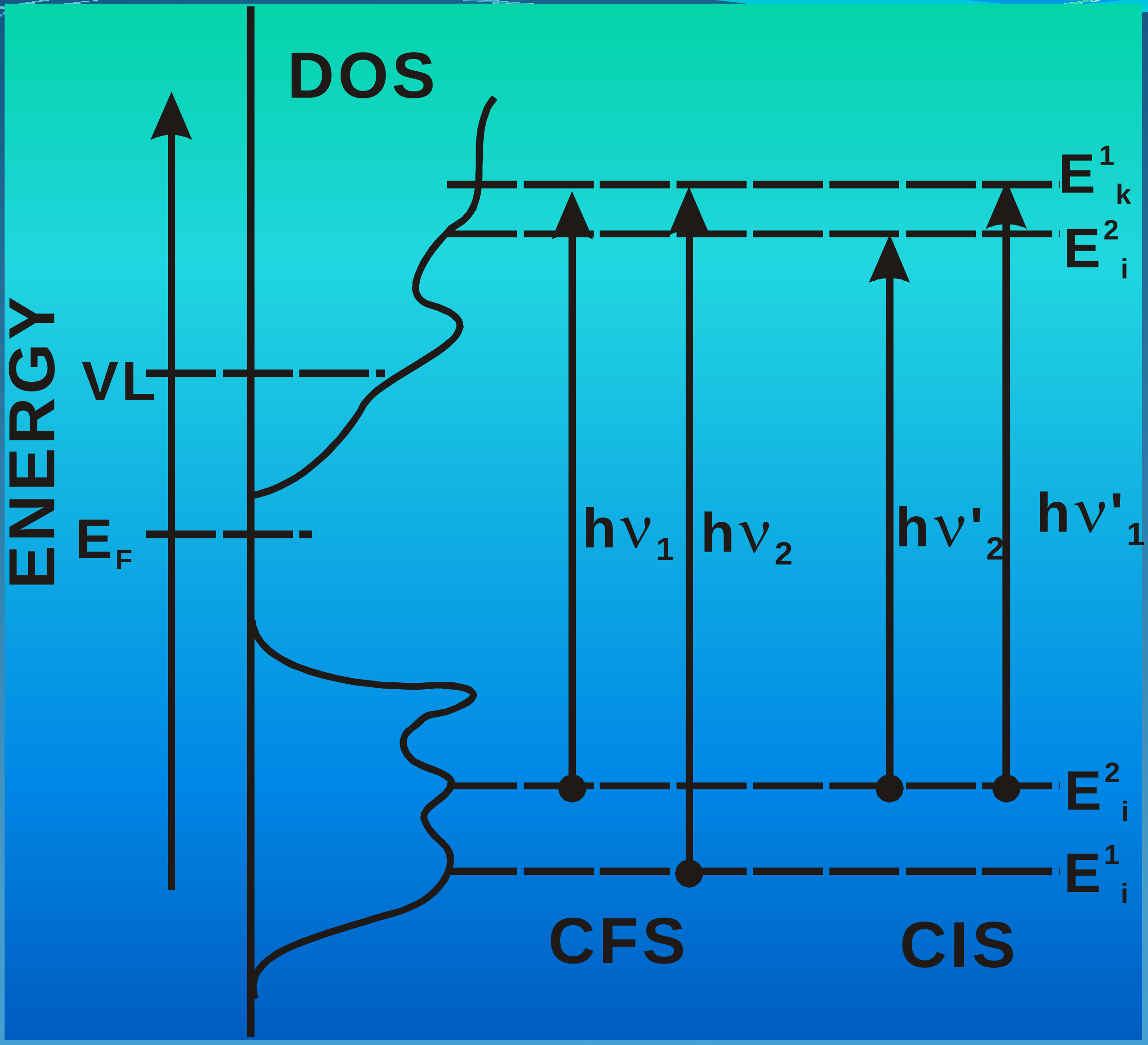

DOS
ENERGY
VL
E_F
E^1_k
E^2_i
$h\nu_1$
$h\nu_2$
$h\nu'_2$
$h\nu'_1$
E^2_i
E^1_i
CFS
CIS

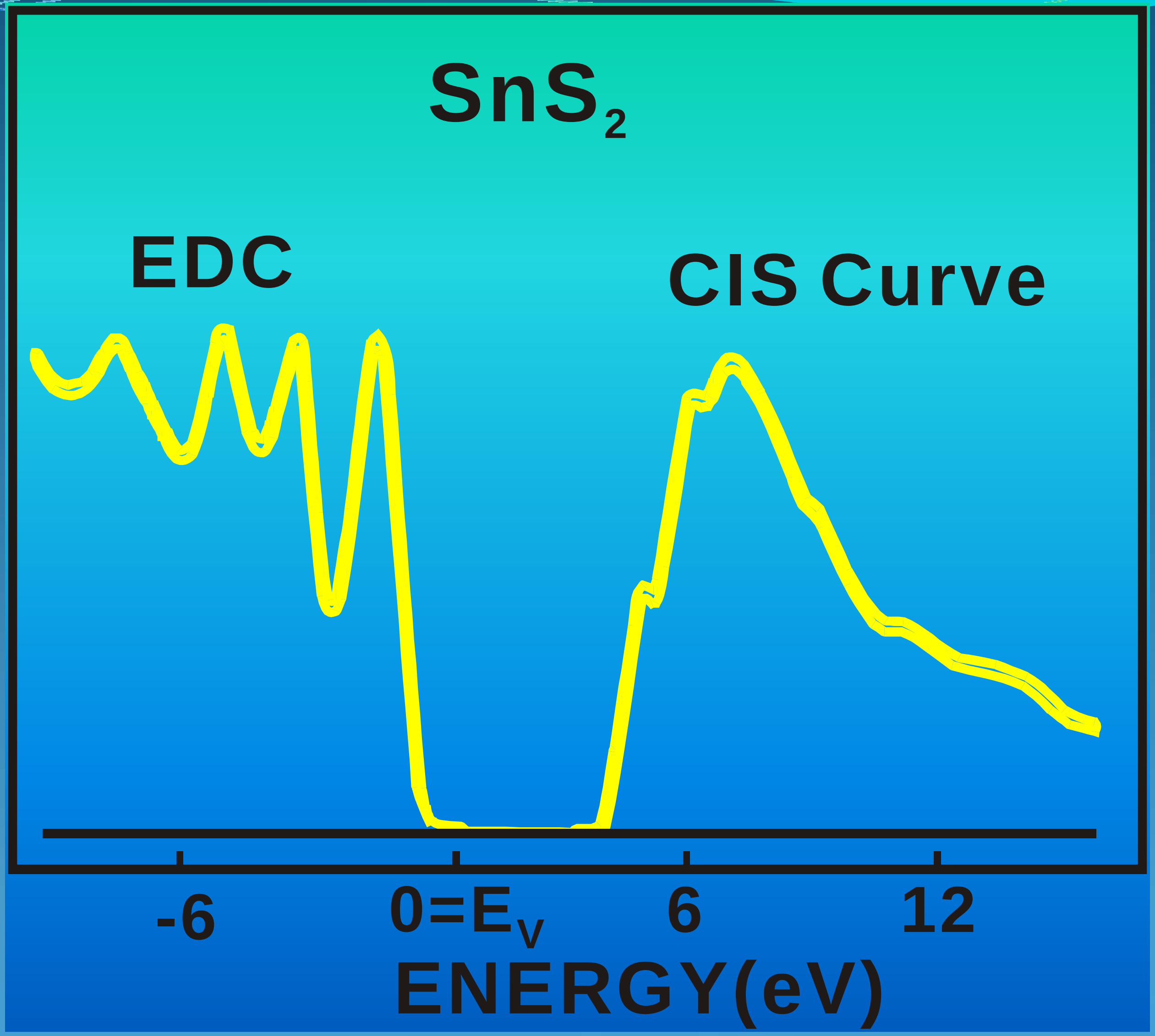

SnS_2
EDC
CIS Curve
-6
$0=E_V$
6
12
ENERGY(eV)

Spin-Polarized PES

- Energy bands in ferromagnetic metals are split by the exchange interaction into the
  - up-spin (majority spin) and
  - Down-spin (minority spin) band
- First experimentally observed by PES in Ni
- Spin polarized detectors
- Total PES

Spin-Resolved Electron Detectors

Mott
Detecto
r

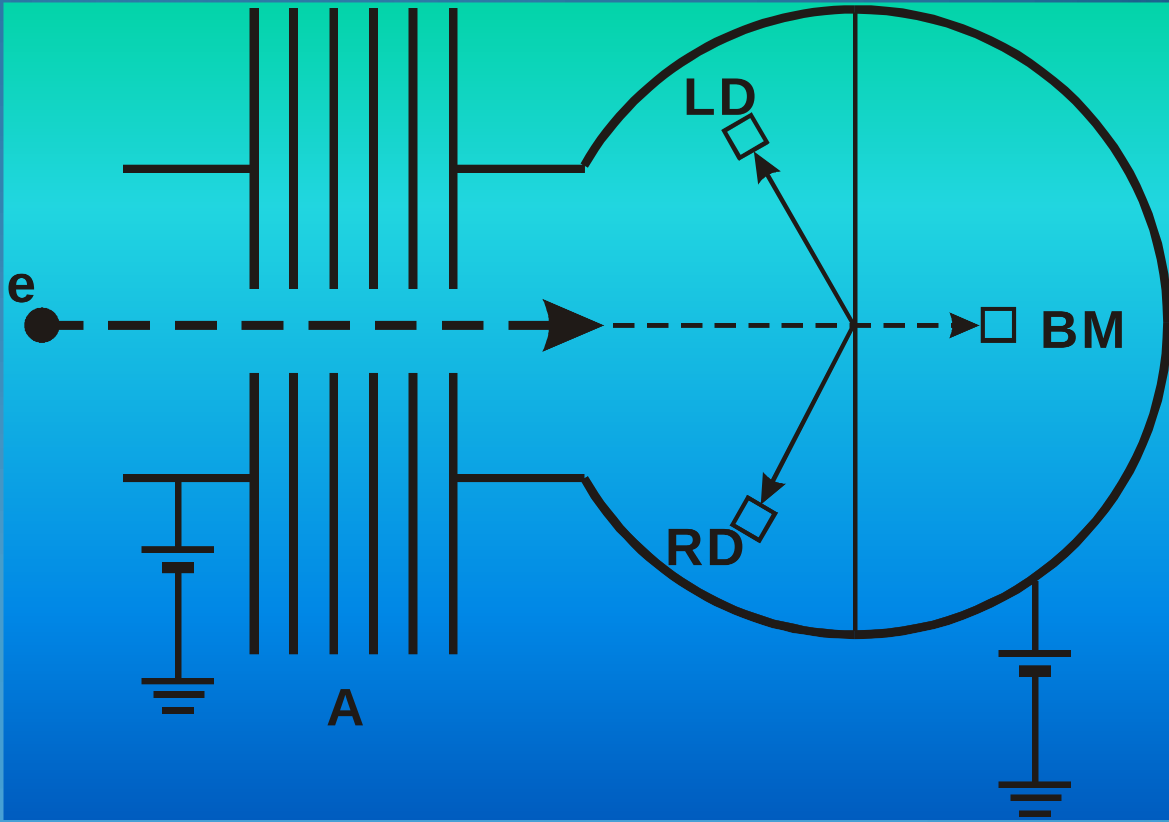

Magnetic bands

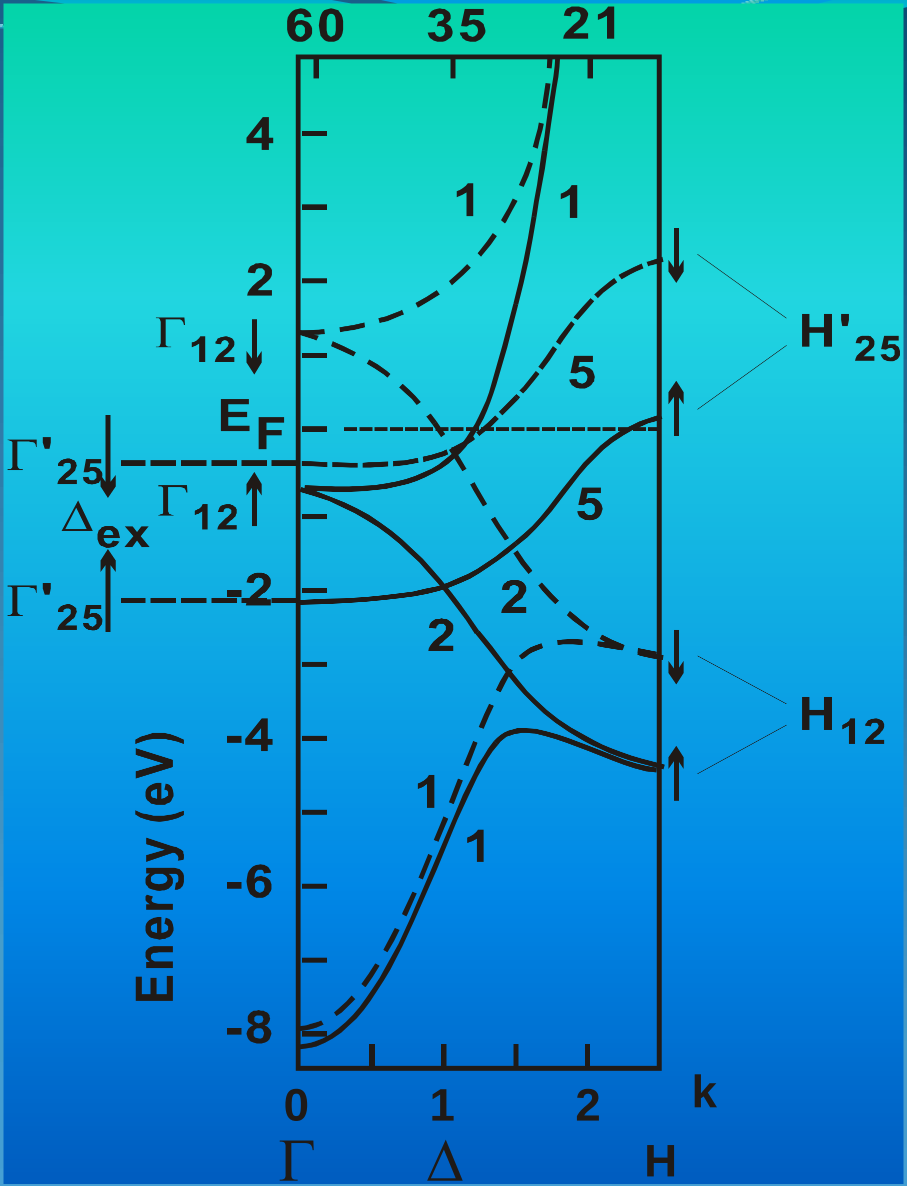

Spin-polarized photoelectron EDC's corresponding to the spin-up and spin-down polarizations

T is the Curie of Iron

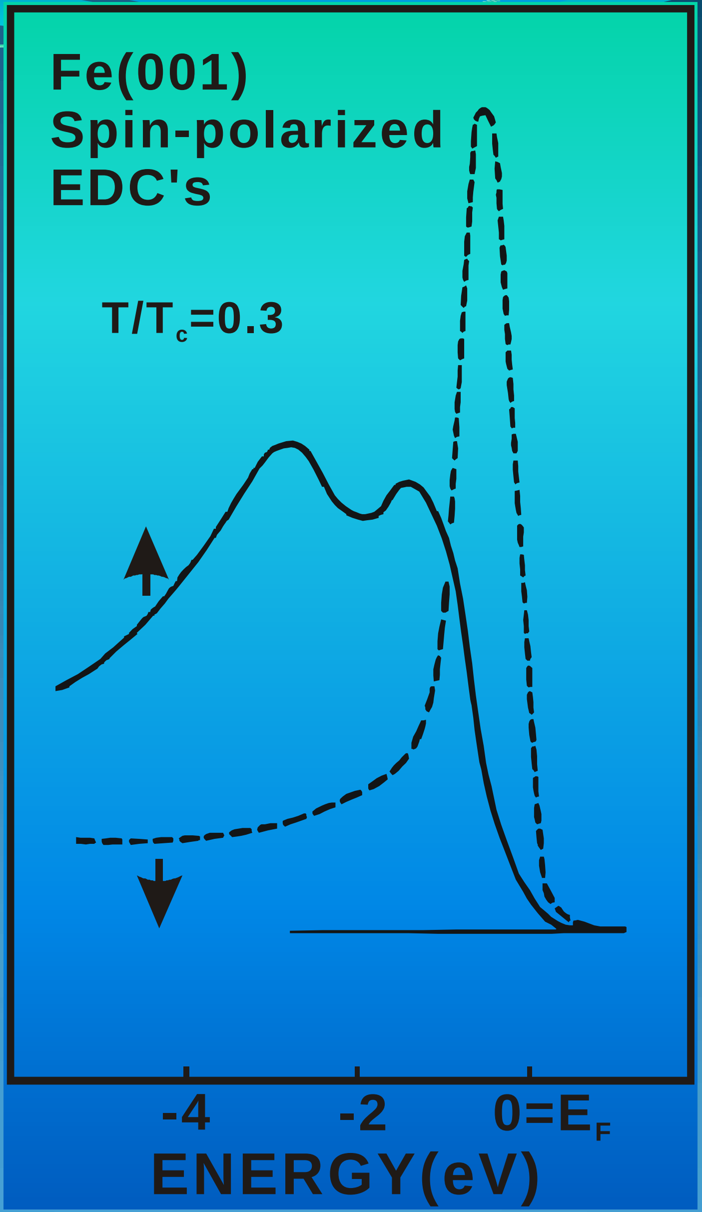

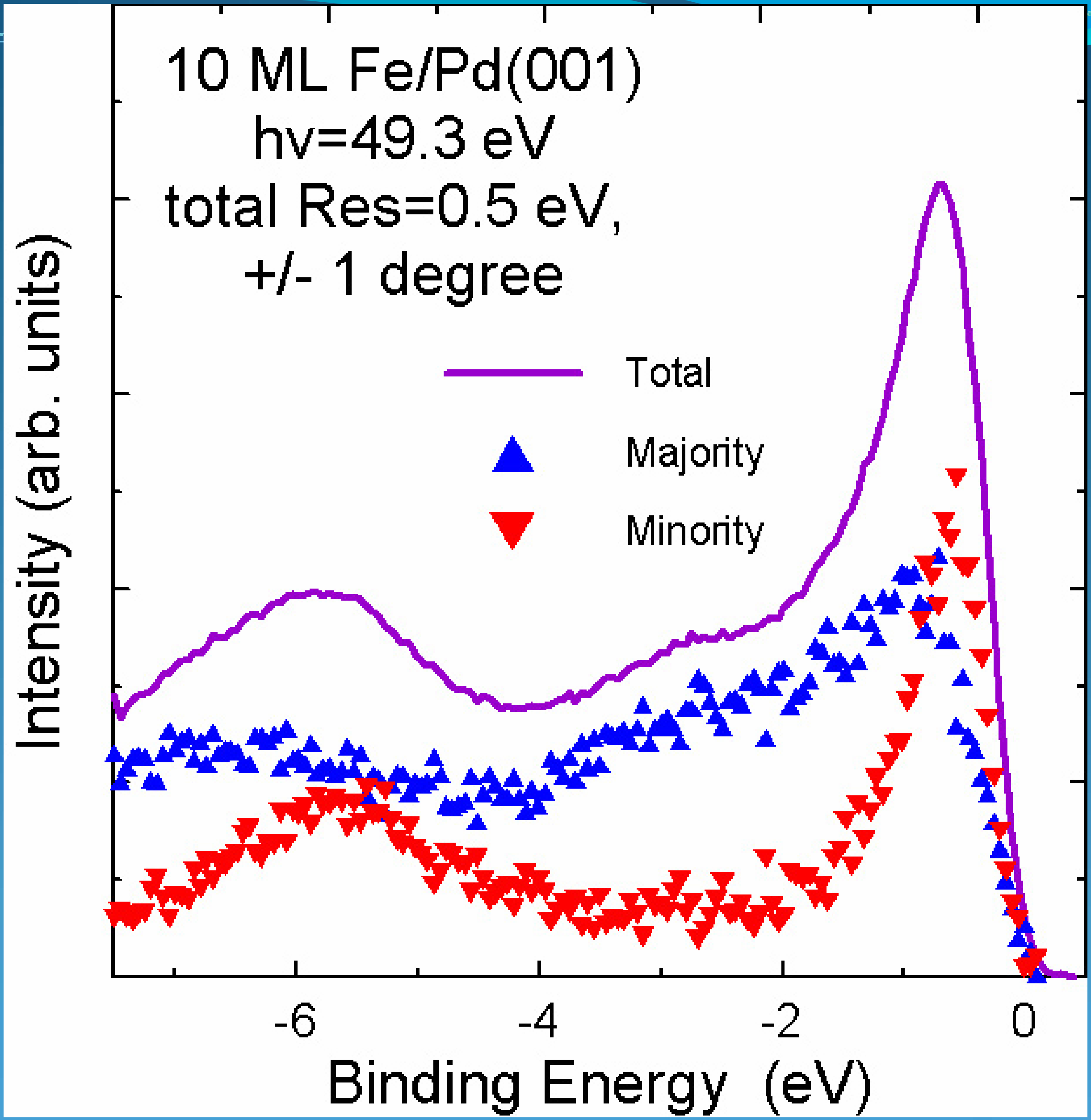

10 ML Fe/Pd(001)
hv=49.3 eV
total Res=0.5 eV,
+/- 1 degree
Total
Majority
Minority
Intensity (arb. units)
-6
-4
-2
0
Binding Energy (eV)

Recent developments

- Complete photoemission experiment:
- Very high energy (< 5meV) and angular (<0.5°) resolution
- Strongly correlated electronic systems
  - High T_c Supercondutors
  - Heavy Fermion system
  - Quantum Well State
- PhD and Photoelectron Holography

Fermi edges

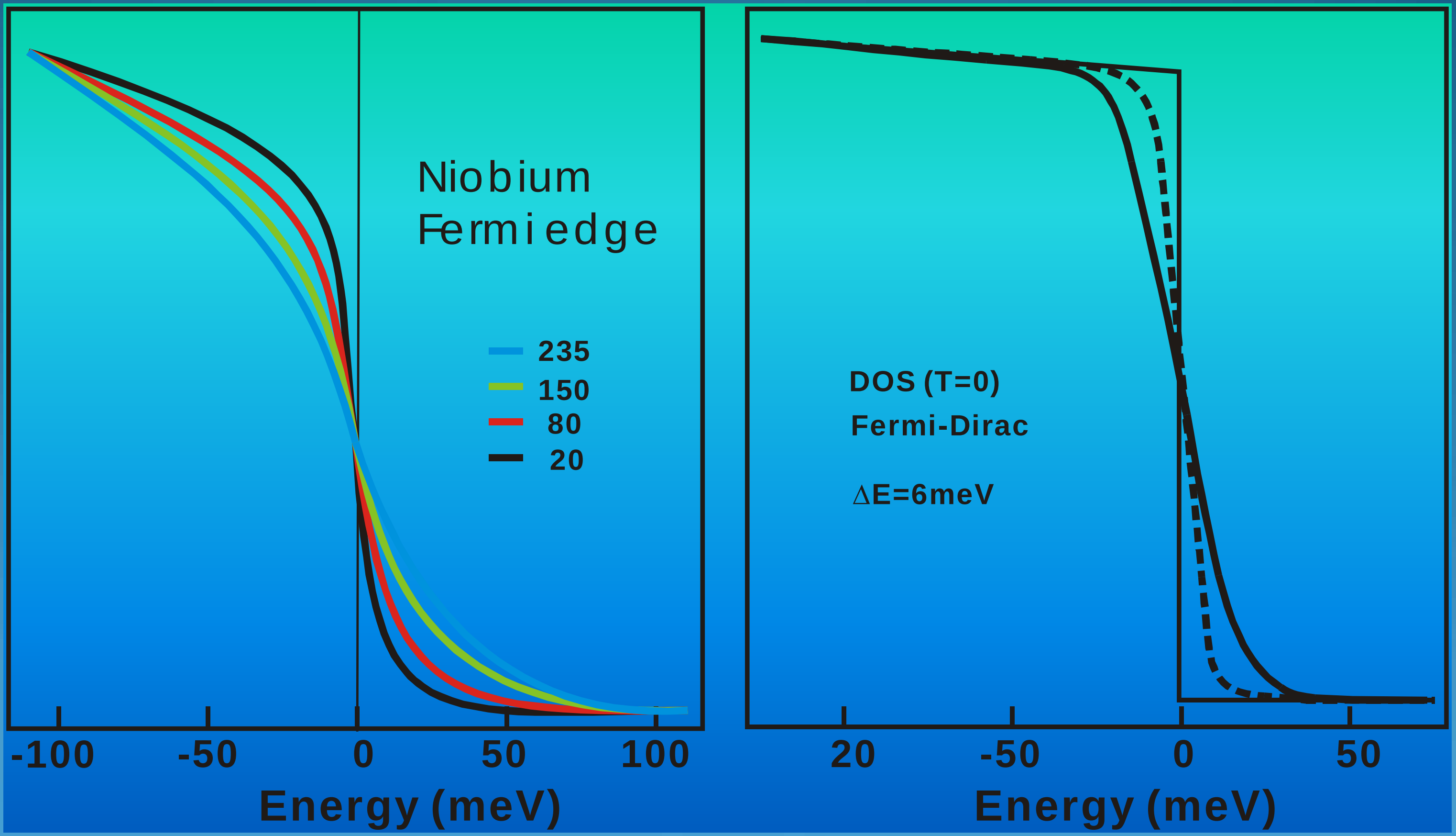

Niobium
Fermi edge
235
150
80
20
-100
-50
0
50
100
Energy (meV)
DOS (T=0)
Fermi-Dirac
ΔE=6meV
20
-50
0
50
Energy (meV)

HTC Gap Spectroscopy

Pseudo-Gap

- Special to HTSC. It persists at temperatures up to three times as high as the limit of superconductivity, in some cases even at room temperature.
- The properties of the pseudo-gap were determined using the highly energy-resolved SR-ARUPS. It was found that the pseudo-gap and the superconducting gap have the same angular symmetry, suggesting they are related.
- The temperature dependence of the pseudo-gap was determined as well.

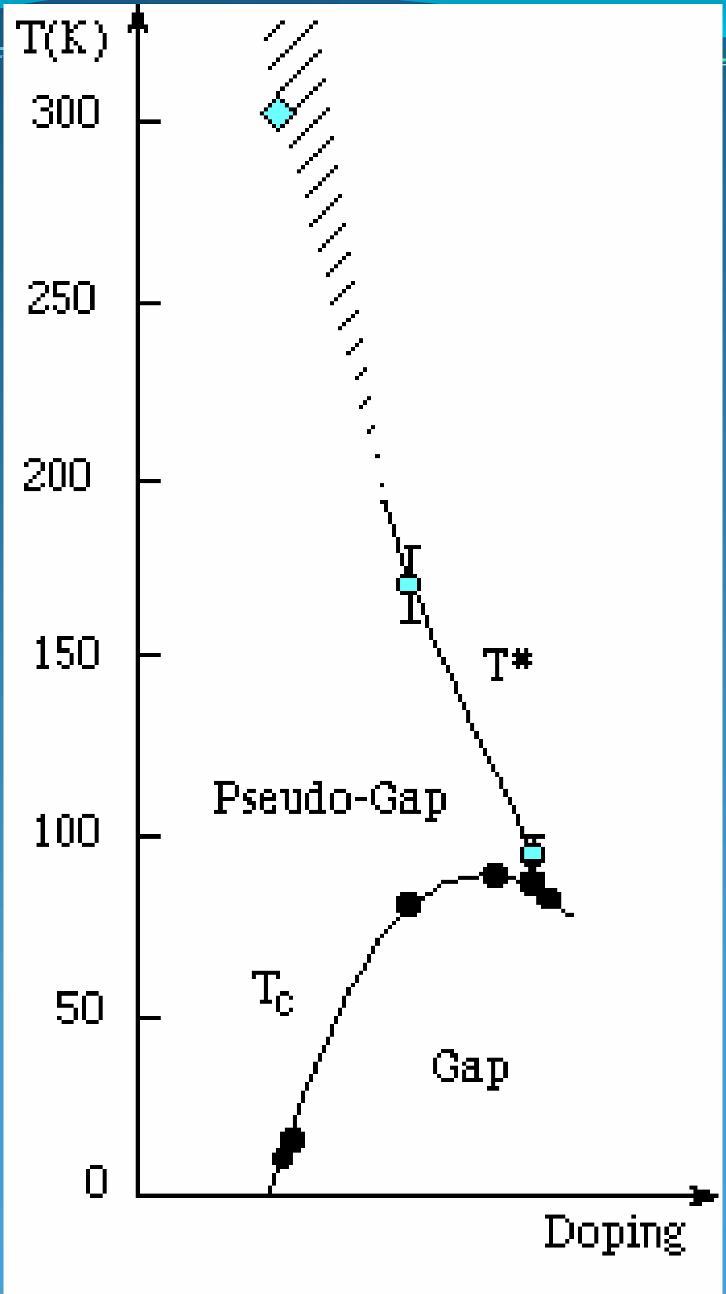

Temperature regions where the gap and the pseudo-gap exist. The maximum temperature where a pseudo-gap is still observed (T*) can be much higher than the maximum temperature for superconductivity (Tc) and as high as room temperature (about 290 K).

The results are reported by H. Ding and coworkers in Nature **382**, 51 (1996) and in Physical Review Letters **78**, 2628 (1997). Highlights can be found in Physics Today, June 1996, p. 17.

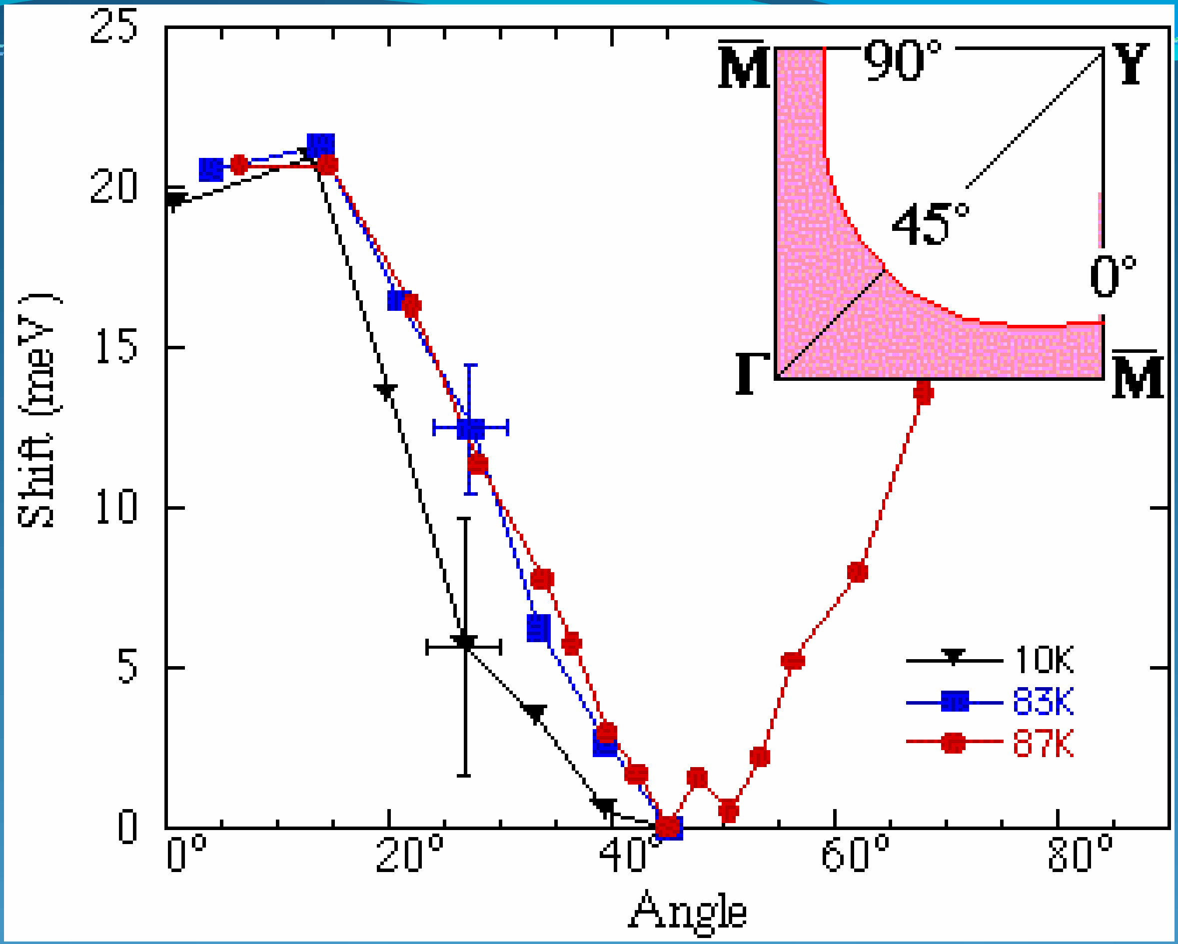

Symmetry of the pseudo-gap when the sample is rotated.
The characteristic minimum at 45 degrees is observed for the superconducting gap and the pseudo-gap, suggesting they are related.

Quantum Well State

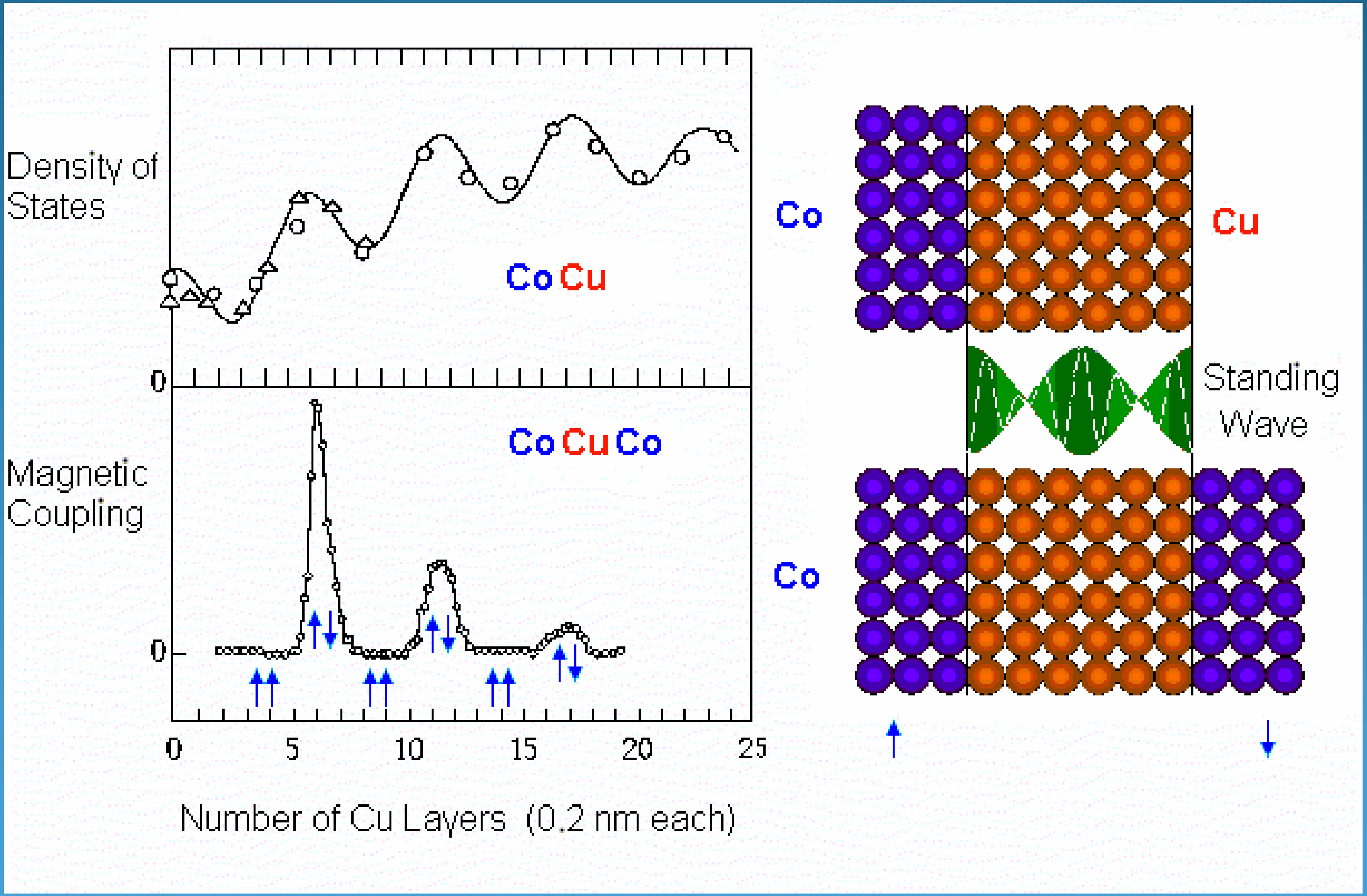

Quantum Well States

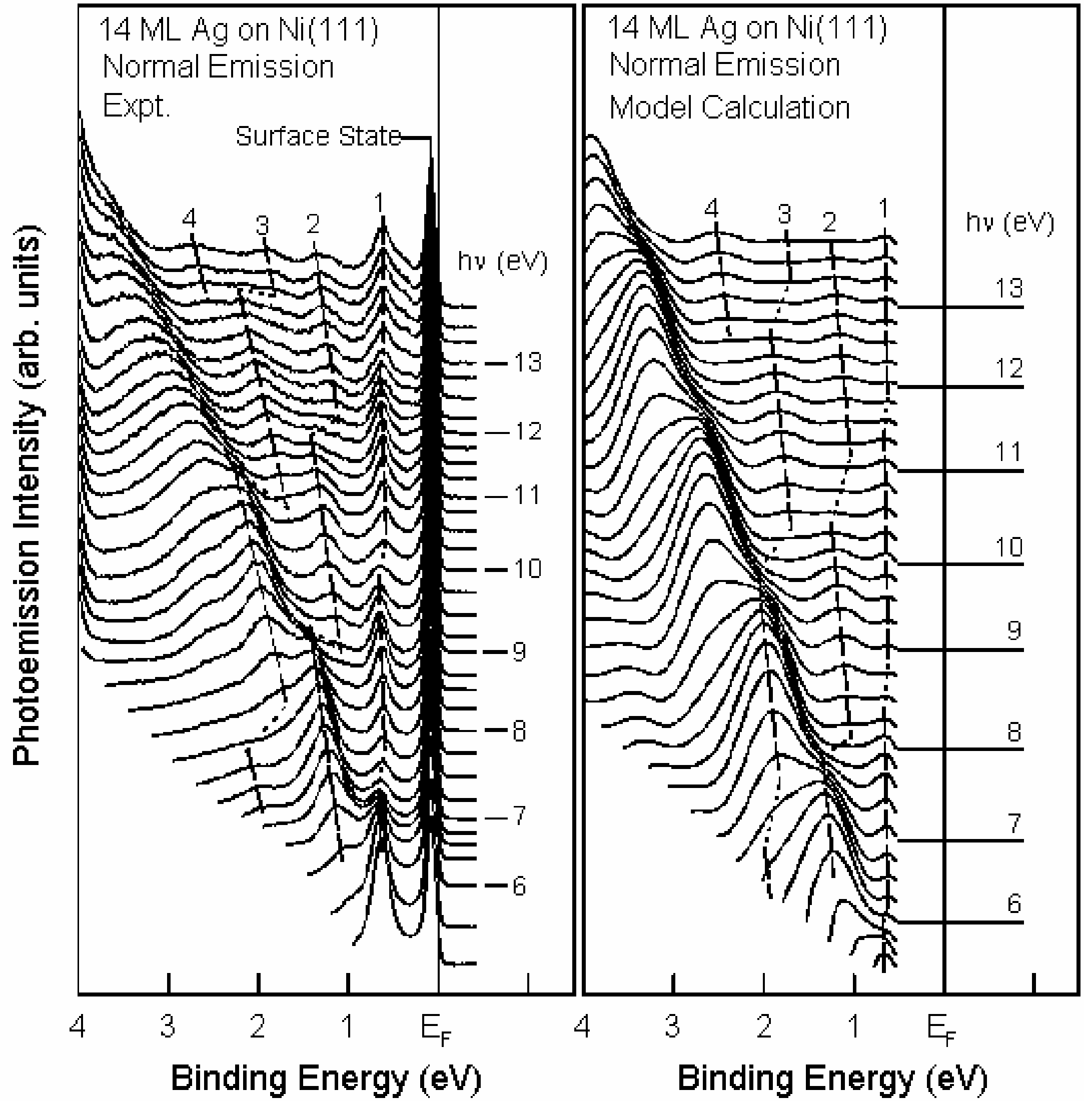

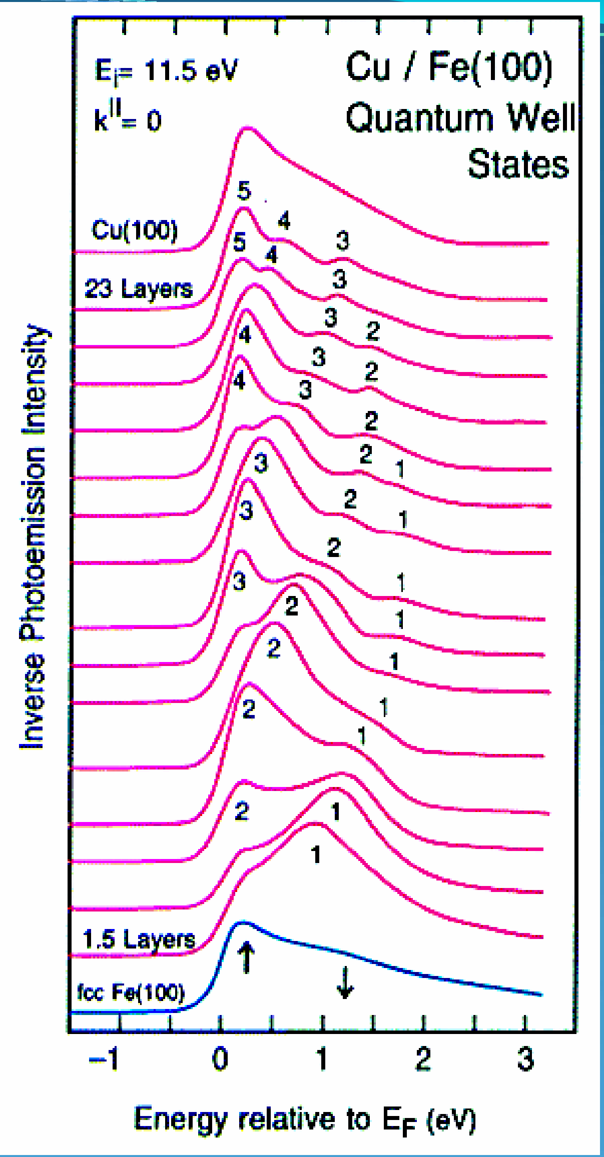

Ei= 11.5 eV
k||= 0
Cu / Fe(100)
Quantum Well
States
Cu(100)
23 Layers
1.5 Layers
fcc Fe(100)
Inverse Photoemission Intensity
−1
0
1
2
3
Energy relative to EF (eV)

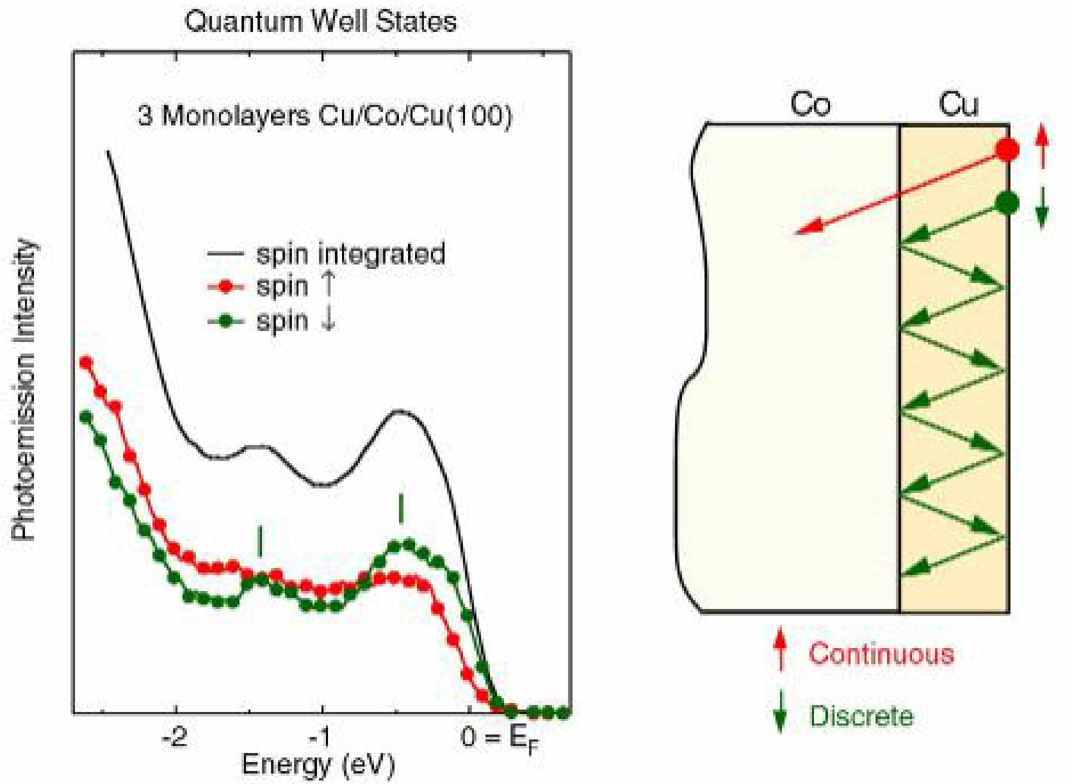
Quantum Well States
3 Monolayers Cu/Co/Cu(100)
spin integrated
spin ↑
spin ↓
Photoemission Intensity
-2
-1
0 = E_F
Energy (eV)
Co
Cu
Continuous
Discrete

Further readings:

- Review of magnetic nanostructures:
  Himpsel et al., Advances in Physics **47**, 511 (1998).
- Basic principles of magnetic recording:
  Grochowski and Thompson, IEEE Trans. Magn. **30**, 3797 (1994)
- Measurement of magnetic quantum well states:
  Ortega et al., Phys. Rev. Lett. **69**, 844 (1992) and Phys. Rev. B **47**, 1540 (1993).
  Himpsel, J. Phys. Cond. Matter **11**, 9483 (1999) and Science **283**, 1655 (1999).

Diffraction and Holography

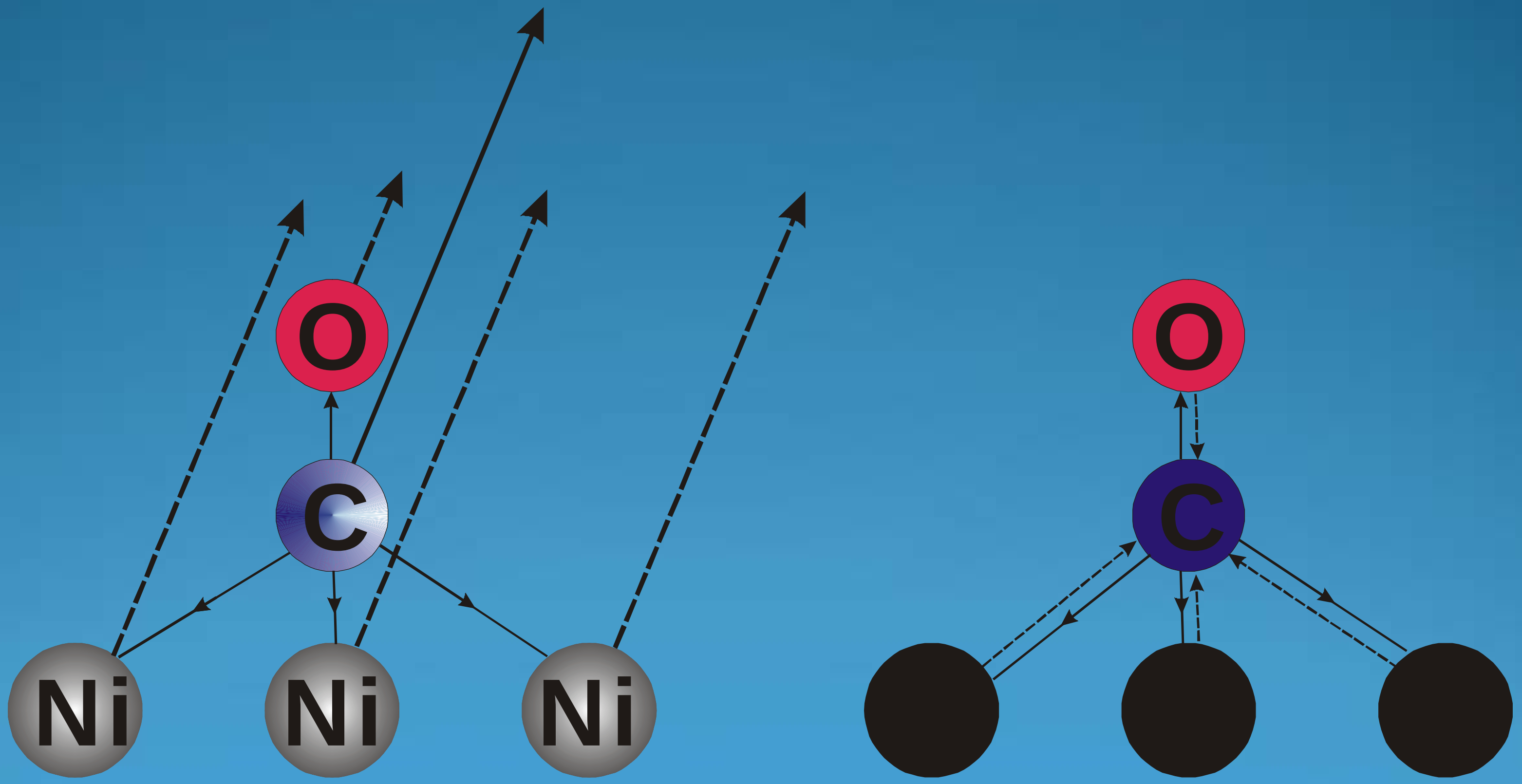

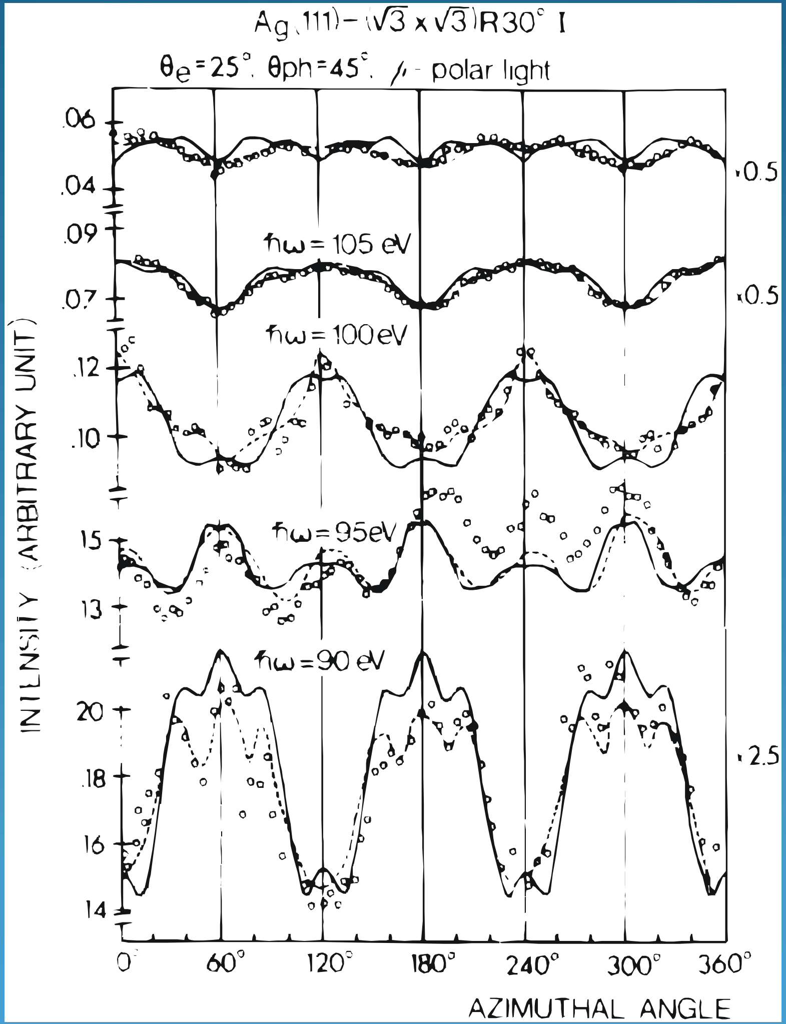

Ag (111) − (√3 x √3) R30° I
θe = 25°, θph = 45°, // - polar light
ħω = 105 eV
ħω = 100 eV
ħω = 95 eV
ħω = 90 eV
INTENSITY (ARBITRARY UNIT)
AZIMUTHAL ANGLE
x0.5
x0.5
x2.5
0°
60°
120°
180°
240°
300°
360°

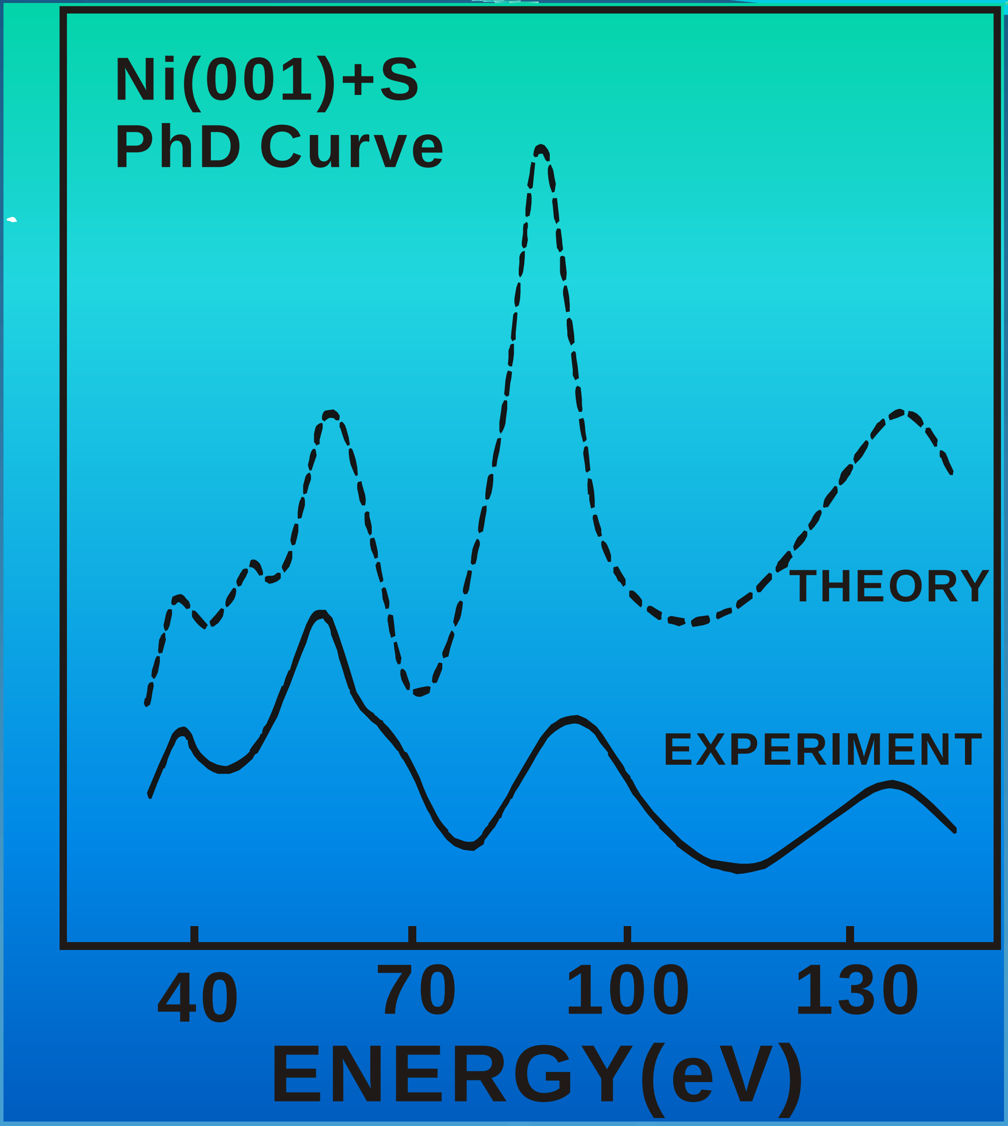
Ni(001)+S
PhD Curve
THEORY
EXPERIMENT
40
70
100
130
ENERGY(eV)

Photoelectron Holography

- Produces 3-D pictures by superimposing two beams, one coming directly from a laser,the other reflected off the three-dimensional object. Using electrons instead of light one can produce three-dimensional pictures of very tiny objects, because the wavelength of electrons is much shorter that that of light.

X-Ray Photoelectron Diffraction of Copper (100): Volume Data Set

ALS

Researchers at the ALS have been able to obtain richly detailed diffraction data for copper (100). The data can be used to test holographic methods for analyzing crystal structure.

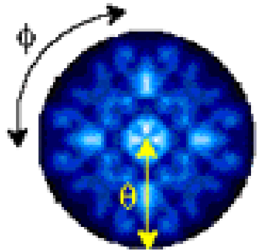

Angle-dependent diffraction pattern
(Conventional data set: fine detail in angle for only one energy)

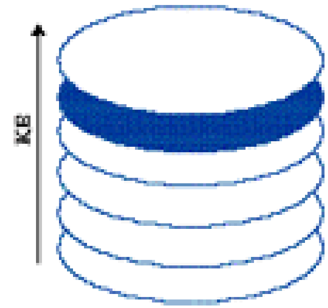

Diffraction patterns stacked according to kinetic energy

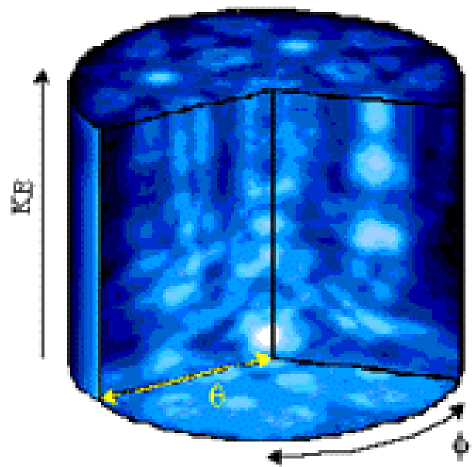

Volume data set
(Fine detail for angles as well as kinetic energies)

Beamline 7.0.1: U. of Wisconsin-Milwaukee, U. of Oregon, LBNL

A 3-D picture of atoms at a silicon surface that was obtained using electrons emitted from the surface under irradiation with SR.The analog to the direct laser beam are electrons emitted directly from the red atom, the analog of the reflected light are electrons scattered by neighbor atoms (green).

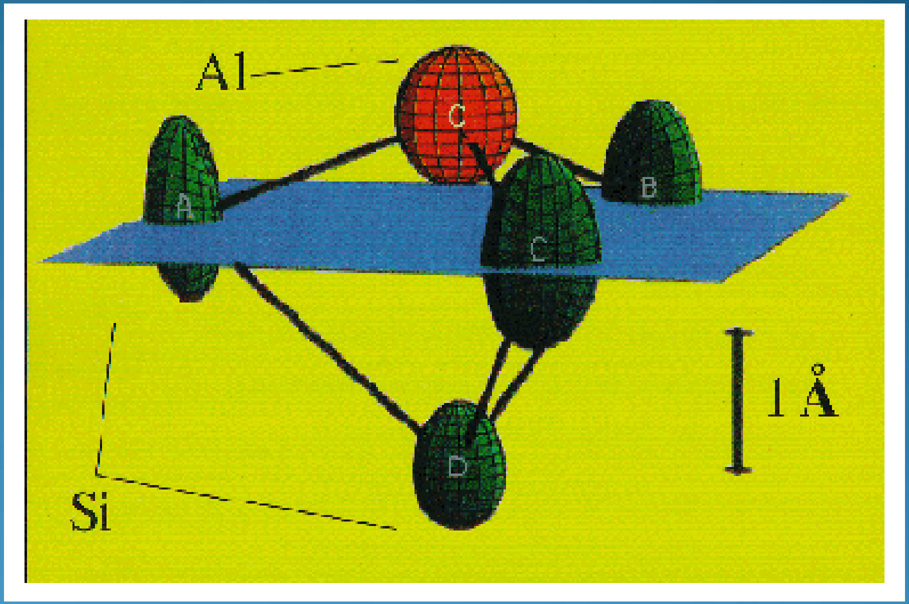

H. Wu and G.J. Lapeyre, Phys. Rev. B 51, 14549 (1995)

References:

Books on photoelectron spectroscopy

- Cardona M. and Ley L., editors, *Photoemission in Solids I & II*, Springer Verlag, Berlin 1978
- Kevan S.D, editor, *Angle-resolved Photoemission - Theory and current application*, Elsevier, Amsterdam 1992